DEVELOPMENT OF NEW ENVIRONMENT FRIENDLY ADSORPTION MEDIA FOR THE REMOVAL OF HAZARDOUS ANIONS FROM WATER

Dissertation submitted in partial fulfillment
of the requirements of the degree of

Doctor of Philosophy

in

Chemistry

by

Tapaswini Padhi

(Roll No. 509CY607)

based on research carried out

under the esteemed Supervision of

Prof. Rajkishore Patel

Department of Chemistry

National Institute of Technology Rourkela

December, 2018

Department of Chemistry
National Institute of Technology Rourkela

September 02, 2019

Certificate of Examination

Roll Number: 509CY607

Name: **Tapaswini Padhi**

Title of Dissertation: **Development of New Environment Friendly Adsorption Media For Removal of Hazardous Anions from Water**

We the below signed, after checking the dissertation mentioned above and the official record books of the student, hereby state our approval of the dissertation submitted in partial fulfillment of the requirements of the degree of Doctor of Philosophy in Department of Chemistry at National Institute of Technology Rourkela. We are satisfied with the volume, quality, correctness, and originality of the work.

Raj Kishor Patel
Supervisor

Sabita Patel
Member (DSC)

Rupam Dinda
Member (DSC)

Manoranjan Barik
Member (DSC)

Braja Gopal Mishra
Chairman (DSC)

Satya Narayan Naik
IIT,Delhi
Examiner

Department of Chemistry
National Institute of Technology Rourkela

Supervisor's Certificate

This is to certify that the work presented in the dissertation entitled *DEVELOPMENT OF NEW ENVIRONMENT FRIENDLY ADSORPTION MEDIA FOR THE REMOVAL OF HAZARDOUS ANIONS FROM WATER*, submitted by *TAPASWINI PADHI (Roll No.509CY607)* to National Institute of Technology, Rourkela, is a record of bonafide research carried out by her under my supervision and guidance in partial fulfillment of the requirement of the degree of Doctor of Philosophy in Chemistry. Neither this dissertation nor any part of it has been submitted earlier for any degree or diploma to any institute or university in India or abroad.

_____

Prof. Rajkishore Patel

(Supervisor)

Place: NIT, Rourkela

Date:

Declaration of Originality

I, Tapaswini Padhi, Roll Number 509CY607 hereby declare that this dissertation entitled "*Development of new environment friendly adsorption media for the removal of hazardous anions from water"* presents my original work carried out as doctoral student of NIT Rourkela and, to the best of knowledge, contains no material previously published or written by another person, nor any material presented by me for the award of any degree or diploma of NIT Rourkela or any other institution. Any contribution made to this research by others, with whom I have worked at NIT Rourkela or elsewhere, is explicitly acknowledged in the dissertation. Works of other authors cited in this dissertation have been duly acknowledged under the sections "Reference" or "Bibliography". I have also submitted my original research records to the scrutiny committee for evaluation of my dissertation.

I am fully aware that in case of any non-compliance detected in future, the Senate of NIT Rourkela may withdraw the degree awarded to me on the basis of the present dissertation.

December, 2018 Tapaswini Padhi

NIT Rourkela

Acknowledgement

To begin with, I might want to pass on my extraordinary gratitude to my supervisor, Prof. Rajkishore Patel, for his direction, inspiration and support to finish this work. I am grateful to him for giving me a great situation to research and concentrate in the Environmental Laboratory and Research Laboratory at the National Institute of Technology, Rourkela. I truly value his guidance, technical insight, commitment and patience. I took in the importance of genuine logical meticulousness by interacting with him. I completely respect his ability for scientific generalization, his ability to dismember an unpredictable issue into littler, and less difficult ones, breaking down them and reproducing it by and by with outright lucidity.

I am always gratified on The Ministry of Environment & Forests (MoEF) for engaging me in the project entitled "Development of new Environment friendly adsorption media for the removal of hazardous anions from water" under Ref: F.No.-19-109/2008/RE, Dated 21.09.2009.

Finally, I owe everything to my loving parents, parents in law, husband, brother and all family members for their patience, sacrifice and support during my research work.

I am to a great degree appreciative to Dr. Sanjay Swain, BITS, Mesra for his magnificent help in doing some portion of this examination work at BITS, Mesra. I am especially grateful to Director of NIT Rourkela for allowing me to join and proceeding with my research work in this institute. Additionally, I am expressing thanks to the DSC members related with my research work for giving me significant recommendations to to strengthen this thesis.

I need to thank the researcher scholar friends in the Environmental Laboratory and Research Laboratory at the National Institute Technology, Rourkela for their help, advice and friendship. My life and research at NIT, Rourkela would have never been the equivalent without them.

Finally, I owe everything to my loving parents, parents in law, husband, brother and all family members for their patience, sacrifice and support during my research work.

Tapaswini Padhi
Department of Chemistry
NIT Rourkela, India

Place: NIT, Rourkela
Date:

Abbreviations

pH_{ZPC}	Point zero charge
MCL	Maximum contamination level
WHO	World Health Organization
LDH	Layered double hydroxides
GFH	Granulated ferric hydroxide
HFO	Hydrous ferric oxide
SHAB	Soft hard acid base
XRD	X-ray Diffraction
SEM	Scanning electron microscopy
TEM	Transmission electron microscopy
FTIR	Infrared spectroscopy
BET	Brunauer-Emmet-Teller
TGA/DTA	Thermo gravimetric Analysis
AAS	Atomic absorption spectroscopy

List of Symbols

λ	Incident X-ray wavelength
θ	Bragg's angle
D	Mean crystallite size
C_0	Initial concentration (mg/L)
Ce	Equilibrium concentration (mg/L)
V	Volume of the solution (L)
M	Mass of adsorbent (g)
q_e	Adsorbent amount (mg g^{-1}) at equilibrium
q_t	Adsorbent amount (mg g^{-1}) at time 't'
K_f	Rate constant of pseudo 1st order adsorption reaction in (min^{-1})
K_s	Rate constant of pseudo 2nd order adsorption reaction in (min^{-1})
K_L	Langmuir constants in (Lg^{-1})
q_{max}	maximum removal capacity (mg g^{-1})
ΔG	Gibb's free energy change
ΔS	entropy change
ΔH	enthalpy change

List of Figures

List of Tables

Abstract

Over last three decades, the important thrust area among the researches are to provide uncontaminated drinking water and for other domestic uses. New technologies in field of water purification are developing steadily but it almost remains same in actual affected fields. In India, one of the main sources for domestic, industrial, agricultural and other purposes is the ground water. The ground water pollution with hazardous anions like fluoride, arsenate specifically and other anions like nitrate, phosphate, sulphate, chromate etc. is a major issue that causes various adverse health effects. Many domestic purification processes are there in application, but not exactly applicable in rural area due to many factors like regular maintenance, cost and non-availability of electricity. So there is a huge research gap between technology available for water purification and its field application in actual affected area. In this project two specific ions fluoride and anions of arsenic are targeted for its removal from water environment.

This dissertation focuses on the remediation of the above-mentioned anionic pollutants by designing suitable materials. Various techniques were applied for the removal of these anionic contaminants so far. Among them adsorption techniques with suitable adsorbent has been an efficient method.

In this present research work, four different types of materials have been synthesized for adsorption of arsenic and fluoride from contaminated water separately. In the first project, we have prepared Fe-Al

6mixed oxide nanoparticle by precipitation method which was used as an adsorbing material to remove fluoride from synthetic aqueous solution. The results revealed that the Fe-Al mixed oxide nanoparticle results better affinity towards fluoride. The maximum adsorption capacity of the material for fluoride was found to be 103.9 mg g^{-1} with the optimum condition. (0.08 g of the adsorbent, pH 7 and temperature of 40°C). The experimental data are best fitted with Freundlich adsorption isotherm. The pseudo 2^{nd} order kinetic model described the kinetics of adsorption process. In the same direction, in the second project, Chitosan encapsulated magnetic nanoparticle modified was synthesized via co-precipitation method and applied for de-fluoridation of water by adsorption. Experimental results showed that the

prepared material works very well for practical purpose. The magnetic chitosan nano particle acts as a good adsorbent for fluoride ions due to interesting interactions of fluoride with amino functionalized Iron. The pseudo 2^{nd} order kinetics is best fitted to the adsorption with a maximum removal capacity of 33.62 mg g^{-1} calculated from Langmuir isotherm model. In third project, Lanthanum incorporated Zirconium Phosphate mesoporous material was synthesized for remediation of fluoride by precipitation by followed by hydrothermal treatment. The mesostructured Zr-P compounds showed greater removal efficiency due to higher specific surface area. The maximum adsorption capacity of the material for fluoride was 83.90 mg g^{-1} with the optimum condition at adsorbent dose of 0.2 g, pH 6 and temperature of 60°C. The adsorption process was best suited to Langmuir adsorption isotherm model and the pseudo 2^{nd} order kinetic model. In the fourth part of this work, Mg/Fe/carbonate layered double hydroxide was prepared for arsenic decontamination by simple precipitation method followed by heat treatment. Presence of the inter layer anions between two cationic layers, facilitates the ion-exchange mechanism for efficient As(V) removal. The maximum removal of arsenic was 271.00 mg g^{-1} at the optimum condition of 0.1 g of the adsorbent, pH of 7. The equilibrium data of As(V) were best described by Langmuir adsorption isotherm model and kinetics of adsorption followed the pseudo 2^{nd} order kinetic model. To check the role of flow rate, initial concentration and bed volume on adsorption of fluoride ions using synthetic aqueous solution, fixed bed column study was conducted. The mechanism of adsorption process were studied by using analytical methods like SEM, EDX, TEM, XRD, FTIR, TGA-DSC and BET surface area before and after treatment. All the results suggested that the above said materials have a strong and specific affinity towards the anionic contaminants, and can be considered as excellent material for treatment of real contaminated water system.

Keywords: Hazardous anions; adsorption; Fluoride; Arsenic; Mixed oxide; magnetic nano particle; mesoporous; LDH.

Contents

Chapter 1

Introduction

This chapter discusses the background of the problem under study in the is work focusing on the problem associated with drinking water and different treatment technologies. A brief overview of adsorption process is also reported. The chapter subsequently presents detailed literature review on different techniques of fluoride and arsenic removal from drinking water.

1.1 Background of the Study

Industrialization along with the urbanization results in rapid deterioration of water quality. The effluents discharged from various process industries viz., textile, leather, paint etc. composed of toxic and hazardous material. The development of industries without a consistent growth in pollution control mechanisms is resulting in a gradual deterioration of water quality.

Water is vital natural resource for sustainment of life and environment that is always believed to be available in great quantity as free gift from nature. However, the suitability of water for industrial, domestic or agricultural purpose depends on its chemical composition. Fresh water occurs as groundwater and surface water. In spite of the fact that groundwater is just 0.6% of the general water assets accessible on earth, it is the fundamental and the most supported wellspring of savoring water provincial and urban regions, primarily in the creating nations like India, as decontamination is not usually necessary. But in the period of this economic growth, groundwater sources are being polluted because of urbanization and industrial developments.

The increasing urbanization, population, unskilled utilization and industrialization of water resources have resulted in deterioration of water quality in the developing countries over the past few years. Several ecological factors such as either anthropogenic or natural are responsible for ground water pollution. The groundwater source is getting contaminated due discharge of liquid and solid hazardous industrial wastes, deep percolation by cultivation, disposal of sewage etc. Groundwater also undergoes various geological reconstructions resulting in adulteration of shallow aquifers (*Anwar, 2008*).

Contamination of ground water with numerous hazards like arsenic, fluoride, pesticides, sulfate, nitrate and other heavy metals and so on has been accounted for from different parts of India. In some instants, other than human consumption, the water sources have been found hazardous for irrigation and industrial needs (*Ankumah et al. 2005; Mulligan et al. 2001*). Therefore, considering all the related issues, more prominent consideration is required on the future impact of water resources planning and advancements. Arsenic and fluoride are the major inorganic contaminations of normal inception present in groundwater in India. In this

work, adsorption by different Medias is adopted for removal of arsenic and fluoride from drinking water.

1.2 Sources of Fluoride and Arsenic in water and their toxicity

1.2.1 Fluoride

Fluorine is an exceptionally reactive material and found normally as CaF_2, which is a fundamental constituent in minerals like fluorite, cryolite, chlorapatite, fluorapatite, phosphorite, topaz and so forth. *(Maheswari et al. 2001)*. Though drinking water is the principle cause (75~90% of daily intake) for fluoride contamination. The fluoride is available in the atmosphere, soil and water, which enters the soil by precipitation or waste run offs and enduring of rocks. Large amount of surface water contains fluoride not more than 0.3 mg L^{-1} of except if it gets polluted from outside sources. Despite the fact that drinking water is the principle cause (75– 90% of day by day allow) for poisoning due to fluoride, drugs, industrial exposure, nourishment, cosmetics, are also reported to be other media of fluoride poisoning *(Meenakshi et al. 2004)*.

Fluoride upto certain concentration is a necessary element for mineralization of bones and construction of dental enamel *(Bell et al. WHO, Geneva, 1970).* However, excessive intake of fluoride causes slow, progressive crippling scourge recognized as fluorosis. The countries which are endemic for fluorosis are India, Syria, Saudi Arabia, Libya, Morocco, Jordan, Algeria, Turkey, Egypt, Iraq, Sri Lanka, Tanzania, Iran, S. Africa, Kenya, Japan, Thailand, New Zealand, Canada, Australia, USA, Argentina, Persian Gulf, China etc. (*Mameri et al. 1998*).

In many regions of the world, health hazards related to fluoride are main environmental issue. Studying survey uncovers that, India is likewise influenced by medical issue caused because of utilization of fluoride polluted water. Odisha is found to be one of the 17 epidemic states for fluorosis in India. 10 of 30 districts in Odisha are reported to have excess of fluoride contamination in ground water. Following table shows fluoride concentrations in different states of India (Table1.1)

Table 1.1: Fluoride concentrations in different states of India *(A.K. Susheela, 1999)*

Name of the States	**Regions/ Districts**	**fluoride concentration range in** mg L^{-1}
Assam	Nagaon, Karbianglong	0.2 - 18.1
Odisha	Dhenkanal, Phulbani, Koraput, Nuapada	0.6 - 5.7
Delhi	Alipur, Najafgarh, Kanjhwala,	0.4 - 10.0
Bihar	Paschim, Palamu, Gridh, Rohtas, Gopalganj, Daltonganj, Champaran, Gaya	0.6 - 8.0
Haryana	Gurugram, Bhiwani, Karnal, Rewari, Faridabad, Rohtak, Mohindergarh, Sonipat, Jind, Kurukshetra, Hisar, Sirsa, Kaithal,	0.17-24.7
Maharashtra	Yavatmal, Akola, Bhandara, Jalgaon, Nagpur, Amravati, Chandrapur, Nanded, Sholapur, Bulduna	0.11-10.2
Jammu & Kashmir	Doda	0.05-4.2
Punjab	Amritsar, Jallandhar, Mansa, Muktsar, Faridcot, Bhatinda, Moga, Patila, Sangrur, Ludhiana, Fatehgarh sahib, Ropar, Ferozpur,	0.44-6.0
Kerala	Palghat, Allepy, Vamanapuram, Alappuzha	0.2-2.5
Madhya Pradesh	Sehore, Shivpuri, Dindori, Jabua, Mandla, Dhar, Chhindwara, Vidhisha, Bhopal, Raisen and Seoni	0.08-4.2
Gujarat	All districts except Dang	1.58-31.0
Karnataka	Mysore, Bijapur, Dharwad, Tumkur, Manya, Gadag, Banglore, Chikmagalur, Bellary, Gulbarga, Belgam, Raichur, Chitradurga	0.2-18.0
West Bengal	Bhardaman, Birbhum, Bankura	1.5-13.0
Uttarpradesh	Raibareli, Mathura, Allahabad, Unnao, Agra, Meerut, Aligarh	0.12-8.9
Andhra	All districts except Visakhapattnam, Srikakulam,	0.11-20.0

Pradesh	West Godhavari, Vijzianagaram, Adilabad, Nizamabad,	
Tamilnadu	Virudunagar, Dharampuri, Coimbatore, Periyar, Salem, Vellore, Madurai, Tiruchirapalli	1.5-5.0
Rajasthan	All the 32 districts	0.2-37.0

Maximum contamination level (MCL) and health effects of fluoride

Fluoride is a vital micronutrient for both animal and human. Consumption of drinking water fills more than 60% of fluoride demand of our body. Consumption and concentration of total fluoride amount in drinking water decides it's beneficial or detrimental effects on our body. According to (*WHO, 1993*) guidelines, fluoride concentration > 1.5 mg/L in drinking water has adverse effect on human health. A few reports and studies established both the danger of high fluoride dosing and the advantages of nominal exposure. The risk of minimal exposure and high fluoride dosing resulting inhibiting dental caries and permanent dental and skeletal fluorosis respectively are described in several reports.

Maximum contamination level (MCL) of fluoride in drinking water is 1.5 mg L^{-1}. It is found that high fluoride content in ground water is favored by high bicarbonate alkalinity and low calcium concentration. Generally, water having higher concentration of fluoride exhibits high pH and high concentration of silica. The ground water containing natural concentration of fluoride is affected by the following factors (a) geological characteristics (b) the acidity and porosity of the rocks and soil (c) temperature (d) contamination due to other chemicals. As a result, the fluoride concentrations ranges from below 1.0 to above 35.0 mg L^{-1}.

Fluorine is a very electronegative component and has high affinity to get pulled in by positively charged calcium ions. The mineralized tissues of bone and teeth have highest amount of calcium; thus, fluoride gets accumulated as calcium fluorapatite crystals on these tissues resulting in developmental alternations. Most of the ingested fluoride gets combined with the apatite crystal lattice of calciferous tissue enamel forming fluorapatite. As fluorapatite is more stable than hydroxyl apatite present in tooth enamel, the hydroxyl ion gets substituted by fluoride ion. The fluoride intensity isn't just subject to fluoride content in water yet additionally on some different sources like dietary habits and

physical activity. The different types of fluorosis arising because of excessive intake of fluoride are presented in Table 1.2.

Table 1.2: Health effects of fluoride *(Choubisa et al. 1996)*

Concentration of Fluoride in (mg L^{-1}**)**	**Remark**
<1.5	Safe
1.5 – 3.0	Dental fluorosis
3.0 – 4.0	Stiffened and weak bones and joints
4.0 – 6.0 and above	Paralysis due to deformities in hip bones and knee

Dental fluorosis

The inordinate admission of fluoride influences lacquer to lose its shine. In mellow shape, dental fluorosis is sorted by serious setting of the teeth, yellowish dark colored to dark stains, white and hazy territories on the tooth surface.

Skeletal fluorosis

Both children and adults are affected by skeletal fluorosis and cannot easily diagnosed until it reaches an advanced stage. Fluoride gets accumulated mainly in the joints of neck, knee, shoulder and pelvic bones results in hard to walk and move. The symptoms are arthritis, bending of bones and spondylitis. The excess ingestion of fluoride leads to low hemoglobin and muscle fibre degeneration.

1.2.2 Arsenic

Arsenic [As (III) and As (V)] is found in all segment of the environment mainly within the superficial zones of groundwater of many countries like Canada, Hungary, Mexico, Mongolia, Argentina, Germany, Bangladesh, Thailand, India, Chile, Pakistan, Nepal, China, Cambodia, USA, Vietnam, Romania, Myanmar, etc. with varing concentrations. In some places of Bangladesh the arsenic concentration is reported to be as high as 1mgL^{-1} *(Harvey et al. 2002)*. Usually arsenic is found to be associated with the contaminants like sulfate, chloride, bicarbonate, magnesium, calcium and iron. Arsenic is highly toxic and is

generated as waste byproducts of dyes, glassware, pesticides and other chemical industries, which are discharged to water bodies and other segments of environment.

Arsenic fits in to the metalloid group and co-exists with Cu, Zn, Ni, Fe etc., as oxide or sulfide ores. Arsenic can be converted from one form to other as it can't be destroyed. Arsenic in aqueous oxic environments is present as arsenate [As(V) as H_3AsO_4, $H_2AsO_4^{-1,}$ $HAsO_4^{-2}$ and AsO_4^{-3}] and anoxic environment is present as arsenite [As(III) as H_3AsO_3 and $H_2AsO_3^-$] *(Oremland et al. 2003)*. Arsenic usually found in more than two hundred different mineral forms consisting 20% sulfides, 60% are arsenates, and sulfosalts; the rest 20% comprises arsenites, elemental arsenic (As), silicates, oxides and arsenides.

The sources of arsenic contamination in ground water are:

i. ***Natural*** *(Leist et al. 2000)***:**

Dissolution of arsenic adsorbed onto the pyrite ores in water by bio geo chemical geo hydrological and geothermal factors.

ii. ***Anthropogenic*** [*(Leist et al. 2000)*, *(McNeil et al. 1997)*]:

a. processing of ores such as Cu, Au, Ni, Pb, and Zn.

b. constituents of many herbicides and insecticides.

c. wool and cotton processing.

d. wood preservative (arsenic based)

e. feed additives (mining and metal alloys)

f. seepages (hazardous waste sheet)

g. areas near cemeteries (arsenic is used as embalming fluid)

h. power generation (burning of arsenic contaminated coal)

i. glass manufacturing and semiconductor

It is found that the arsenic concentration in drinking water (river water) increases when contaminated by geothermal, industrial or mining waste. The highest arsenic concentration was reported to be 85 mg/l from an acid seep in the Richmond mine at Iron Mountain, California *(Nordstorm et al. 1999)*. The ground water arsenic concentration is

dependent on factors like (a) thick clay barrier surrounding the aquifer, (b) depth of tube well (c) presence of large concentrations of phosphate or silicate etc. The mobilization of arsenic in aqueous phase is affected by adsorption affinities of arsenic on common metal surfaces like ferrihydrite, alumina etc. *(Banga et al. 2005)*.

Maximum contamination level (MCL) and health effects of Arsenic

Presence of arsenic in high concentration (> permissible limit) has large impact on humans, animals and plant health. The consequences of arsenic poisoning are skin or lungs cancer, white or dark spot on the skin, hardening of skin, kidney cancer and breakdown of central Nervous System (CNS). Due these adverse health effects of arsenic, the maximum allowable level of arsenic by WHO is of 0.01mg/L in drinking water (*WHO, 2001*).

The maximum contamination level of arsenic in various countries is shown in Table 1.3.

Table 1.3: Arsenic poisoning scenario for drinking water in various countries

Name of the Country	**Permissible national limit (mg/L)**	**Reference**
Bangladesh	0.05	*Harvey at al, 2002*
India	0.05	*Bhattacharjee et al. 2005*
Pakistan	0.05	*Nickson et al. 2005*
Taiwan	0.05	*Bhattacharjee et al. 2005*
China/Mongolia	0.05	*Bhattacharjee et al. 2005*
USA	0.01	*Bhattacharjee et al. 2005*
Germany	0.025	*Bhattacharjee et al. 2005*
Vietnam	0.05	*Berg et al. 2005*
Japan	0.01	*Bhattacharjee et al. 2005*

Toxicity order of arsenic is: AsH_3 (arsine) > As(III) (inorganic) > As(III) (organic) > As(V) (inorganic) > As(V) (organic) > AsH_4^+ (arsonium) compounds and elemental arsenic. The effect of arsenic on human health effect can be classified as sub-acute (can be alterable), acute and chronic effects. Chronic poisoning is caused due to arsenic ingestion for a longer

period while subacute and acute poisoning is caused due to ingesting of arsenic polluted water in large quantity for shorter period of time. The disease is commonly called Arsenocosis *(Abdul et al. 2015)*.

The symptoms of Arsenocosis are swelling of the eyelids, feet and hands, abdominal pain, diarrhea, vomiting, skin rashes and muscular pain. Effects of arsenic poisoning on heart, lungs, and kidneys can be fatal. After prolonged exposure of arsenic, hematological effects including anemia and leukemia or breakdown of central nervous system may occur *(Yoshida et al. 2004)*. At the exposure of arsenic (0.005~0.01mg L^{-1} Kg^{-1} day^{-1}) in drinking water our skin gets affected by pigmentation and hyperkeratosis (*Abdul et al. 2015)*.

1.3 Processes for the separation of Fluoride and Arsenic from contaminated water

The primary technique for the remediation of inorganic pollutants from waste waters are briefed in Table1.4.

Table 1.4: Description of methodology for removal of inorganic contaminants

Methodology	Description	References
Precipitation	A precipitate is formed by addition of a reagent with the solution of chemicals which is to be removed. Then the precipitate is separated by filtration, sedimentation, and/or flocculation process. The sludge produced is considered as hazardous material due to presence of high amount of contaminant results in increasing the cost of the method.	*Matlock et al. 2001* *Matlock et al. 2002* *Hu et al. 2005* *Turner et al. 2005* *Huisman et al. 2006* *Blue et al. 2008* *Blue et al. 2010* *Li et al. 2010* *Drouiche et al. 2012*
Ion-exchange	Anion from the solution to be removed is replaced with another ion present in an immobile solid phase called ion exchanger. When it becomes exhausted it can be regenerated by the	*Korngold et al. 1996* *Feng et al. 2000* *Ruixia et al. 2002* *Zhao et al. 2002* *Oehmen et al. 2006*

	appropriated solutions.	*Meenakshi et al. 2007* *Meenakshi et al. 2009* *Virolainen et al. 2014* *Nikoloski, et al. 2015* *Zewail et al. 2015*
Membrane filtration	This process is quite costly in terms of installation, operation and membrane degradation. The process does not require additives having advantage of transport selectivity of the membrane. Eg. electro-dialysis, nano-filtration, dialysis and reverse osmosis	*Bhandare et al. 2002* *Qdais et al. 2004* *Hu et al. 2006* *Tahaikt et al. 2007* *Kabay et al. 2008* *Sehn et al. 2008* *Algarra et al. 2014* *Cui t al, 2014* *Mehdipour, 2015* *Stajcic, et al. 2015* *Zhu et al. 2015* *Aftab et al. 2017* *Iben Nasser et al. 2016*
Adsorption	It might be characterized as variety in concentration of a part in the surface layer in examination with the bulk phase identified with unit surface zone by including interface collection of substances at an interface in which the mass exchange occurs by physical and chemical interactions.	*Cobelo-Gracia et al. 2007* *Li et al. 2011* *Gong et al. 2012* *Tomar et al. 2014* *Arce et al. 2015* *Cai et al. 2015* *Madrakian et al. 2015* *Yari et al. 2015* *Zhang et al. 2015* *Elwakeel, 2013* *Lopez-Munoj et al. 2016*

Fluoride

The process of defluoridation may be defined as removal of fluoride from drinking water. Industrial affluent and excess of fluoride from drinking water can be removed by different

treatment methods like (a) precipitation, (b) ion exchange, (c) electrolysis, (d) membrane and adsorption process. In adsorption process fluoride contaminated water passes through a contact bed and fluoride is separated by surface chemical reaction or ion exchange. Removal of fluoride is tested by different adsorbents such as waste carbon slurry *(Gupta et al. 2007),* trimetal oxide *(Yang et al. 2007)* and many low-cost materials *(Simurali et al. 1998)*. Different fluoride removal techniques based on advantages and disadvantages are summarized in Table 1.5.

Table 1.5: Advantages and dis advantages of different fluoride removal Techniques

Techniq ue	**Adsorption**	**Ion Exchange**	**Coagulation-Precipitation**	**Membrane Process**
Remarks	**Adsorbents:** calcite, activated saw dust, activated alumina, activated coconut shell carbon and activated fly ash, activated carbon, soil sorbent, rice husk, bone charcoal, activate etc.	basic anion exchange resin with ammonium functional group	**Nalagonda technique:** precipitation by lime followed by addition of alum for coagulation.	NF and RO is generally used for fluoride removal
Advanta ge	Cost effective and removes fluoride upto 90%.	Removes fluoride up to 90–95%. Holds the colour and taste of water intact.	Most effective technique approved by NEERI under **Rajiv Gandhi Drinking Water Mission**. Realtime application in rural areas.	highly effective, No chemicals required, fuctions at wide range of pH, no effect of competitive ions
Disadvan tage	The removal is highly affected by competition of carbonate,	Expensive due to cost of resin, efficiency decreases in	adverse effect of silicates on defluoridation, erroneous, removes only a	is expensive compared to other options

	phosphate or sulfate.	presence of other ions.	lesser percentage of fluoride precipitates (18~33%) and converts ionic fluoride into soluble aluminum fluoride complex ion	

Arsenic

Removal of arsenic from waste water and drinking water are done by various techniques such as ion-exchange and reverse osmosis (*Clifford, 2006*), coagulation and precipitation with iron and aluminium salts *(Hering et al. 1996), using* iron oxide coated sand *(Joshi et al. 1996)*, adsorption onto activated alumina, manganese dioxide coated sand *(Bajpai et al. 1999)*, activated carbon and activated bauxite *(Gupta et al. 1978)*, oxidation and adsorption by green sand filtration *(Christen, 2000)*, zero-valent iron *(Fendorf et al.1997),* ferruginous manganese ore *(Chakravarty et al. 2002)*, ferrihydrite *(Jain et al. 1999)* and clay minerals *(Manning et al. 1997)*. The techniques of precipitation coagulation, adsorption by activated alumina are found to be inefficient for removal of As (III) and As (V) due to use of external oxidizing agent that detoriate the water quality *(Krishna et al. 2001)*.

In perspective of past exchange, it is clear that As(III) removal is preferred by oxidation from As(III) to As(V) followed by adsorption on to adsorbent. Comparison of conventional processes of arsenic removal is summarized in Table 1.6.

Table 1.6: The comparison amongst the conventional processes *(Kartinen et al. 1995)*

Process	**Removal efficiency (%)**	**Advantages**	**Disadvantages**
Precipitation with alum	20 – 90%	suitable for domestic use	highly influence the removal efficiency is affected by highly contaminated oxidizing chemicals
Precipitation with iron	60 – 90%	Reliable	highly influence the removal efficiency is influenced by high dose of oxidizing chemicals
Precipitation	40 – 90%	Reliable	Variation of pH reduces removal

with iron/ manganese			efficiency; highly influence the removal efficiency is influenced by high dose of oxidizing chemicals
Lime softening	0 – 90%	reliable and reduces corrosion	removal efficiency is influenced by sulphate ions and needs secondary treatment
Reverse osmosis	≥ 90%	Removes dissolved salts, minerals; turbidity; Highest water quality	Expensive to install and operation; membrane corrosion
Electro dialysis	≥ 95%	Pure quality water	needs oxidizing agents and costly
Ion exchanges	≥90%	treat water with As concentration less than 2 μgL^{-1}	Presence of nitrates, sulfate, TDS, fluorides ions, selenium, etc. affects efficiency
Adsorption in activated alumina	≥ 90%	suitable for domestic use; inexpensive; improves test and odour	bacteria may grow on alumina surface; Careful monitoring required.
Adsorption on activated carbon	30 – 90%	Inexpensive; improves test and odour	Efficiency affected by the metal concentration and ash content in the carbon.

The above mentioned methods other than adsorption used for removal of arsenic and fluoride are not widely affected due to cost and maintenance of process, so adsorption is developing as beneficial method for decontamination of arsenic and fluoride hazardous ions Removal of arsenic and fluoride in aqueous solution is favored by adsorbents containing iron compounds. Recycling, conservation of resources and environmental protection are now the demanding situation due to increase in amount of wastes in environment.

1.3.1 Adsorption

Adsorption is defined as deposition of adsorbate (solid/ gas) on the surface of adsorbent (solid) used to eliminate the contaminants from liquid phases *(Kammerer et al. 2011), (Worch et al. 2012)*. Schematic description of adsorption process and the components involved in this procedure are shown in Figure 1.1. By changing the circumstances of the

system, such as concentration, pH, temperature, the adsorbate can be released to the liquid phase again, known as desorption.

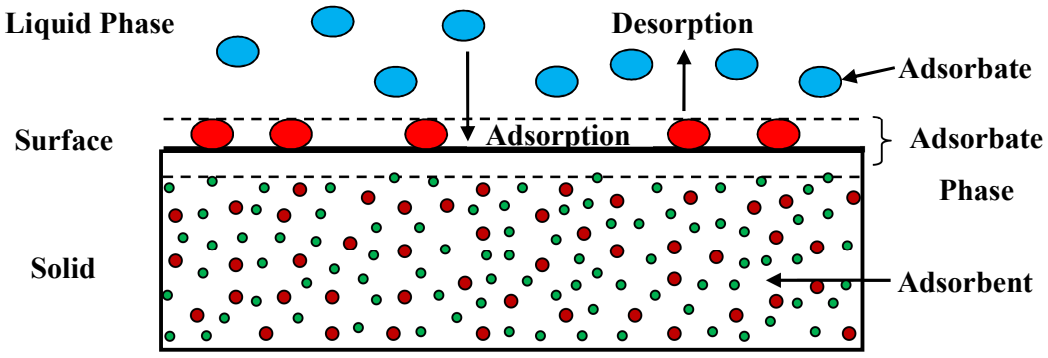

Figure 1.1 Schematic description of adsorption

Characteristics of adsorption

Adsorbents are classified on the basis of their chemical and physical resistance matrix composition, density, polarity, surface area, the pore radius distribution, porosity and particle size distribution.

Adsorption in water treatment

Contrary to the method of separation such as precipitation, that generates hazardous sludge. Adsorption processes does not generate any undesirable byproducts while treatment of contaminated water. Due to simplicity of design and operation, adsorption is established as a better process for water treatment *(Lafrano et al. 2012)*.

The adsorption takes place in following three steps *(Mohapatra et al. 2009)*

i. contaminant diffusion from solution to surface of adsorbent
ii. adsorption on the adsorbent surface
iii. transportation of the pollutants within the adsorbent due to elemental exchange with elements present in adsorbent.

While designing a suitable adsorption process, the main aspect considered are *(Oller et al. 2011), (Zhang et al. 2010)*

i. initial concentration and nature of adsorbate
ii. pH
iii. temperature

iv. interfering ions
v. specific surface area
vi. dose of adsorbent
vii. cost-effectiveness

1.4 Scope of Study

In this thesis, research has been focused on the synthesis of various adsorbent medias like mixed metal oxide nano particles *(Waghmare et al. 2015)*, hybrid materials of metal oxide nanoparticles *(Philips et al. 2018)*, mesoporous materials *(LI et al. 2011)* and layered double hydroxides (LDH) *(Ge et al. 2013)*.

1.4.1 Adsorbents used for removal of Fluoride and Arsenic

The aim of our research is to develop effective adsorbent materials for remediation of fluoride and arsenic from water. Among various materials applied for fluoride and arsenic adsorption, iron, aluminium, zirconium, lanthanum and magnesium are most popular. The adsorbent materials prepared using these elements are most effective for treatment of these anionic hazards due to it's stability in water without shrinking, high surface area and porosity, swelling or softening, *(Serbezov et al. 2011)* and low solubility in extensively PH range *(Kim et al. 2004)*.

In First part, Iron-Aluminium mixed oxide nano particle, in second part Chitosan modified magnetic nano particle, in third part Lanthanum doped Zirconium phosphate mesoporous material, in last part Magnesium- Iron layered double hydroxide were selected all these elements used have strong affinity towards fluoride as well as arsenic.

Iron-Aluminium mixed oxide nano particle

Iron-based adsorbents have been extensively reported to exhibit the highest adsorption capability towards As while aluminium-based adsorbents have been shown to have affinity towards F *(Ku et al. 2002), (Prathna et al. 2017)*. Few studies have been carried out exploring the efficacy of iron and aluminium-based binary oxides and hydroxides for the simultaneous removal of F and As *(Qiao et al. 2014), (Liu et al. 2012)*.

The possible mechanism of anion adsorption can be demonstrated by the reaction under

mentioned in Figure 1.2.

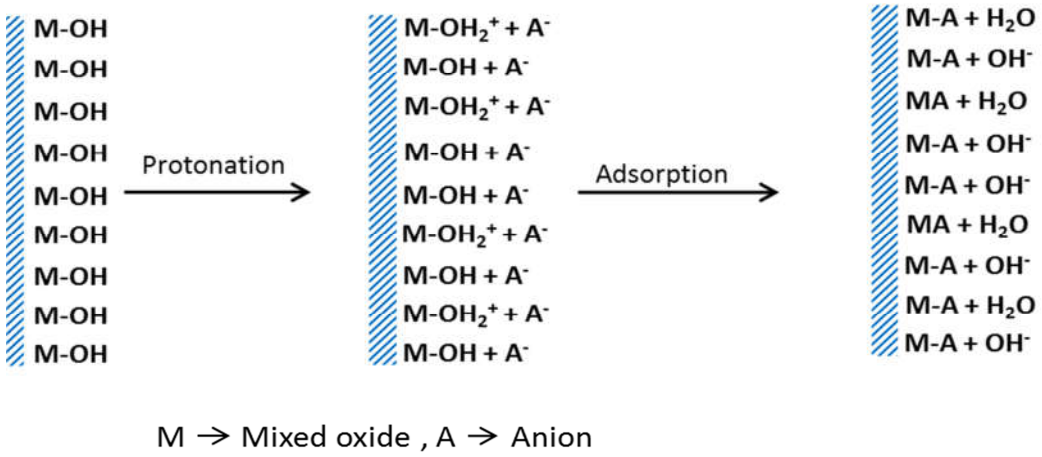

Figure 1.2 Schematic diagram of possible anion adsorption reaction by mixed oxide materials *(Lu et al. 2013)*

Magnetic chitosan nano particle

Chitosan derivatives, prepared by chemical and physical modifications, cross-linking, modifying its physical structure, immobilizing it on insoluble supports, or impregnating it with metals, are applied as fluoride and arsenic removing agents. Nanochitosan (*Kwok et al. 2014*), zero valent iron encapsulated chitosan (*Gupta et al. 2012*), mixed metal oxide impregnated chitosan beads (MICB) (*Yamani et al. 2012*), TiO_2-impregnated chitosan bead (*Miller et al. 2010*), aluminum and doping chitosan–Fe(III) hydrogel (*Ma et al. 2014*), and chitosan complexed with transition metalions (*Shinde et al. 2013*)were used to remove arsenic and fluoride.

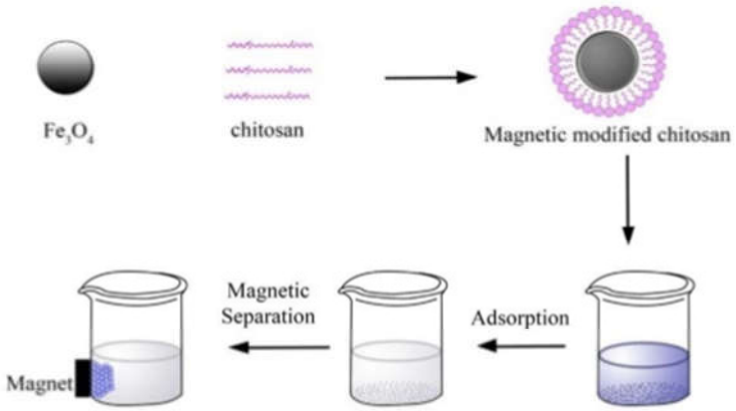

Figure 1.3 Synthesis route and application of magnetic chitosan nanoparticle for removal of anions *(Chang et al. 2006)*

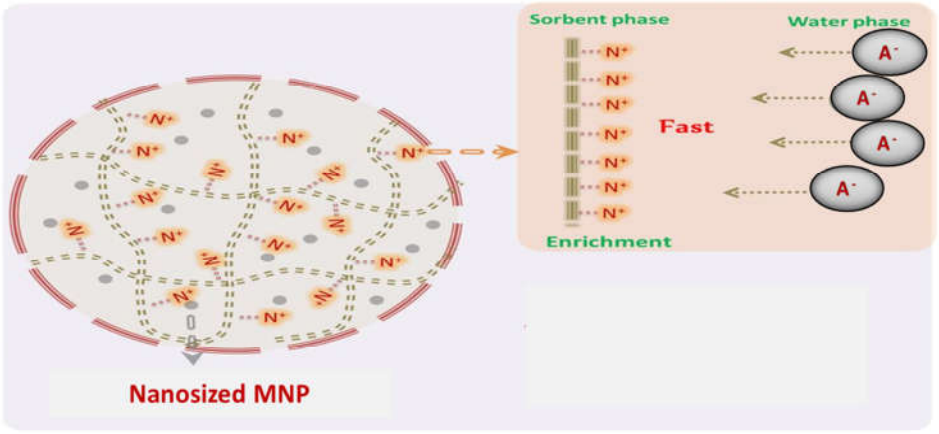

Figure 1.4 Possible mechanism of anion removal by magnetic chitosan *(Chang et al. 2006)*

A detailed diagram of synthesis and mechanism of removal procedure of anions by magnetic chitosan nanoparticle is given in Figure 1.3 and Figure 1.4 respectively.

Zirconium phosphate mesoporous compounds

Porous materials are important due to high adsorption capacities *(Bian et al. 2009), (kim et al. 2004)*. Favorable features of this material for removal of arsenic and fluoride are narrow pore-size distributions, large surface areas and highly uniform channels. For removal of the anions, commercial zirconium phosphate may be used as adsorbent material due to its high affinity, large-scale production and selectivity *(Song et al. 2011)*.

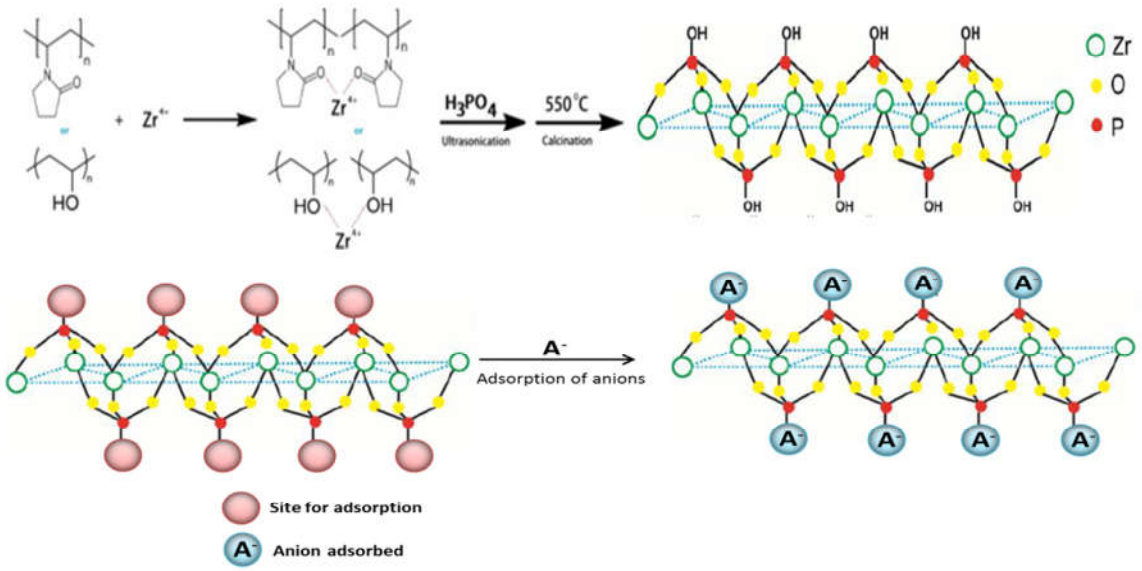

Figure 1.5 Possible mechanism of anion removal by magnetic chitosan *(Hajipour et al. 2014)*

Synthetic procedure and and probable mechanism for anion adsorption on Zirconium phosphate surface is demonstrated in Figure 1.5.

Magnesium-Iron layered double hydroxide

Layered double hydroxide (LDH), also termed as hydrotalcite like (HTLC) compounds or anionic clays are of great importance due to vast application in adsorption, catalysis, biotechnology and nanotechnology. The general formula of LDH can be described as $[M_{1-x}^{2+}M_x^{3+}(OH)_2]^{x+}(A^{n-})_{x/n}.mH2O$, where M^{2+} and M^{3+} is divalent (Mg^{2+}, Zn^{2+}, Ni^{2+}, Fe^{2+}, Cu^{2+}, etc.) and trivalent cation (Al^{3+}, Mn^{3+}, Fe^{3+}, Cr^{3+}, etc.) in octahedral positions of brucite-like layers *(Tadanaga et al. 2010)* respectively. A^{n-} is interlayer anions (CO_3^{2-}, NO_3^-, Cl^- etc.) located in the interlayer space between two brucite sheets *(Han et al. 2010), (Shao et al. 2012)*, and x is $M^{3+}/M^{2+} + M^{3+}$ ratio with various values between 0.17 and 0.5. Due to large surface areas (20~120 m^2/g) and high anion-exchange capacities (3.0~4.8 meq/g), LDH and its calcined products can be considered as potential adsorbents for removal of hazardous anions from aqueous media *(Zhao et al. 2010), (Chen et al. 2011), (Xu et al. 2010)*.

The schematic synthetic procedure and possible removal mechanism has been illustrated in Figure 1.6 and Figure 1.7 respectively.

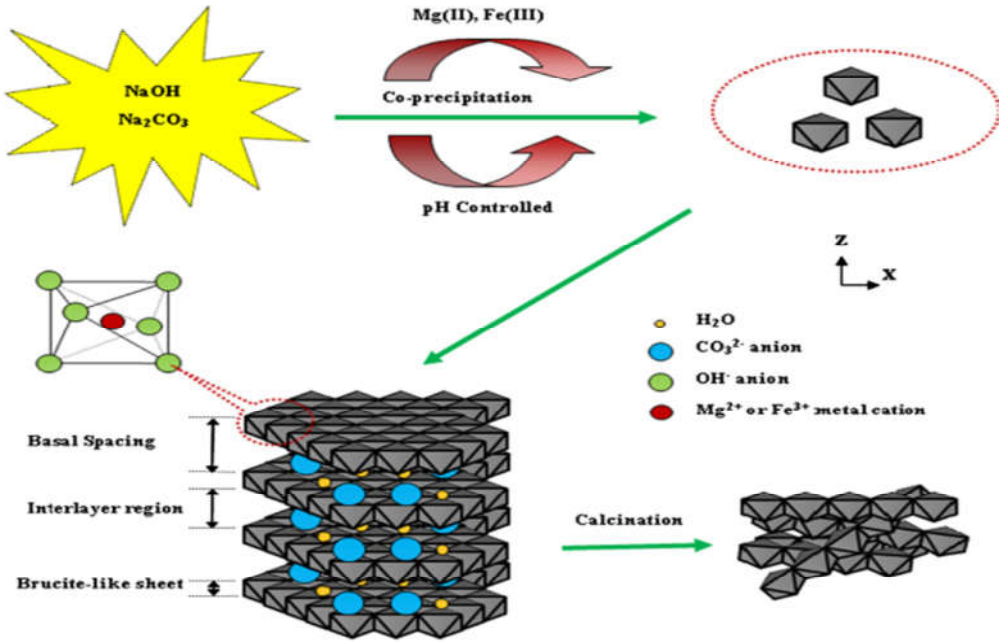

Figure 1.6 Synthesis of (Mg/Fe) LDH*(Kang et al. 2014)*

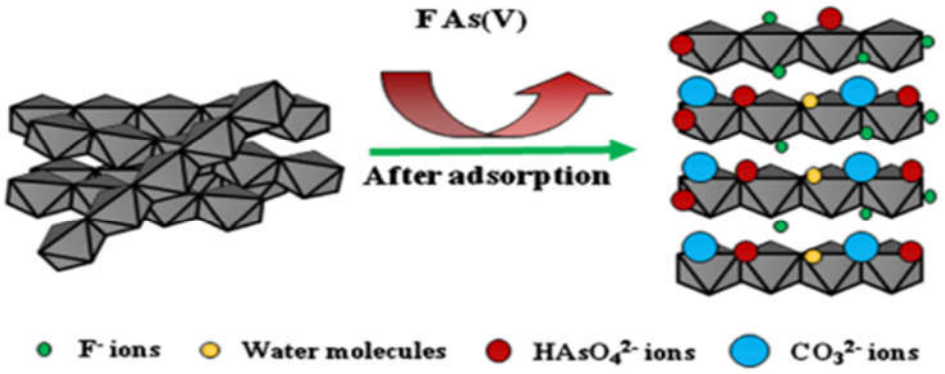

Figure 1.7 Possible mechanism of anion removal by LDH *(Kang et al. 2013)*

1.5 Organization of Thesis

The present thesis is sorted out into eight chapters. The current chapter (**Chapter-1**) gives an overview of the problem undertaken in this work i.e. the problem associated with the presence of fluoride and arsenic in water. A brief overview of adsorption-based separation processes is discussed in this chapter. It also discusses the features of different techniques and different adsorbent materials used for the treatment of fluoride and arsenic contaminated water. A comprehensive literature review on synthesis of different adsorbent materials by different wet chemical method and their application for adsorption of negative anions from aqueous solution are presented in **Chapter-2**. **Chapter-3** represents the principle and experimental procedure adopted for preparation and characterization of adsorbent and batch mode as well as column mode removal of the adsorbate. **Chapter-4** discusses the characterization of Fe-Al mixed oxide rod shaped nanoparticle synthesized via precipitation technique and its application for remediation of fluoride from synthetic aqueous media. **Chapter-5** describes characterization of magnetic chitosan nanoparticle and their application towards adsorptive removal of fluoride aqueous solution. **Chapter-6** contains characterization of Lanthanum doped Zirconium phosphate (La-ZrP) mesoporous material and their application towards adsorptive removal of fluoride aqueous solution. In **Chapter-7**, the characterisation of Mg/Fe LDH and adsorption behavior of As(V) from aqueous media have been discussed. The conclusions the research work with highlighting the contribution are drawn in **Chapter-8**.

Chapter 2

Review of background literature

This chapter, reports detail survey of advancements in the region of synthesis and characterisation of various adsorbate compounds that are mentioned (Fe-Al mixe oxide nanoparticle, magnetic chitosan (Ch-Fe_3O_4) nanoparticle, La-ZrP mesoporous compound and Mg/Fe LDH) by various wet chemical process for example precipitation, co-precipitation, hydrothermal etc. All pertinent information as described in the literature has been reviewed thoroughly and exhibited in brief the knowledge of the research work. Further, the environmental application of these adsorbent materials such as adsorption hazardous anions by batch and column method has also been discussed.

2.1 Mixed oxide nanoparticle

2.1.1 Remediation of selected anions from aqueous media

Wu et al. (2008) prepared Fe-Al-Cetrimetal hydroxide with acrylic-styrene copolymer latex as binder for spray coating on sand for remediation of fluoride from drinking water. The stable coating of 75 μ was done by latex/Fe-Al-Ce ratio of 0.8 and its defluoridation capacity was 3.46 mg/g at pH7.0 and initial fluoride concentration of 50 mg/l. This sand coated Fe-Al-Ce adsorbent was used effectively in a packed bed column for defluoridation from drinking water.

Tang et al. (2009) used granular ferric hydroxide for defluoridation of water in batch study. Ionic strength did not affect equilibrium adsorption at the pH range of 2~11. The optimum pH range was 3~6.5 where maximum fluoride removal took place. The experimental data were followed both of pseudo 2nd order kinetic and Freundlich isotherm model. Desorption of fluoride was conducted at alkaline solution and 65% of fluoride release at pH of 7.0. The presences of co-anions affect the fluoride remedial efficiency in the order of $H_2PO_4^-$>HCO_3^->SO_4^{2-}>Cl^-.

Kumar et al. (2009) describe the fluoride remediation capacity of granulated ferric hydroxide (GFH) in batch mode from water. The adsorption process was rapid and 95% of adsorption was finished between 10 minutes and equilibrium was accomplished within 60 minutes. The maximum defluoridation capacity of GFH was 7.0 mg/g. The optimal pH range was found to be 4~8. The adsorption has followed the both Langmuir isotherm model and pseudo 2nd order kinetic model. The adsorption procedure was endothermic in nature. The co-anion was reduced the fluoride adsorption in order of phosphate > carbonate > sulphate. The adsorption process was occured by ion exchange mechanism.

Biswas et al. (2010) synthesized hydrous iron (III) –chromium (III) bimetal mixed oxide (HICMO) adsorbent for fluoride decontamination. The optimal pH for maximum fluoride adsorption was 3.0 and then adsorption declined in the pH range of 3~5. The adsorption followed the Langmuir isotherm model and pseudo 2nd order kinetic model. The maximum adsorption capacity of HICMO was 16.34 mg/g. The thermodynamic study revealed that the adsorption process was endothermic and spontaneous. The adsorption was

basically represented by an ion-exchange mechanism. The bicarbonate ions reduced the fluoride adsorption capacity strongly. 91% of desorption was achieved by 0.5M NaOH solution. The column breakthrough capacity of HIMCO at a flow rate of 1 to 2 ml/min was 7.47 mg/g. The HIACMO dose of 0.2 g/50 ml reduced the fluoride solution of 10mg/l to 1.5 mg/l.

Dou et al. (2011) used granular Zr-Fe oxide (GZI) comprised of nano-scale oxides particles and amorphous synthesized by extrusion method for fluoride decontamination. The maximum equilibrium adsorption capacity of GZI was 9.80 mg/g for fluoride solution (10mg/l) at pH of 7.0. The GZI performed well at pH of 6-8. The batch experiment data follow the pseudo 2^{nd} order kinetic model and Freundlich isotherm model. The Langmuir adsorption capacity of GZI was 22.82 mg/g at neutral pH and more than activated alumina (7.728mg/g at same pH). The bicarbonate ions were influenced by the defluoridation capacity of GZI whereas in presence of others co-anions adsorption was not affected. Toxicity characteristic leaching procedure (TCLP) leachability results revealed that spent GZI was not toxic and can dispose directly. The successful regeneration of GZI was done by 0.01M NaOH solution. The ground water was treated about 370, 239 and 128 bed volumes before breakthrough was accomplished under space velocity of 0.5, 1 and 3 h-1 respectively for fluoride concentration of 3.59 mg/l, pH of 8.3 and TOC of 7.6 mg/l.

Chen et al. (2011) studied the fluoride adsorption capability of iron impregnated granular ceramics (GC) from aqueous solution. The ceramic granules made by Kanuma mud, zeolite, starch and $FeSO_4.7H_2O/Fe_2O_3$ mixed at a ratio of 4:3:2:1 by granulation method at room temperature. The granular ceramic (GC) with $FeSO_4$ was more effective than the granular ceramic with Fe_2O_3. The optimum pH for GC with $FeSO_4$ and GC with Fe_2O_3 was 7.0 and 4.0 correspondingly. The adsorption followed both Langmuir and Freundlich isotherm models for GC with $FeSO_4$ and GC with Fe_2O_3. Both these adsorption processes showed thermodynamically spontaneous and endothermic in nature.

Chen et al. (2011) studied defluoridation capability of Fe-Al-Ce (FAC) trimetal oxides sprayed with acrylic-styrene copolymer latex onto glass beads. The maximum fluoride adsorption of 2.77 mg/g was found when the granules were covered at 65°C utilizing a latex/FAC proportion of 0.5:1 for 0.001M of initial fluoride concentration at pH

of 7.0 and a granule dose of 5g/l for adsorption time of 36 h. The Langmuir maximum adsorption capacity of adsorbent was found to be 5.9 mg/g.

Liu et al. (2012) used iron, iron oxyhydroxide (FeO*x*H*y*) and aluminum mixed oxide (FeAlO*x*H*y*) and aluminum oxyhydroxide (AlO*x*H*y*) for both simultaneous and competitive adsorption between fluoride and arsenate. Iron oxyhydroxide (FeO*x*H*y*) showed a high removal capacity toward arsenate (As (V)) than fluoride (F) especially at pH above 6.5 whereas aluminum oxyhydroxide (AlO*x*H*y*) showed good adsorption capability toward As(V) and F but maximum removal was found at weak acidic pH of 6.0. To overcome the drawback of pH and competition between As(V) and F, combine iron oxyhydroxide (FeO*x*H*y*) with aluminum oxyhydroxide (AlO*x*H*y*) to form iron and aluminum binary oxide (FeAlO*x*H*y*). In comparison to FeO*x*H*y*and AlO*x*H*y*, FeAlOxHy showed superior performance for simultaneously remove As (V) and F. The removal of fluoride by FeAlOxHy, AlO*x*H*y* and FeO*x*H*y*were 64.5%, 29.4% and 18.4% respectively.

Mohapatra et al. (2012) used Mg-doped nano ferrihydrite for defluoridation of water. The fluoride removal was increased from 66% to 91% when Mg doping on nano-ferrihydrite was varying from 0.39% -0.98%. The experimental results followed well with the Langmuir adsorption isotherm model. Highest defluoridation capacity of 0.98%. Mg-doped nano-ferrihydrate was 64 mg/g at optimum condition (temperature=30^{o}C, pH=5.75, dose=1g/l, initial fluoride concentration=30 mg/l and contact time=5h). The adsorption was endothermic in nature, spontaneous, and followed the pseudo 2nd order kinetic model and the adsoprion process. The presence of sulphate and chloride reduced the defluoridation efficiency from 91.2% to 53.8% and 72.5% as their concentration was enhanced from 5 to 50mg/l. Desorption of 89% was done by 1M NaOH solution.

Sanchez et al. (2013) examined the defluoridation efficiency of aluminum impregnated iron oxides in a fixed bed column for simulated water and drinking water. The experiment was carried out in borosilicate glass column of 9 mm diameter with fluoride solution of 4 mg/l at pH 6.4 for aqueous solution and at pH 7.4 for drinking water. The experiment was run for 2, 4 and 6 g of aluminum impregnated iron oxides with a bed depth of 3.5, 7 and 10.5 cm at flow rate of 1 ml/min. The column study observed that the maximum adsorption of 0.509 mg/g was obtained at bed height of 3.5cm and 2g of adsorbent after 254.3 minutes for aqueous solution whereas adsorption capacity of 0.296

mg/g was obtained at same condition after 148 minutes for drinking water. The pH of water was 7.2 and 7.3 for model solution and drinking water respectively. The experimental data of breakthrough curve was fitted well with bed depth service time (BDST) and Thomas, Bohart-Adams model.

Nur et al. (2014) used hydrous ferric oxide (HFO) for defluoridation of drinking water in both fixed bed and batch column experiments. The fluoride uptake of HFO was founded more than four anion exchange resins and three multivalent metal oxides. The adsorption data of HFO follow both the Langmuir and Freundlich models. The pHpzc of HFO was calculate to be 5.0. The maximum removal capacity of HFO was 6.71 mg/g at pH 6.5. Desorption of HFO was done by 0.1M NaOH. The column adsorption capacity of adsorbents (10% or 20% HFO + 90% or 80% anthracite) was observed to be 3.26 mg/g after three consecutive adsorption-desorption cycles. The breakthrough data of column experiment was described by Thomas model. The model capability is used to improve by artificial neural network.

Gitari et al. (2015) used Fe^{3+} mixed bentonite clay and raw bentonite for defluoridation of aqueous solution. He optimum loading was obtained at 30 min by mixing with 100 ppm of Fe^{3+} solution. The modified bentonite had a large surface area and micropore area than raw bentonite. The modified bentonite removed fluoride more efficiently than raw bentonite. The fluoride removal of ≈ 100% was achieved over wide pH range of 2-10 by Fe^{3+}-modified bentonite clay whereas raw bentonite released fluoride at alkaline pH > 10. The adsorption capacity of Fe^{3+}-modified bentonite clay was 2.91 mg/g. The experimental data follow the Langmuir isotherm model indicating a monolayer coverage of the adsorption. The Fe^{3+}-modified bentonite clay removed the fluoride from groundwater at neutral and optimum pH well below the WHO guidelines but pH of treated water was becoming acidic in nature (pH drops) and need pH adjustment. The Fe^{3+}-modified bentonite clay used effectively for treatment of borewell water with high fluoride concentration.

The subsurface soil, which is a complex blend of inorganic and organic materials, contains fluoride. So, the mixed oxides of some polyvalent metals found in subsurface soil can be a better adsorbent for fluoride and arsenic remediation from affected groundwater. As Fe^{3+} and Al^{3+} oxides are easily found in the earth crust, and have high bonding affinity with

fluoride and arsenic based on soft hard acid base (SHAB) idea; they can be considered to be good for fluoride and arsenic adsorption from aqueous media. On this premise, the present work has been attempted and this work reports (i) preparation of Fe(III)- Al(III) bimetallic mixed oxide, and (ii) study of fluoride and arsenic adsorption on the synthesized mixed oxide.

2.2 Magnetic chitosan nanoparticle

Magnetic nanoparticles can be easily separated from its solution by applied magnetic field *(Sharma et al. 2009; Mahmood et al. 2013).* Other than the magnetic properties, magnetic nanoparticles show high surface to volume ratios. Thus, the chemical modification of the surface enhances the removal capacity of toxic anions in water treatment process *(Mahmood et al. 2013).* Magnetite nanoparticles have gained much interest due to its high adsorption capacity for of fluoride and arsenic from polluted water and simple removal and dispersion from aqueous media *(Van Dorn et al. 2011; Sharma et al. 2018).*

There are different methods for the synthesis of magnetic nanoparticles such as co–precipitation, hydrothermal, solvochemical, micro–emulsion, sonochemical etc. In Co-precipitation method, a stoichiometric ratio of Fe^{2+} and Fe^{3+} is used as an iron source, which under suitable alkaline medium gives Fe_3O_4 magnetic nanoparticles *(Gehrke et al. 2015; Laurent et al. 2008*). In hydrothermal method, single crystals of are synthesized in an autoclave with high pressure and temperature *(Fan et al. 2001)*. In solvochemical method, an organic solvent is used as dispersion media in place of water *(Heyon et al. 2001)*. In sonochemical method, ultrasonic waves generate high temperature to activate the internal liquid which can trigger reduction, decomposition, hydrolysis and oxidation *(Mukh-Qasem et al. 2005)*. In microemulsion method, two types of immiscible liquid are mixed in presence of surfactant. In this method different shapes of nanoparticles can be obtained. Micro emulsion can be used to obtain the uniform size, morphology, good disparity. Zhang et al. (2001) reported that using solvothermal analysis at pH = 8.5, a mixture of spherical particles and needle like rods can be obtained on the other hand at pH=10.5, spherical nanoparticles can be obtained.

2.2.1 Remediation of selected anions from aqueous media

Asgari et al. (2017) synthesized Fe_3O_4 magnetic nanoparticles and modified the surface using Ga (III) porphyrin complex and 3-aminopropyltriethoxysilane. They tested the sample for fluoride adsorption and found that the concentration of fluoride reduced from 10 mg/L to 0.3mg/L in contact time of 30 minutes. They also tested the reusability and they found that removal efficiency of fluoride in 5 cycles reduced from 97.2% to 87%.

Markeb et al. (2017) synthesized Ce–Ti@Fe_3O_4nanoparticles for fluoride removal. They found the maximum removal capacity of 91.04 mg/g at pH=7 and also showed a fast adsorption rate. They also observed that it can be used for 5 cycles without significant loss of adsorption capacity. Similarly, Zhao et al. (2010) prepared Fe_3O_4@Al $(OH)_3$ nanoparticles which combines the advantages of magnetic separation and high affinity of aluminum oxide towards fluoride.

Liu et al. (2016) synthesized Fe-Al oxide magnetic nanoparticles anchored on graphene oxide (IAO/GO). They found that IAO/GO exhibits super paramagnetism, good selectivity for fluoride, high removal capacity and better acid alkali stability. The maximum removal capacity from Langmuir model was calculated to be 64.72mg/g. They also concluded that the IAO/GO can be used for fluoride decontamination of natural water environments due to its good selectivity for fluoride removal when co–anions exist, good removal efficiency, and low residual iron and aluminum concentration after defluoridation. They explained that electrostatic interactions, ion exchange and inner–sphere complexations were the main factors of adsorption mechanisms.

Zhang et al.(2016) synthesized Fe_3O_4 magnetic nanoparticles coated with Fe–Ti bimetallic oxide by co–precipitation method and found that saturation fluoride adsorption capacity of 57.22mg/g. They also found that adsorption was fast and equilibrium reached in 2 minutes. They further used this bimetallic magnetic composite nano-adsorbent (Fe_3O_4@Fe–Ti) in a fluidized bed system for fluoride removal.

Yang et al. (2016) synthesized magnetic alumina aerogel for the decontamination of fluoride from aqueous media. In this research, magnetic alumina hydrogel adsorbent was fabricated by amending alumina aerogel with Fe_3O_4. They found the removal capacity of 32.1 mg/g at pH 5.0. They also tested it for removal of fluoride from well water. They

reported that the as prepared magnetic alumina aerogel was an effective and easily prepared adsorbent and was easily separable after adsorption.

Patel et al. (2012) used granulated barium hexaferrite (BaFe12O19, BHF) and magnetite (Fe_3O_4) in range of 50 to 100 nm for removal of As(III). The BHF showed better adsorption of 75% of As(III) than magnetite. The removal capacities for BHF was 2.27 mgg^{-1} which was more than that of Fe_3O_4(0.7 mgg^{-1}).

Jin et al. (2012) modified Fe_3O_4 by CTAB which enhanced the removal capacity of As(V) from 7.59 to 23.07 mg g^{-1} utilising 0.1 g L^{-1} of Fe_3O_4@CTAB for two minutes at pH 6. The adsorption process fitted well with pseudo 2nd order kinetic model and Langmuir isotherm model with the maximum removal capacity 23.07 mg g^{-1}. That was two times the result calculated for Fe_3O_4. The sample was regenerated upto 85 % and reused up to fifth cycle.

Akin et al. (2012) prepared Fe_3O_4 nanoparticles by utilizing bauxite from red mud and studied the removal efficiency of As(V) from synthetic and groundwater. The water utilized, contained 1570 μgL^{-1} and 2800 μgL^{-1} of As(V) and As(III) respectively. The removal efficiency of As(V) from actual groundwater was found to be 99.2 %. The author carried out two stage adsorption process to bring down the concentration of As(V) upto permissible level of 10 μgL^{-1}.

Bujnakova et al. (2013) used nanocrystalline magnetite for As removal with concentration 5 mg L^{-1} . The maximum removal capacity was found to be 3.65 mg g^{-1} with > 90 % removal efficiency of As.

Lunge et al. (2014) synthesized magnetic nanoparticles utilizing MION-Tea waste template, which removed As(III) and As(V) efficiently due to improved crystalline structure of magnetic nanoparticles. The results obtained followed the Langmuir adsorption isotherm model with removal capacity of 153.8 and 88.69 mg g^{-1} for As(V) and As(III) respectively. Presence of competitive ions affected negatively the adsorption of As(III).

Monarez-Cordero et al. (2014) used magnetite nanoparticles synthesized by aerosol-assisted chemical vapor deposition (AACDV) method for remediation of As. The

equilibrium was obtained within one minute of contact time with 100 % of adsorption efficiency. So the rate of removal was very fast with great affinity of Fe towards As.

Here various magnetic nanoparticles for the removal of fluoride has been discussed depending upon their adsorption capacities, contact time, dosage, pH etc. With a little surface modification, the targeted contaminant can be effectively removed with these MNPs. Magnetic nanoparticles are already being used for adsorption of fluoride and arsenic from waste-water. It was also concluded that, coating with some green organic material like Chitosan can also be used for adsorption of contaminants. Therefore, magnetic nanoparticles have a huge potential for water treatment processes.

2.3 Mesoporous materials

The porous materials can be differentiated into three groups based on their pore diameter: macroporous (d> 50nm), mesoporous (2nm <d< 50nm) and microporous (d< 2nm) according to the IUPAC classification, *(Sing et al. 1985).*

Due to promising physicochemical properties like large pore volume and high surface area, mesoporous Zirconia and alumina are better for water treatment *(Cao et al. 2011; Badoga et al. 2015)*.

Mesoporosity provides increased number of active sites as well as favourabla dispersion enhancing the diffusion of reactant molecules, (*Badoga et al. 2015)* thus making mesoporous as a great adsorbent material for water treatment, *(Cai et al. 2014; Han et al. 2013)* organic dyes, *(Shen et al. 2014; Yahyaei et al. 2014)* inorganic anions, *(Lee et al. 2010; Jagtap et al. 2011)* or rare earth elements (*Sun et al. 2012)*.

As mesoporous compounds are prone to hydrolysis, phase transformations and redox reactions, their synthesis is quite difficult *(Kleitz et al., 2002)*. By calcination >500^{o}C, the surfactant gets removed from the material resulting in collapse of pore structure due to oxide crystallization making less stable *(Kleitz et al., 2002; Ciesla et al., 1999)*. Hence during the synthesis process, sulfate and phosphate anions are introduced in porous structure to increase the stability as sulfate and phosphate reduces the time of crystallization of porous oxides *(Shen et al., 2003; Samantaray and Parida, 2001)*, *(Ciesla et al., 1999)*.

2.3.1 Summary of Previous Work

Jimenez-Jimenez et al. (1998) synthesized mesoporous ZrP in an aqueous media of cetyltrimethyl ammonium bromide (CTAB), zirconium *n*-propoxide and orthophosphoric acid by sol-gel method. Another similar method was proposed using acid-ethanol extraction *(Jimenez-Jimenez et al. 1998)*.

Tarafdar *et al.* (2006) prepared spherical mesoporous ZrP using zirconium carbonate $(NH_4)_2HPO_4$ and TTBr by precipitation/ hydrothermal treatment for first time in basic medium. The synthesized meso-structured compound had specific surface area = 299 m^2/g and was used as catalyst for ethyl acetate hydrolysis.

Tian et al. (2010) derived mesoporous ZrP from glucose yeast biotemplate showing wormhole-like structure, with surface area = 217 m^2/g and narrow pore size of 2.7 nm. The synthesized ZrP used as air electrode for oxygen reduction reaction. The synthesis, properties and applications of mesoporous ZrP is given in Table 2.1.

Table 2.1: Summary on synthesis, properties and applications of mesoporous ZrP

Material	Synthesis	properties	Applications	Reference
ZrP	Decomposition of mesoporous Zr-phosphate/ diphosphonate (Thermal decomposition)	Particle size= 10~20 nm, BET surface area = 215 m^2/g, pore size = 4.0 nm	acid catalyst	*(Alberti et al. 1999)*
	Zirconium Phosphate, C18BDAC (Self-Assembly)	Ia3d (Cubic structure)	acid catalyst	*(Kleitz et al. 2002)*
	$(Zr(OC_3H_7)_4$, Brij 56, (Precipitation of hydrothermal treatment)	Super-microporous walls, pore diameter= 300 ~ 800 nm	catalysis	*(Yuan et al. 2005)*
	P-123, zirconium isopropoxide and triethyl phosphate	hexagonal mesoporous films	conducting devices	*(Nishiyama et al. 2006)*

	(Spin coating method)			
	AOT "Surfactant-assisted"	BET surface area= 83 m^2/g, pore diameter = 2~30 nm	protein adsorption	*(Bellezza et al. 2006)*
	zirconium carbonate Precipitation at pH = 8.0	BET surface area= 299 m^2/g, pore diameter = 3.91 nm	hydrolysis of Ethyl acetate	*(Um et al. 2007)*
	zirconium butoxide, pluronic F-127, phosphorous trichloride (Co-assembly Method)	BET surface area = 84 m^2/g, pore size = 17 nm	Composite membranes	*(Tian et al. 2003; Sahu et al. 2009)*

Dey et al. (2011) investigated fluoride adsorption capacity of mesoporous ZrP at pH=6.0. By evaluating the D-R adsorption isotherm data, it was found that, adsorption occurred through an ion exchange process. The presence of competitive ions facilitated the adsorption in positive manner. The fluoride loaded ZrP was effectively regenerated and used for several cycles.

Though porous transition-metal compounds were synthesized successfully, their application for water treatment was reported in very few literature and the no previous work regarding dopping of ZrP with Lanthanum was reported. In this work, Lanthanum doped MZrP was synthesized by sol–gel method and characterized using various phisico-chemical techniques for fluoride remediation.

2.4 Layered double hydroxide

There are many uses of Layered double hydroxide (LDH) like polymers additives, nano-composite formation, precursors, medicinal applications and environmental waste treatment (*Lin et al. 2005; Rivers, 2001; Rivers, 2002*). The structure of LDH is similar to that of brucite [$Mg(OH)_2$] where Mg^{2+} ions acquire octahedral positions in layered structure. But in LDH, the Mg^{2+} ion is replaced with trivalent cations like Al^{3+}. LDH can be synthesized by using different combination of divalent and trivalent

cations. Figure 2.1 shows LDH, represented by the formula $[M_{1-x}^{2+} M_x^{3+} (OH)_2]^{x+} (A^{n-})_{x/n} .mH_2O$.

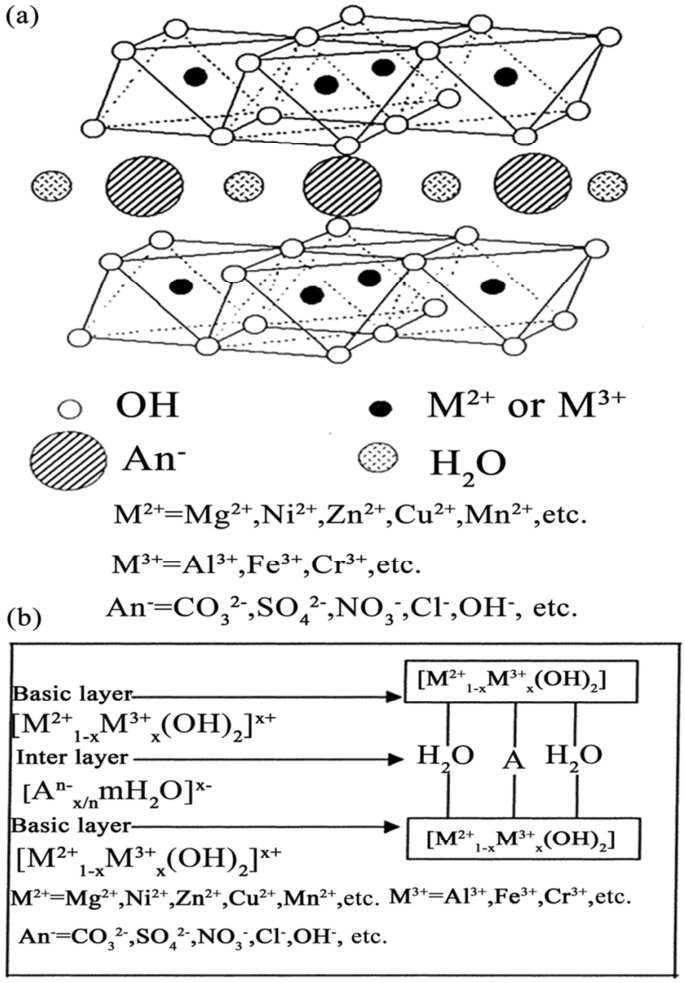

Figure 2.1 Structure models for LDHs (a) 3D structure and (b) 2D structure *(Huang et al. 2014)*

The brucite like structure of the LDHs has an anion exchange capacity making them unique for anion adsorption from aqueous media. There are two different mechanisms that are proposed for removal of anions from aqueous solution;

i) **Anion exchange:** Though LDH show anion exchange behavior remediation of anionic pollutants from water, thermally activated LDH is show better anion exchange property *(Miyata et al. 1983; Palmer sara et al. 2009)*.

ii) **The reformation effect:** The LDH get thermally activated (TA) when heated between 300 to 500°C thereby removing the interlayer anion and water

molecule. The TALDH when comes in contact with water and other anions get restructured by sorption process *(Erickson et al. 2004; Lv et al. 2006)* which is called reformation/ memory effect (*Palmer sara et al. 2009)*. The reformation effect increases when large number of anions get removed by thermal activation *(Wang et al. 2007)*.

The optimum temperature at which the LDH get thermally activated (TA) and highest possible number of interlayer anions are eliminated without damaging the cation layers is called optimum TA temperature. Thus TA temperature plays an important role in uptake of anion.

2.4.1 Summary of Previous Work

The research work reporting remediation of fluoride and arsenic by LDH and TALDH have are discussed below.

Das et al. (2002) studied fluoride removal efficiency of thermally activated Zn/Al LDH synthesized by coprecipitation and at 450°C. The maximum fluoride uptake was found to be 85.5% reaching equilibrium after 4 hours at pH = 6. The removal process was spontaneous and exothermic in nature and followed Freundlich adsorption isotherm. The presence of competitive anions had negative effect on removal of fluoride.

Wang et al. (2007) synthesized TA Mg/Al LDH by co-precipitation method and calcination at 500°C and examined its fluoride uptake capacity. The LDH showed maximum fluoride uptake of 75.8% and attained equilibrium during the first 15 min of their action, at which point the reaction reached equilibrium during 15 min.

Zhang et al. (2012) studied the, fluoride removal capacity of Li/Al LDHs synthesized by coprecipitation method showing higher fluoride removal under acidic condition. Adsorption followed both Langmuir and Freundlich isotherm model indicating the process to be heterogeneous or multilayer adsorption. The kinetics followed pseudo 2^{nd} order model with regression coefficient $R^2 > 0.99$.

Chetia et al. (2012) synthesized calcined Mg/Al–CO_3 LDH and studied the removal efficiency of As from aqueous media. The LDH removed As upto 99.99% acquiring

equilibrium during 90 mins pH = 7.5. The maximum adsorption capacity was found to be 100 mg/gm and the process followed the Freundlich model.

Huang et al. (2015) Mg/AlCO_3 LDHs by solvothermal process for remediation of As(V) and F from aqueous media. The LDH showed maximum uptake capacity of 28.6 and 125.8 mg g^{-1} for F and As(V) respectively and the adsorption occurred by anion exchange.

Ma et al. (2017) prepared Mg/Al LDH by intercalation with MoS_4^{2-} for removal of As(III)/As(V). The LDH removed both the ions up to 99% and the maximum removal capacity for As(V) and As(III) were found to be 56 and 99 mg g^{-1} respectively.

Here most of the previous works are focused on Aluminium based hydrotalcite like compounds and their calcined compounds. As, exposure of drinking water to Al for prolonged period of time during treatment process can cause potential risk for both human health and environment, various Fe based layered double hydroxides are also reported showing better adsorption results for removal of hazardous anions. However almost no reports are available regarding simultaneous removal of Arsenic and Fluoride and removal mechanism using these compounds. Thus understanding the removal mechanism of above said anions calcined Fe/Mg LDH can be used for their remediation form water.

2.5 Research Gap

Numbers of literatures were studied reporting the synthesis and environmental application of various adsorbent materials as mentioned above for remediation of arsenic and fluoride from contaminated water. A number of research are done on preparation and adsorption of the above said materials and observed to be showing adsorption properties for environmental applications. Although these compounds have drawn much attention for remediation of hazardous anions from aqueous media, the surface modification of these materials by incorporating doping agent or surfactants, or bio-organic compounds for enhanced adsorption capacity for arsenic and fluoride has not been demonstrated.

The previously carried out studies, clearly indicate a great gap between the requirements of adsorbents to be used and adsorbent already reported. To fill the research gap, adsorbents are

prepared that could match the desired parameters without any additional complication in the formation of any type of pollutants. The following points are considered while synthesizing adsorbent.

- The developed adsorbent should be environmentally friendly during the synthesis, and remediation subsequently.
- The efficiency of adsorbent should not be less than the reported materials.
- The regeneration of the adsorbent must be simple and involving less cost.
- The adsorbent should be used for a number of cycles without losing its efficiency.
- Sufficient evidences can be gathered to establish the mechanism of adsorption process.
- The results of the studies can be extended subsequently for pilot scale studies.

Therefore more advanced studies are needed to develop better materials with different morphology and functionality which can be used for cost effective environmental clean-up process. This fact encourages undertaking the present work.

2.6 Research Objective

By keeping the knowledge of research gap in our mind, attempt has been made to develop some environmental friendly adsorbent medias by surface modification of above said materials. The major objective of the research work is to eliminate arsenic and fluoride from synthetic aqueous media.

The objectives of the research are:

- To synthesize novel adsorbents like (Fe-Al mixed oxide nanoparticle, magnetic chitosan (Ch-Fe_3O_4) nanoparticle, La-ZrP mesoporous compound and Mg/Fe LDH) using different wet chemical methods for sustainable drinking water remediation of fluoride and arsenic.
- To determine the physico-chemical characteristics by characterization of the selected adsorbents to focusing on their surface chemistry, mineralogy, specific surface area and

- porosity using different sorptometric, scattering, spectroscopic and microscopic analytical techniques.
- To examine the removal capacity of arsenic and fluoride from synthetic and actual polluted water by these materials by conducting kinetic and equilibrium isotherm using the synthesized adsorbents and estimate their adsorption capacities.
- To determine the mechanisms of anion removal onto above adsorbents and examine the feasibility of the process for regeneration of exhausted adsorbents.
- To conduct column adsorption studies on both fluoride and arsenic from synthetic and ground water by above materials as a function of
    a) flow rate effect on breakthrough
    b) initial concentration effect on breakthrough
    c) adsorbent mass/bed height effect on breakthrough
- To design a model implementing kinetics and isothermic results to remove fluoride and arsenic from water.

Chapter 3

Materials and Methods

This chapter describes the detail experimental methods carried out in the research work. The glassware and chemicals used in this research are mentioned in materials section. This also includes synthesis procedure of adsorbents and instrumental technique used for characterization along with the elaborated study to know the adsorption capacity in batch mode as well as column mode. The theories used for explanation of the results obtained are also discussed in this chapter.

3.1 Reagents and Chemical

All chemicals used are of analytical grade without further purification. The chemicals were obtained from Merck (Germany, and India), Rankem (India), Sigma-Aldrich and Steinheim (Germany).

3.2 Adsorbate preparation

Stock As(V) and As(III) (1000mg/L) was prepared by diluting required amount of corresponding arsenic salts (Merck) using 1000 ml double distilled water. Likewise, fluoride stock solution (1000mg/L) was prepared by diluting required amount of NaF salt (Merck) using 1000 ml double distilled water. Solutions of required concentrations were obtained by serial dilution of the stock solutions. pH of the solutions was maintained by addition of 0.1M HCl and 0.1 M NaOH.

3.3 Adsorbent preparation

In this study, four different adsorption medias were prepared and examined to study the removal efficiency of arsenic and fluoride.

3.3.1 Synthesis of Fe-Al mixed oxide nanoparticle

Fe-Al mixed oxide nanoparticle was prepared by co-precipitation technique using $Fe(NO_3)_3.9H_2O$ and $Al(NO_3)_3 \cdot 9H_2O$ as salt precursor, mixture of ethanol and double distilled water as solvent and Triton[(R) X-100] as structure directing agent. 100mL of 1 $molL^{-1}$ $Fe(NO_3)_3.9H_20$ and $Al(NO_3)_3 \cdot 9H_2O$ homogeneous solution in 1:1 mixture solution of ethanol and water was taken and 2 ml of Triton[(R) X-100] was added to it with continuous stirring. Then NaOH solution (1 mol/L) was added drop wise up to pH = 10.0 with continuous stirring forming a brown gel-like ppt with aging for 24h at ambient temperature. Then the precipitate was washed with double distilled water to make it free from nitrate, filtered and dried at 373K to form Fe-Al mixed oxide nanorods. The above method was repeated twice with two different ratios of ethanol and water (i.e. 0:1 and 2:1). The material synthesized in (1:1) mixture of ethanol and water was then calcined at 700°C.

A weighed amount of sample was wet chemically analyzed by tri-acid digestion for quantitative analysis of iron and aluminium *(Vogel, 2000)*.

3.3.2 Synthesis of magnetic chitosan nanoparticle

The Fe_3O_4-Chitoasan nanoparticle was synthesized by the following method:

Required quantity of Ferrous chloride salt solution was taken to prepare of 0.2 M of Ferrous chloride solution. The $FeCl_2$ solution was stabilized by adding some amount of 0.5 M HCl. 0.25M NaOH salt solution was then prepared. Then desired amount of CTAB was dissolved in n-octane followed by addition of 1-butanol and $FeCl_2$ aqueous salt solution in different ratios to form a microemulsion. The above mixture was stirred slowly till a transparent microemulsion was obtained. The above steps were repeated to produce the second microemulsion, which contained 0.25M NaOH solution.

The second microemulsion was then mixed at a volumetric ration of 1:1. After the addition, a dark green precipitate was obtained and gets transformed to black after some time. The same was washed with acetone and double distilled water at room temperature (leveled as S1).

The same procedure was continued, in which Chitosan nanoparticles were synthesized. This technique includes formation of the chitosan nanoparticles in aqueous core of reverse micellar droplets cross-linked through glutaraldehyde. In this method chitosan was first dissolved in acetic acid and water with constant stirring at 60^oC. Then, first microemulsion was prepared by addition of n-butanol and n-octane to desired amount of CTAB which forms a transparent emulsion. Ferrous chloride was added to previously prepared chitosan solution. Then both CTAB solution and Fe-Chitosan solution was mixed together to form second microemulsion. Then 3 ml of glutaraldehyde was added and heated at 60^oC for 15 min. The Microemulsion 2 was prepared by a mixture of CTAB, Butanol, Octane and 0.5 molar NaOH solutions. Then with the same procedure it was washed and dried at room temperature.

3.3.3 Synthesis of Lanthanum based Zirconium phosphate (La-ZrP)

The mesostructured LaZrP was synthesized by following method:

Desired amount of $ZrOCl_2.8H_2O$ and $La(NO_3)_2.6H_2O$ were dissolved in double distilled water (100ml). To above solution 3.78 gm of solid $(NH_4)_2CO_3$ was added with continuous stirring till clear solution of zirconium carbonate was obtained. Then 1.47 g $(NH_4)_2HPO_4$ was dissolved in the solution. Then desired amount of CTAB was added. The clear solution obtained was aged in polypropylene bottle at 80^oC for 3 days for complete precipitation and microwaved at 100^oC for 2 hrs. Then the precipitate was filtered and washed thoroughly followed by drying and calcination at 500^oC for 2 hours.

3.3.4 Synthesis of Mg/Fe-CO_3 LDH

The LDHs of different ratios of Mg/Fe were prepared by hydrothermal process. 16 mL of ammonia solution (NH_4OH) was added to 80 mL of solution mixture of $Mg(NO_3)_2.6H_2O$ (7.5, 10, 12.5 mmol) and $Fe(NO_3)_3.9H_2O$ (2.5mmol) under rigorous stirring. After 30 minutes, the mixture was heated at 180°C for 12 hours in a 120 mL Teflon-lined stainless-steel autoclave. A white powder obtained after synthesis was washed with ethanol and double distilled water followed by centrifuge for several times, and vacuum dried at 60 °C for 6 hours.

3.4 Characterization of the adsorbent

Various analytical techniques are used for characterizing the adsorbents. Here, the basic principles of techniques utilized in the experimental part is described in this section. The techniques include are (a) X-ray Diffraction (XRD), (b) Scanning electron microscopy (SEM), (c) Transmission electron microscopy (TEM), (d) Infrared spectroscopy (FT-IR), (e) Brunauer-Emmet-Teller (BET) surface area, (f) Thermogravimetric Analysis (TGA/DTA) and (g) Atomic absorption spectroscopy (AAS).

3.4.1 Zero point charge (pH_{ZPC})

The zero point charge (pH_{ZPC}) of the synthesized material are determined by studying the electro chemical properties of the surface. It can be defined as the pH at which the charge of the adsorbent suface is zero. The value of pH_{ZPC} increases in presence of acidic functional group due to H^+ release and decreases in presence of basic functional group due

to OH^- ion. A mass titration method was adopted for determination of pH_{ZPC} value inthis study.

40mL of KNO_3 solution (0.01 $molL^{-1}$) was taken in 125 ml PVC flask with pH adjustment of 1 to 10 by of HCl adding (0.1 mol L^{-1}) and of NaOH (0.1 $molL^{-1}$) solution. The volume of solution in each bottle is adjusted to 50mL with double distilled water. Then 0.2 g of adsorbent was added to it and initial pH (pH_i) for each bottle was measured. Then after 72 hrs, of continuous shaking, shaking, the final pH of the (pH_f) was noted for each bottle. Then pH_i value was plotted against ΔpH (difference between pH_i and pH_f) and the pH at which ΔpH becomes 0 is known as pH_{ZPC} of the sample.

3.4.2 X-ray diffraction study (XRD)

XRD analysis plays an important role in characterization of nanocrystalline materials. This technique is mainly used to determine crystallite size and phase of materials. The patterns of diffraction are recorded Cu Kα radiation (λ = 1.5418 Å) with the help of a X-ray diffractometer. Crystalline phase of nanomaterial may be identified by investigating diffraction pattern based on the principle of Bragg's law:

$$n\lambda = 2d\sin\theta \tag{3.1}$$

where, d – distance between the lattice planes,

λ - incident wavelength

θ - Bragg's angle

The peak width of diffraction pattern gives information about size distribution and strain of crystalline structure. In case of nanomaterials a broad peak is obtained due to decrease in size. The peak width of particular diffraction plane calculated using the Debye-Scherrer equation:

$$D = (0.9\lambda)/\beta\cos\theta \tag{3.2}$$

where, D - the mean crystallite size, λ - incident wavelength, θ - Bragg's angle and β - width of the peaks in radians.

The XRD pattern of synthesized material was obtained by Philip's PAN analytical X'Pert X-ray diffractometer using Cu Kα radiations at 35 kV and 30 mA with variation of

2θ (10^0~80^0) at rate of 2°min^{-1}. The diffraction planes obtained were analyzed with the help of X'Pert high score software.

3.4.3 Scanning electron microscopy (SEM)

SEM is used for imaging sample surface by detecting signals of interaction between sample surface and the incident electron. When the beam of electron falls on the surface of secondary electrons (energy < 50 eV) gets emitted from the surface. Efficiency of emission depends on bulk chemical composition, chemical characteristics and geometry of sample surface. Thus, from SEM analysis information about chemical composition and surface morphology of the compound are obtained (*Deng et al., 2014*).

The SEM and EDAX analysis were done by JOEL model JSM-6480LV, Japan with an accelerating voltage (20 keV). The sample is coated with platinum before the analysis.

3.4.4 Transmission electron microscopy (TEM)

TEM is chemical characterization instrument with high spatial resolution. An advanced TEM images crystalline sample with resolution of 0.1 nm smaller than interatomic distance. Quantitative analysis is also possible by focusing on electron beam to a diameter < 0.3 nm. Interparticle interaction, shape and particle size can determined TEM (Zhang, 2009).

The TEM and selected area electron diffraction (SAED) pattern of the synthesized material were done using high-resolution (HR) TEM (JEM-2100 HRTEM, Make-JEOL, Japan) with voltage of 200KV.

3.4.5 Fourier transforms infrared spectroscopy (FTIR)

FTIR spectroscopy is used to determine the functional proof of sample by characterizing vibrational frequencies of molecules and phonons. The intensity of IR spectrum transmitted through the sample reflects the vibrational mode ode of the functional group by selection rule. The interaction of a surface molecules and nanoparticles usually changes the vibrational frequencies. Thus, the change in frequency gives information about the interaction of the surface molecules and nanoparticles (*Zhang, 2009*).

FTIR study was done by PerkinElmer FTIR Spectrometer Spectrum RX-I (USA). The spectrum obtained in range of 400 - 4000 cm^{-1} wave number are analyzed.

3.4.6 Brunauer-Emmett-Teller (BET) analysis

Calculation of the amount of N_2 gas adsorbed physically correspond to a monolayer coverage, which determines specific surface area of the adsorbent. Volumetric of continuous flow method was used to calculate the amount of adsorbed N_2 gas. This technique is also helpful for determination of pore size, pore volume, pore density and pore diameter.

The surface area of sample was measured by BET (Quantachrome AUTOSORB-1, USA) at liquid N_2 temperature. The samples were degassed at 100~150℃ by considering Helium as carrier gas. The surface area of the adsorbent were calculated using N_2 adsorption/ desorption method.

3.4.7 Thermogravimetric analysis (TGA-DTA)

In TGA mass of the material is calculated against time or temperature while temperature constantly changes. This method determines purity of sample, carbonate or organic content, water content and decomposition reactions. The plot of change in mass with temperature is known as thermogravimetric curve (*McMahon G., 2007*) which measures the kinetics. The TGA detects small changes in mass of the sample kept in the thermobalance caused due to the change in temperature of the furnace in both inert or air atmosphere. The factors that affect TGA measurement are heating rate, sample size, electrostatic effects, buoyancy, sample holder and gas flow.

Differential thermal analysis (DTA) analysis detects the phase transitions, physical properties and thermal behavior of a sample in terms of the temperature change. Any physical or chemical change occurs due to change in heat contain of the material. DTA results helps in studying phase transition, change in enthalpy and construct phase diagram.

3.4.8 Atomic absorption spectrometer (AAS)

After adsorption, concentration of As(V) was measured using VARIAN, AA240 AAS. The instrument is calibrated by taking standard solutions of variable concentration (by serial dilution from stock solution).

3.5 Batch adsorption study

3.5.1 Adsorption study

The adsorption study of fluoride and arsenic from it's synthetic aqueous solution was done by treatment of 50mL of anionic solution with required amount of absorbent varying the parameters such as pH, adsorbent dose, initial concentration, contact time, and temperature to optimize the adsorption process in batch mode. Then bottle containing anionic solution were subjected for shaking in a water bath shaker with a shaking speed of 300 rpm. After certain time, the adsorbent was separated through cellulose acetate filter paper (0.45μm). The filtrate was analyzed for As concentration by AAS and tested for fluoride concentration by Orion 720 A^+ Ion analyser using ion selective electrode method.

For percentage removal before and after adsorption was calculated by following formula

$$\% \text{ Removal} = \frac{(C_0 - C_e)}{C_0} \times 100 \tag{3.3}$$

$$q(mg/g) = \frac{(C_0 - C_e)}{m} \times V \tag{3.4}$$

where m is the adsorbent mass (g), C_0 , Ce represents initial and equilibrium concentration of adsorbent respectively, V is the volume of the adsorbate solution (L), q represents loading capacity mg/g.

3.5.2 Desorption Study

In this process, anion loaded adsorbent (0.5g) was stirred in 50 mL aqueous solution of different pH maintained by the addition of 1.0 M NaOH and 1.0 M HCl solution for

30mins. Then, the residual solution was filtered and tested for the anion concentration by instrumental techniques mentioned above.

3.5.3 Reuse Study

After first adsorption experiment, the loaded adsorbent was separated from the adsorbent solution and dried at 70^{o}C which was used for further adsorption of arsenic and fluoride in different cycles to evaluate the extent of adsorption.

3.6 Adsorption kinetic models

The kinetics study is carried out to evaluate the mechanism and the rate determining step of the adsorption. In the study two kinetic models were used to evaluate the order of reaction between the adsorbate and adsorbent and rate of adsorption. The kinetic models used are pseudo 1st and pseudo 2nd order model.

3.6.1 Kinetic Model (pseudo 1st order)

The pseudo 1st order rate equation for liquid phase adsorption developed was by Lagergren in the year 1898. The integrated pseudo 1st order rate equation can be represented as (*Ayoob et al. 2008*)

$$\log(q_e - q_t) = \log q_e - {K_f t}/{2.303} \tag{3.5}$$

where q_e , q_t is the concentration of fluoride adsorbed at equilibrium and at time '*t*' respectively (mg g^{-1}), K_f 1st order rate constant (min^{-1}). The slope and intercept obtained from the linear plot of $\log(q_e - q_t)$ vs *t* gives the value of q_e and K_f.

3.6.2 Kinetic Model (pseudo 2nd order)

The pseudo 2nd order kinetic model can be expressed by following linear equation

$${t}/{q_t} = \frac{1}{K_s}(q_e)^2 + {t}/{q_e} \tag{3.6}$$

and the *h* represents adsorption rate at $t \rightarrow 0$ (mg/g min^{-1})

$$h = K_s q_e^2 \tag{3.7}$$

where, K_s is the 2nd order rate constant (g mg^{-1} min^{-1}). Hence from the slope and intercept of the plot between t/q_t vs t, q_e and K_s can be calculated.

3.7 Adsorption isotherm study

The isothermic datas of adsorption can be used to evaluate the mode o on the interaction of adsorbate with adsorbent. Two isotherm models: Langmuir and Freundlich adsorption isotherm model were examined by application of the experimental datas and the better fitted model was found out by comparing the regression coefficient value (R^2).

3.7.1 Langmuir isotherm model

Langmuir adsorption isotherm study is usually assumes adsorption on homogeneous site on adsorbent surface. The Langmuir model is based on the idea of Monolayer adsorption with the following outcomes : i) adsorbate molecule are adsorbed on a particular site of the adsorbent. ii) Each active site on the adsorbent surface is occupied by single adsorbate molecule. iii) All adsorption sites exhibit equal adsorption energy. iv) adsorption is reversible. v) Once adsorbed, the adsorbent molecule cannt move across the adsorbent surface. (*Chatterjee et al., 2009; Bayazit and Inci, 2013*).

The Langmuir equation is given as:

$$\frac{q_e a_L}{K_L} = \frac{K_L C_e}{(1 + K_L C)} \tag{3.8}$$

The linear form of the equation is:

$$\frac{C_e}{q_e} = \frac{1}{K_L q_{\max}} + \frac{C_e}{q_{\max}} \tag{3.9}$$

where a_L (Lmg^{-1}) and K_L (Lg^{-1}) are Langmuir constants,

The maximum adsorption capacity, $q_{\max} = \frac{K_L}{a_L}$ is (mg g^{-1}).

From slope and intercept obtained from the linear plot between $\frac{C_e}{q_e}$ and C_e determines the q_{max} and K_L values are calculated.

3.7.2 Isotherm model (Freundlich)

Freundlich model represents a multilayer adsorption mechanism on heterogeneous adsorbate process (*Namasivayam and Kavitha, 2002*).

The equation of Freundlich model can be represented as (*Inci et al., 2011*):

$$q_e = K_F C_e^{1/n} \tag{3.10}$$

In linear form, the equation can be given as:

$$\ln q_e = \ln K_F + \frac{1}{n} \ln C_e \tag{3.11}$$

where C_e (mg L^{-1}) represents adsorbate concentration at equilibrium, q_e (mg g^{-1}) represents adsorption capacity at equilibrium and K_F and n are represented as Freundlich constants The slope and intercept obtained from the linear plot of $\ln q_e$ and $\ln C_e$ of K_F and $(1/n)$ values can be calculated.

The Langmuir equilibrium parameter (R_L) that expresses characteristics of the isotherm can be expressed as (*Afkhami et al., 2010;Chatterjee et al., 2009; Kumar et al., 2012*):

$$R_L = \frac{1}{1 + a_L C_0} \tag{3.12}$$

The R_L value calculated above expression decides the nature of adsorption. ($0 < R_L < 1$) : favourable adsorption, ($R_L = 1$) : linear adsorption, ($R_L > 1$) : unfavourable adsorption and ($R_L = 0$) : irreversible adsorption. (*Lian et al., 2009*).

3.8 Thermodynamic study

The process of adsorption is also affected by change in temperature of the system. The energy change as the effect of temperature are expressed in form of thermodynamic parameters.

The thermodynamic parameters can be determined from the equations given below:

$$\Delta G^0 = -RT \ln b \tag{3.13}$$

$$\Delta G^0 = \Delta H^0 - T\Delta S^0 \tag{3.14}$$

$$\ln b = \frac{\Delta S^0}{R} - \frac{\Delta H^0}{RT} \tag{3.15}$$

Where, R is ideal gas constant = 8.314 $Jmol^{-1}K^{-1}$, T (K) is represented by adsorption temperature, ΔH^0 (kJ/mol) represents enthalpy change, ΔS^0 (J/(mol K) represents entropy change and ΔG^0 (kJ/mol) represents the change in Gibbs free energy. The Vant-hoff plot ln K_0 vs. 1/T calculates the value of ΔH^0 and ΔS^0 from it's slope and intercept.

3.9 Column adsorption studies

Small-scale fixed bed column experiments were designed and conducted the breakthrough analysis. A cylindrical tube having diameter 2.5 cm and 40 cm height made up of Perspex glass was used to carry out the column adsorption experiment. Then the column was filled with required quantity of the adsorbent to get the required bed height. The schematic diagram and working model of the column is shown in Figure 3.1.

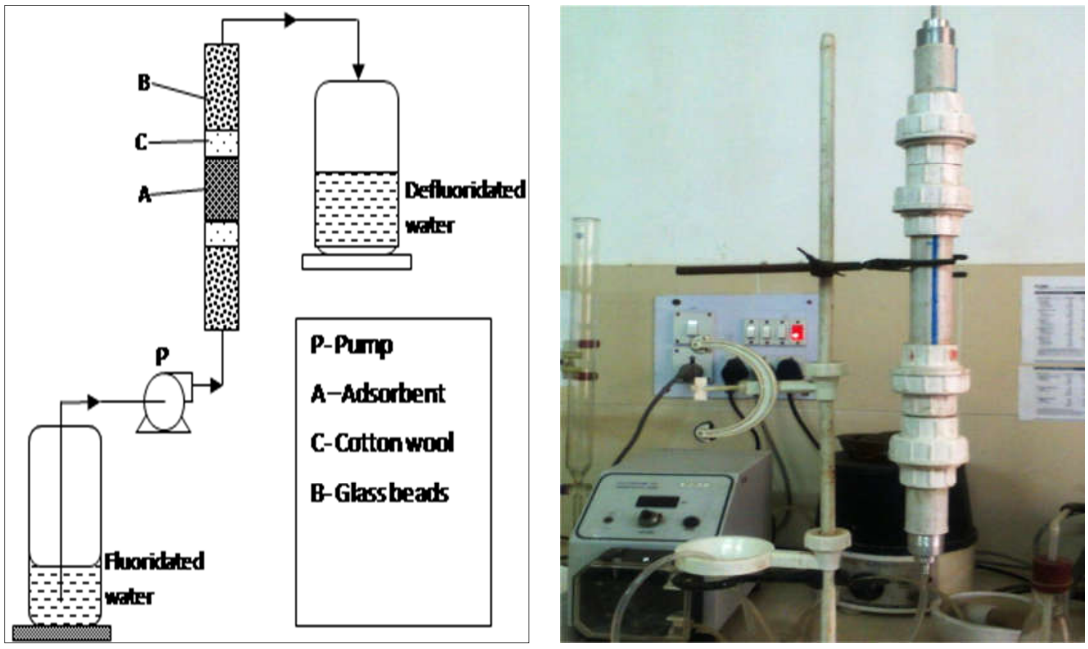

Figure 3.1 (a) Schematic representation (b) working model of Column used in the study

Synthetic aqueous fluoride and arsenic solution were pumped through column with the help of peristaltic pump with the desired flow rate. To minimize channeling inside the column, upward flow of water was undertaken during the study. Samples from the outlet unit were collected at certain time intervals and tested for anionic concentration. The concentrations obtained at different time were used to construct breakthrough curves with variation of flow rate, initial adsorbate concentration and bed mass. The fixed bed column was designed by logit method (*Oulman, 1980*) known as BDST (bed depth service time) model and can be represented as following equation,

$$\ln\left[\frac{C}{C_0 - C}\right] = -\frac{K\, N_0\, X}{V} + K\, C_0\, t \qquad (3.17)$$

where, C is adsorbate concentration at time t, C_0 represents initial solute concentration, approach velocity V= 95.54 cm/hr, bed depth X= 10 cm, K ($Lmg^{-1}hr^{-1}$) rate constant of adsorption and N_0 (mg/L) represents adsorption capacity. K and N_0 were calculated from Slope (KC_0) and intercept ($-K\, N_0X/V$) from the straight line plot of $\ln[C/(C_0 - C)]$ and time 't'.

Chapter 4

Synthesis of rod shaped iron-aluminium mixed oxides and its fluoride sorption behavior at ambient temperature

Nano-structured rod-shaped Iron-Aluminium mixed oxide nano-particles were prepared at ambient temperature. Size and shape of the particles were determined by SEM and TEM. The detail sorption studies in batch as well as column mode for fluoride was conducted to know the removal efficiency. The kinetics and thermodynamics of fluoride removal on mixed oxide nano-particles was carried out with variation of dose, pH, initial fluoride concentration, time and temperature. The reaction rate of fluoride removal was fitted well to Pseudo 2nd order kinetic model. The isothermal data for fluoride removal followed the Langmuir model. The maximum removal capacity of Fe-Al mixed oxide nanoparticle was calculated to be 103.09mg g^{-1}. Fluoride removal capacity increases with increase in Cl^- and SO_4^{2-} concentration. Reusability of the mixed oxide nano-particle was examined up to seven consecutive cycles. Assumption study shows that the mixed oxide nanoparticle has the capacity of lowering concentration of fluoride to acceptable level.

4.1 Introduction

Fluoride is considered as highly hazardous pollutants among all present in groundwater. Considering its adverse health impact, WHO has recommended maximum allowable limits of F as 1.5 mg/L (*WHO, 2011*). The groundwater contamination of fluoride has been reported in various places of the world (*Amini et al. 2008; Qiao et al. 2014*). Hence, removal of fluoride is of crucial importance to simplify treatment processes and to reduce costs (*Liu et al. 2012*). Iron-based adsorbents have been extensively reported to exhibit the highest adsorption capability towards As while aluminium-based adsorbents have been shown to have affinity towards F (*Kumar et al. 2011; Prathna et al. 2017*).

Few researches have been conducted exploring the efficacy of iron and aluminium based binary oxides and hydroxides for the removal of F (*Qiao et al. 2014; Liu et al. 2012*). An increasing interest in the use of nanoparticles in treatment of drinking water in view of increased surface area to volume ratio has been noticed in recent decade (*Upadhyayula et al. 2009*) enabling enhanced adsorption of contaminants. However, the nanoparticles exhibited significant efficacy for fluoride removal was not comparable with aluminium based adsorbents. Some studies have also indicated the potential antimicrobial activity of alumina and iron oxide nanoparticles against common pathogens (*Patra et al. 2017; Prashant et al. 2015*).

The objective of this work was to study the adsorption potential of fluoride by iron/alumina mixed oxide nanocomposites. In order to achieve this, iron/alumina mixed oxide nanocomposites were synthesized, characterized and their simultaneous arsenic and fluoride removal efficiency were studied.

4.2 Results and Discussions

4.2.1 Characterization

The synthesized material consisted of 55.8% of iron as Fe^{3+} and 53.6% of aluminium as Al^{3+}. The pH_{zpc} of the mixed oxide was calculated to be 7.2. he pH_{zpc} decrease with the increase in occurrence of singly coordinated groups. As the pH_{zpc} of the prepared sample is slightly lower, it contains higher fraction of singly coordinated surface groups.

4.2.2 Surface Morphology

Figure 4.1; (a, b. c and d) shows the SEM micrographs of as synthesised Fe-Al mixed oxide(1:1) nanorod, Fe-Al mixed oxide(0:1) nanostructures, Fe-Al mixed oxide(2:1) nanorods and EDAX pattern of calcined Fe-Al mixed oxide(1:1) nanorods respectively. Figure 4.1a suggests that the synthesized Fe-Al mixed oxide(1:1) shows the nanorod morphology having the diameter (100~200nm) and length in micrometre range. The surface of the material was found to be smooth with no defects. Figure 4.1b shows that the SEM morphology of Fe-Al mixed oxide(0:1) retained rod shaped structure in nano range. From Figure 4.1c also represents the SEM micrograph of the Fe-Al mixed oxide(2:1) retaining the morphology of nanorods. Figure 4.1d represents the EDAX analysis of Fe-Al mixed oxide(1:1) nanorods which confirms that Al, Fe and O are present in the mixed oxide.

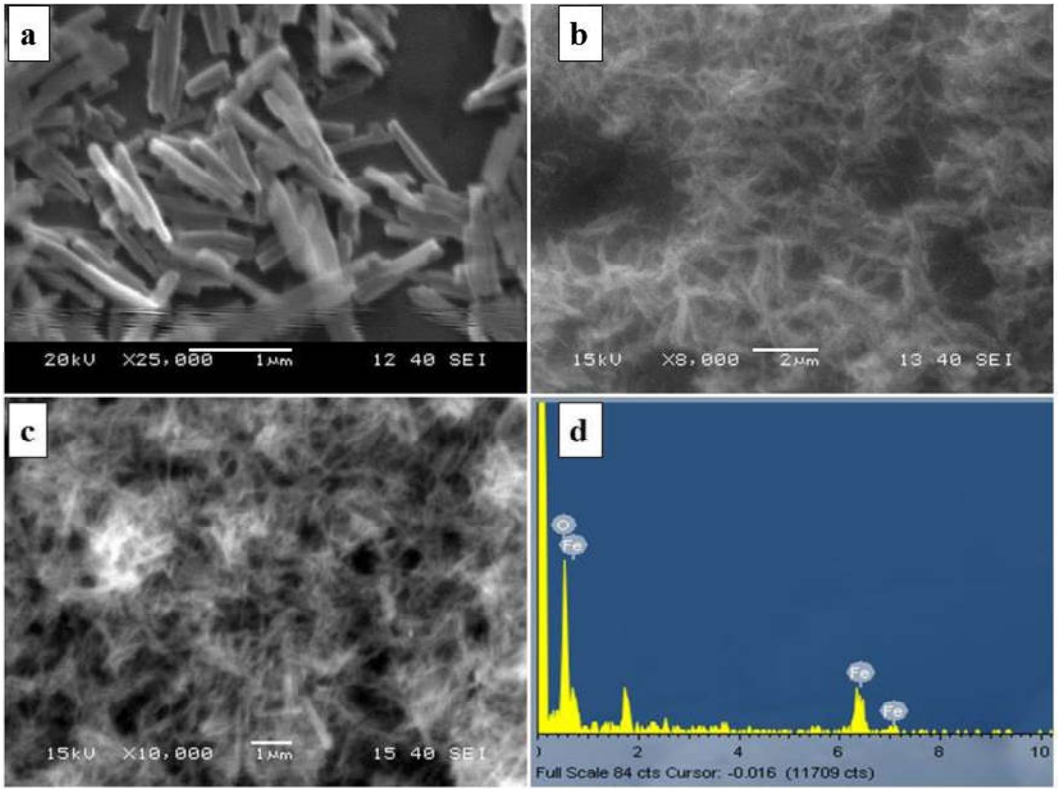

Figure 4.1 SEM morphology of a) Fe-Al mixed oxide(1:1) nanorod, b) Fe-Al mixed oxide(0:1), c) Fe-Al mixed oxide(2:1) and d) EDX of Fe-Al mixed oxide(1:1) nanorod

4.2.3 TEM analysis

From TEM micrograph of Fe-Al mixed oxide(1:1) (Figure 4.2a), it is found that the particles obtained are of rod-shape having width (7~10nm), and length (50~200nm) with spherical particles of size (2~10nm). The (SAED) patterns of (Figure 4.2b) exhibits strong diffraction patterns at 0.197nm and 0.151nm and weak diffraction patterns at 0.22, 0.251 and 0.17 nm.

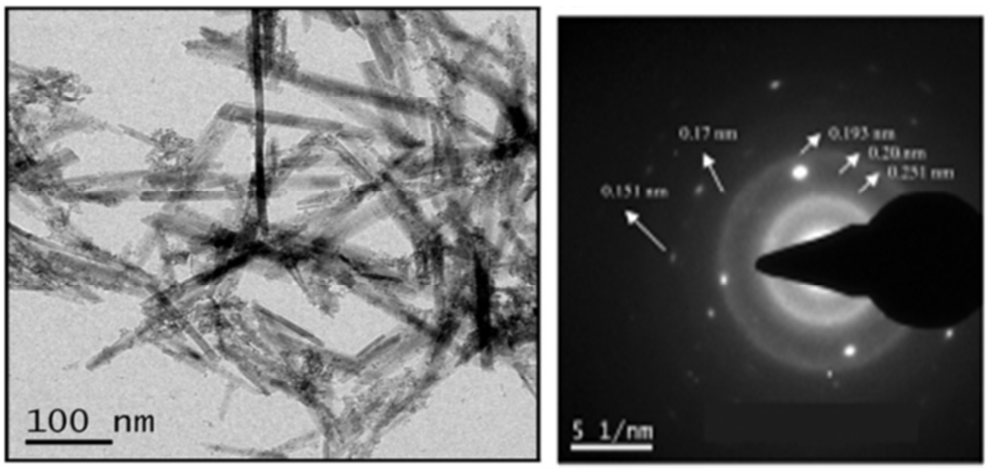

Figure 4.2 (a) TEM and (b) SAED image of Fe-Al mixed oxide (1:1) nanorod

4.2.4 XRD analysis

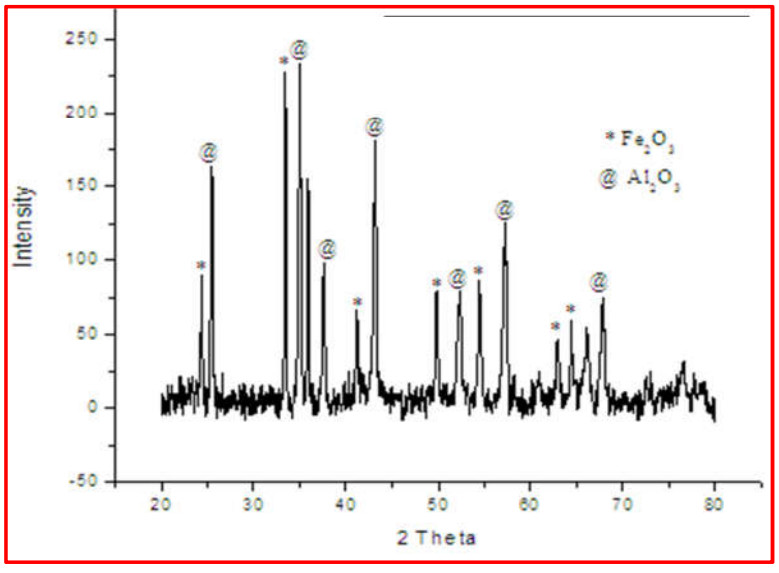

Figure 4.3 XRD patterns of calcined Fe-Al mixed oxide (1:1) nanorod

The XRD pattern of the mixed oxide nanorod [calcined Fe-Al mixed oxide (1:1)] presented in Figure 4.3 determined the structure and purity of the synthesized material. The XRD data confirmed the crystalline structure of nanorod composites. The diffraction peaks representing the α-Fe_2O_3 and Al_2O_3 were obtained with reference pattern (JCPDS CARD No: 84-0311 and No: 83-2081). No other peaks related to impurities or other crystalline phases are observed in the XRD profile.

4.2.5 Thermal (TGA/DTA) analysis

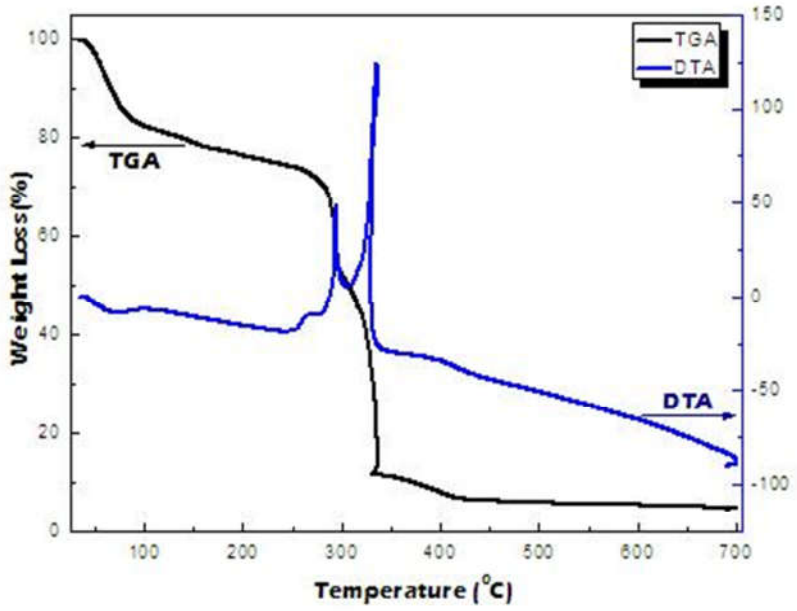

Figure 4.4 TGA/DTA profile of Fe_2O_3-Al_2O_3 mixedoxide(1:1) nanorod

Thermal analysis of the Fe-Al mixed oxide was conducted by TGA-DTA analysis in air upto 700°C with rate of heating 10°C/min. The TGA-DTA curve (Figure 4.4) of mixed oxide nanoparticle illustrates three major weight loss regions. The first weight loss region between 50-150°C, may corresponds to desorption of water (physically absorbed) from the sample. The second weight loss region between 260°C-290°C can be ascribed to the decomposition of $Fe(OH)_3$ thermally. in DTA curve, strong exothermic peak corresponding to decomposition of $Fe(OH)_3$ precursor into γ-Fe_2O_3 is observed at 275°C. Similarly, in the temperature range of 290°C to 335°C in the DTA curve, a strong exothermic peak was observed corresponding to phase transformation of γ-Fe_2O_3 to α-Fe_2O_3. The loss of weight at around 400°C indicates the decomposition of AlOOH to Al_2O_3.

4.2.6 FTIR study

FTIR analysis was done to study further transformation and formation. The peaks at 3358, and 496 cm^{-1} in Figure 4.5(a) are ascribed to O-H, and Fe-O functional groups, respectively. The peak at 632 cm^{-1} and at 1637 cm^{-1} is obtained in Figure 4.5(b) due to Fe-O (maghemite) and water of crystallisation respectively. New peaks (565~880 $cm^{-1)}$ may be due to the presence of alumina, which is also confirmed by XRD results.

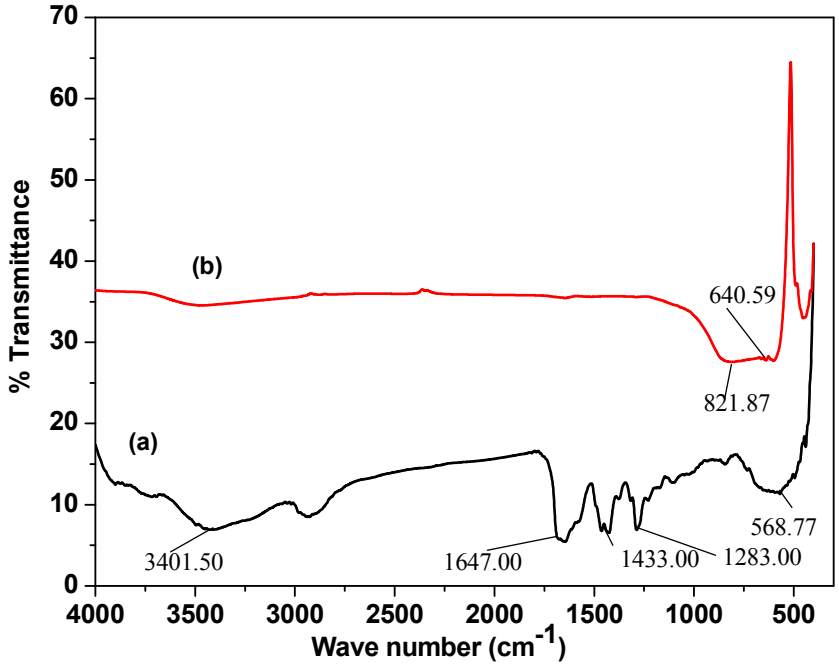

Figure 4.5 FTIR Analysis a) Fe_2O_3 and b) Fe_2O_3-Al_2O_3 mixed oxide (1:1) nanomaterial

4.2.7 BET Isothermic analysis

Figure 4.6 shows the BET surface area and porosity analysis of the prepared material using N_2 adsorption-desorption technique. From Figure 4.6(a), the Langmuir and BET surface area of the prepared Fe-Al mixed oxide (0:1) were found to be 24.945 and 27.550 m^2/g. From figure 4.6(b), the Langmuir and BET surface area of Fe-Al mixed oxide(1:1) nanoparticle were found to be 107.35 and 129.74 m^2/g. Similarly, Figure 4.6c gives the Langmuir and BET surface areas of Fe-Al mixed oxide(2:1) were found to be 20.575 and 22.785 m^2/g. Thus it is concluded that Fe-Al mixed oxide(1;1) exhibited highest surface area among the prepared nanorods.

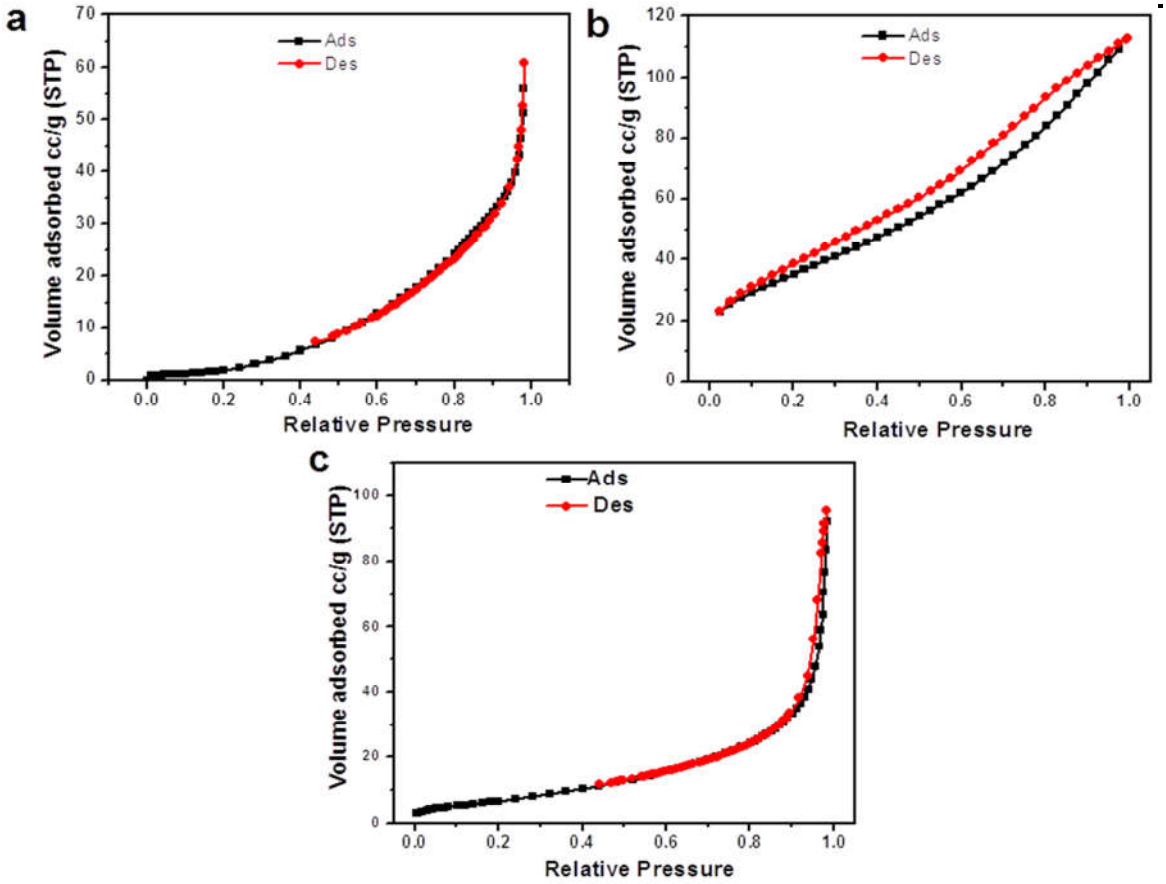

Figure 4.6 BET isotherm of (a) Fe-Al mixed oxide(0:1), (b) Fe-Al mixed oxide(1:1), (c) Fe-Al mixed oxide(2:1)

4.3 Sorption studies

4.3.1 Effect of dose

The absorbent dose is considered to calculate the optimum condition of absorbent amount required for adsorption. By optimizing the significant amount of dose, the cost of dosing and sludge formation can be minimized for better performance in treatment. Figure 4.7 demonstrates the variation of dose by Fe-Al mixed oxide(1:1), Fe-Al mixed oxide(0:1) and Fe-Al mixed oxide(2:1) nanorods at pH=7.0 for 50 ml of 10 mg/L (F^-) solution at 60 min. The fluoride removal increased continuously with increasing adsorbent dose (0.01~0.08 gm) which can be due to increase in number of active sites with increasing adsorbent dose. After 0.08 gm, the adsorption remains constant. Therefore 0.08 g was considered as the optimum

dose. Among the three adsorbents prepared, Fe-Al mixed oxide(1:1) nanorod shows the highest removal percentage of fluoride .

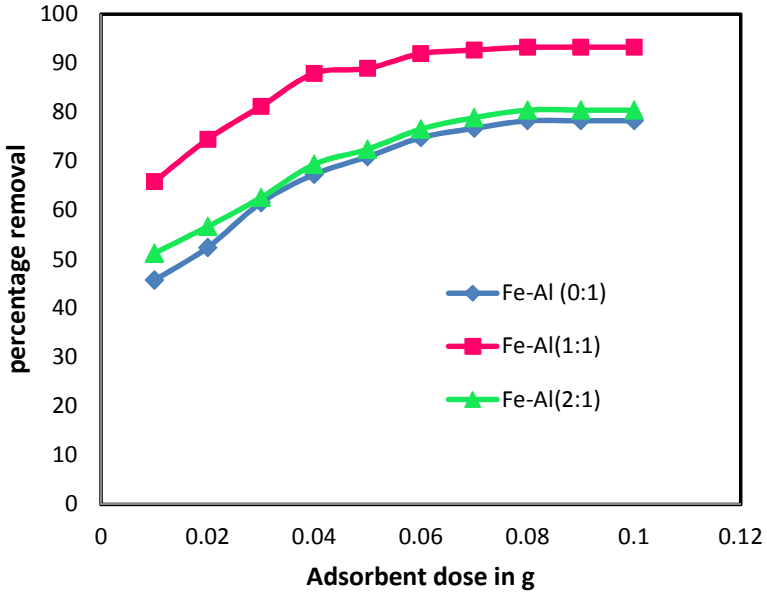

Figure 4.7 Dose effect on fluoride removal

4.3.2 Effect of pH

The pH variation study of Fe-Al mixed oxide nanoparticles for removal of fluoride was conducted with pH (2~12) using 0.08g for the material and fluoride concentration (10mg/L) (Figure 4.8). With increase in pH up to 7, the fluoride removal capacity increases and with further increase in pH, removal capacity decreases due to competition of OH^- ion with F^- ion. Less adsorption occurs in acidic condition due to formation of H_2F^- ions.

The mixed oxide nanoparticles were supposed to remove fluoride by hydroxyl ion exchange (4.2) or by electrostatic force (4.1) at $pH_{ZPC} < 7.2$,

$$MOH_{(s)} + H_3O + F^- \rightarrow MOH_2^+ - - - F^-_{(s)} + H_2O \quad (4.1)$$

$$MOH + F^- + H_3O^+ \rightarrow M^+_{(s)} - - - F^- + 2H_2O \quad (4.2)$$

The removal of fluoride at pH_{ZPC}=7.2 can be demonstrated by (4.3)

$$MO^{\delta-}H^{\delta+}_{(s)} + F^- \rightarrow MO^{\delta-}H^{\delta+} - - - F^-_{(s)} \quad (4.3)$$

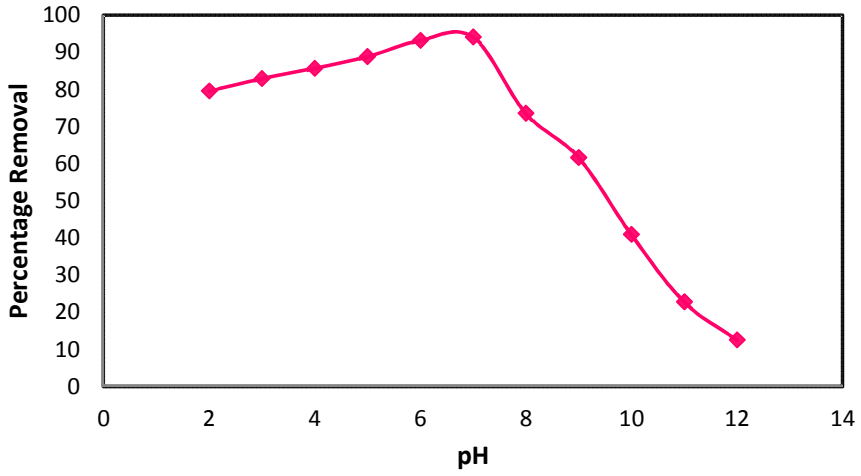

Figure 4.8 pH variation effect on fluoride adsorption

4.3.3 Effect of initial fluoride concentration

The concentration study of Fe-Al mixed oxide nanoparticle was done with 0.08 g of for 50 ml of fluoride solution at pH=7 varying concentration from 10 ~ 100mg/L for 60 mins. Figure 4.9 showed that the removal percentage of fluoride decreased with increasing fluoride concentration i.e. adsorption capacity increases with increasing concentration. This may be due high availability of adsorption site at lower concentration, compared to that of at higher concentration, hence adsorption decreases.

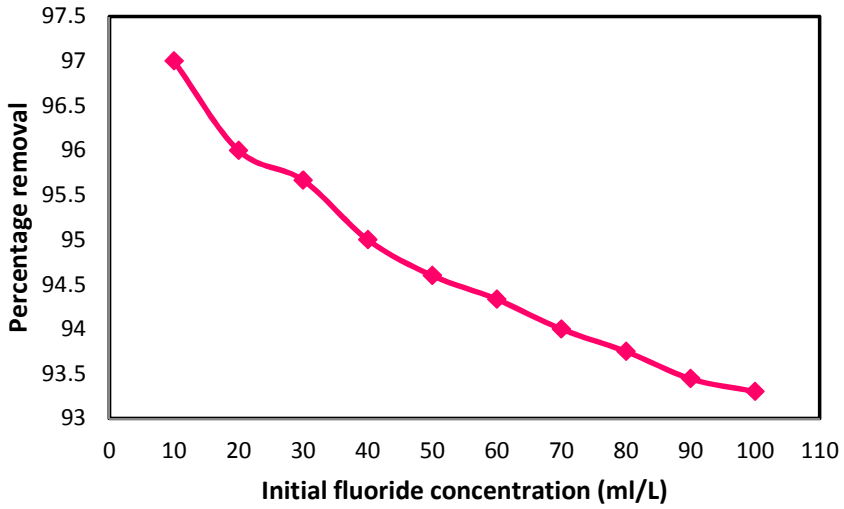

Figure 4.9 variation of fluoride concentration

4.3.4 Adsorption isotherm

The adsorption isotherm study was carried out using Langmuir and Freundlich equations (Figure. 4.10). The parameters obtained from the above the equations are given in Table 4.1. Among both the models, the Langmuir model fitted better as its correlation coefficient (R^2) nearly equal to 1.

Table 4.1: Aadsorption isotherm constants

Langmuir	**Adsorbent**	**a_L (Lmg^{-1})**	**K_L (Lg^{-})**	**q_{max} ($mg\ g^{-1}$)**	**r_L^2**	**R_L**
	Fe-Al mixed oxide(1:1)	0.0022	0.224	103.09	0.9 96	0.82
Freundlich	**Adsorbent**	**K_F**		**1/n**		**r_F^2**
	Fe-Al mixed oxide(1:1)	26.5		0.3493		0.95 7

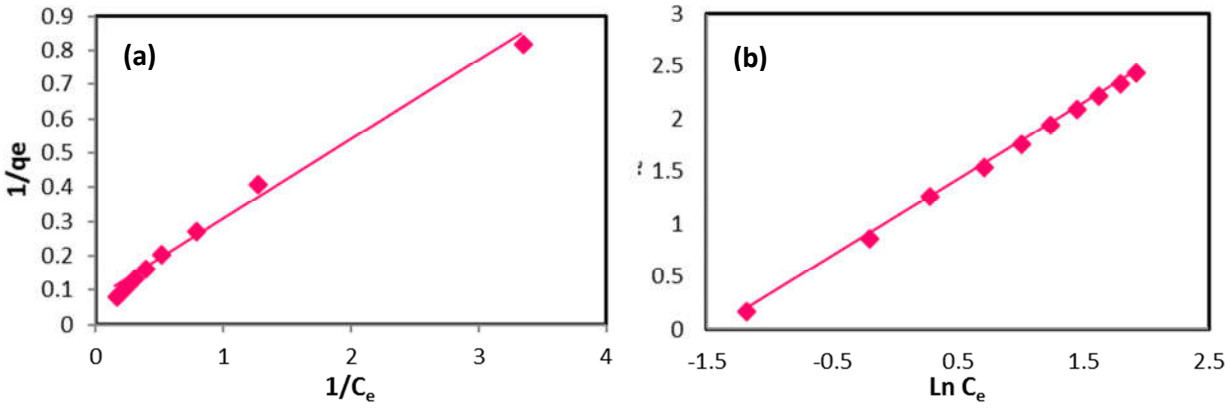

Figure 4.10 (a) Linear form of Langmuir and (b) Freundlich isotherm model

4.3.5 Effect of contact time

Figure 4.11 showed the variation of contact time (5 ~ 50 min) for fluoride adsorption on Fe-Al mixed oxide nano particle. Initially adsorption of fluoride increases with increase in time and decreases after equilibrium point at 40 mins. This may be due to availability of higher number of active sites at initial stage and after equilibrium the binding sites were fully occupied.

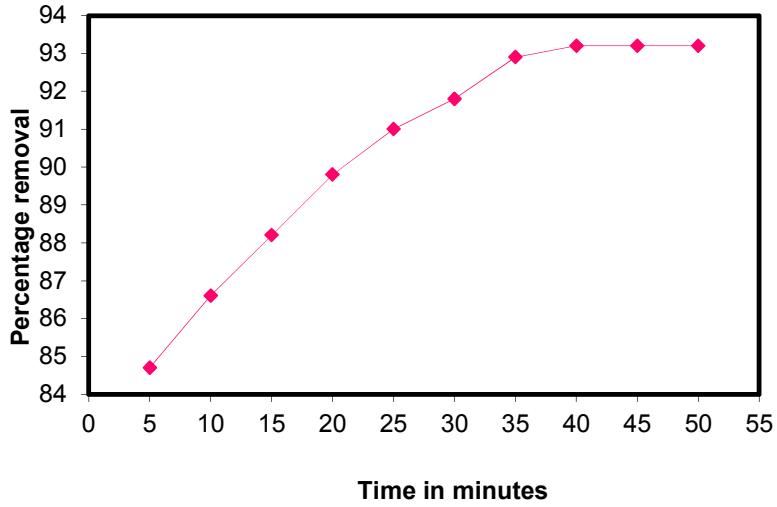

Figure 4.11 Time variation study

The kinetic study was done by investigating pseudo 1st order and pseudo 2nd order rate equations (Figure 4.12 (a), (b)). The kinetic parameters obtained from above kinetic model given in Table 4.2. By comparing the parameters of both the model, the fluoride removal process was found to be better fitted pseudo 2nd order kinetic model with regression coefficient 0.99.

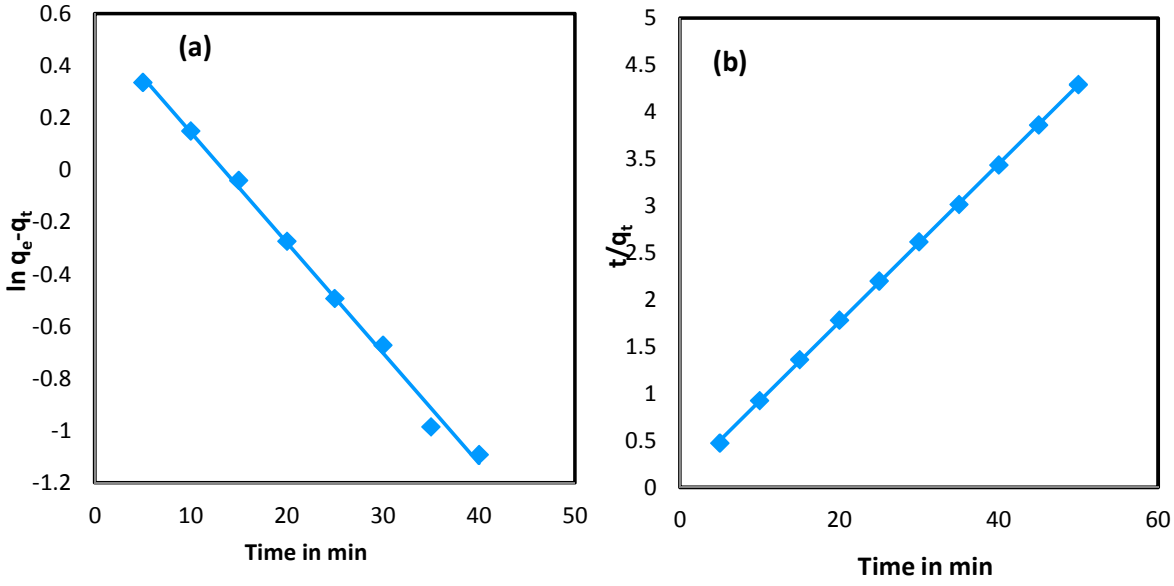

Figure 4.12 Linearised plots of (a) pseudo 1st order and (b) pseudo 2nd order kinetic model

Table 4.2: Parameters of pseudo 2nd order kinetic model

Adsorbents	K_2 (g mg^{-1} min^{-1})	q_e (mg/g)	q_e (mg/g) (Experimental)	r^2
Fe-Al mixed oxide(1:1)	0.0999	40	39.19	1
Fe-Al mixed oxide(2:1)	0.0933	39.53	39.7	1
Fe-Al mixed oxide(0:1)	0.00891	36.23	34.23	0.9986

4.3.6 Effect of temperature and thermodynamic study

Figure 4.13 showed variation of temperature (283~323K) on fluoride decontamination at pH = 7. The efficiency of decontamination increased with increasing temperature indicating exndothermic nature of the process. The figure demonstrated that 323K is the optimum temperature for fluoride adsorption.

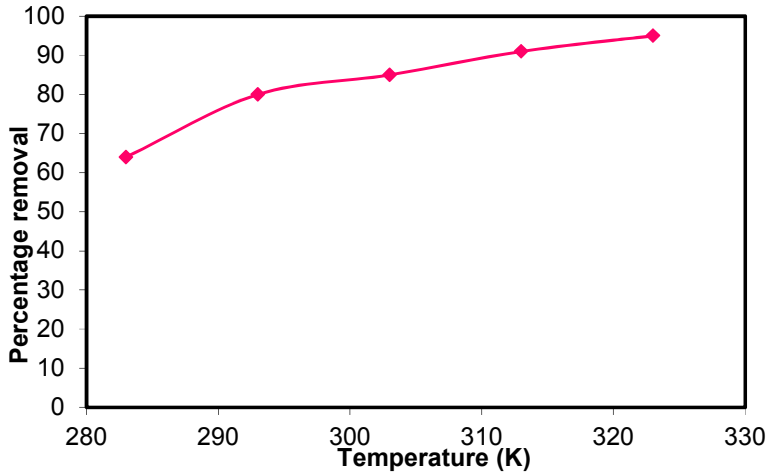

Figure 4.13 Temperature variation

4.3.7 Effect of competitive ions

The removal efficiency of fluoride in presence of different co-ions (nitrate, sulphate, bicarbonate, chloride and phosphate) was examined with variation of concentration of competitive ions (25~600 mg L^{-1}) with fluoride concentration (10mg/L) (Figure 4.14). The results showed that, the adsorption was slightly affected in presence of Cl^-, NO_3^-, SO_4^{2} ions, while presence of PO_4^{3-} and HCO_3^- had a negative effect on removal process.

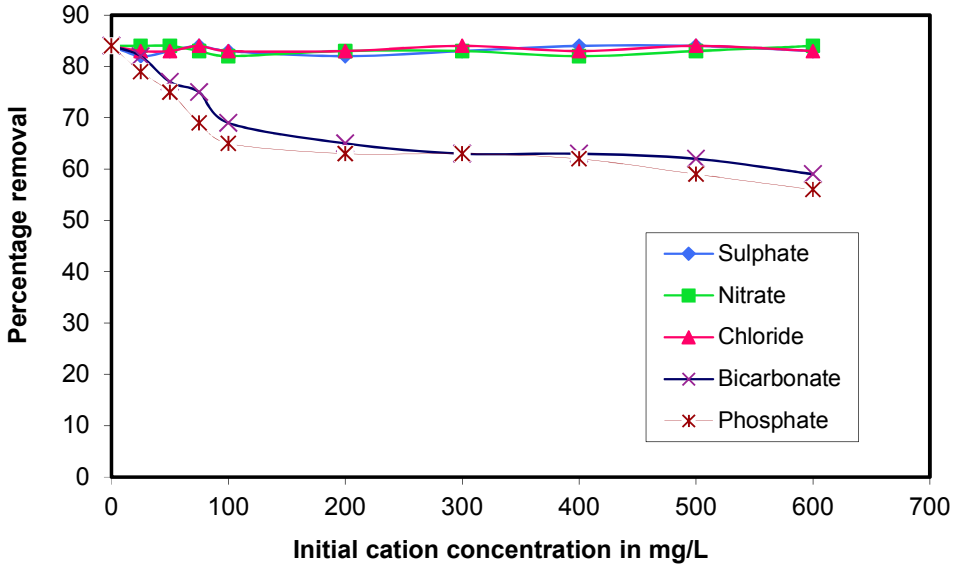

Figure 4.14 Effect of competitive ions

4.3.8 Regeneration study

The adsorbent material gets exhausted and its removal capacity decrease at the end of the process. So, it needs to be regenerated for further use. In this study regeneration was carried out by leaching out of fluoride at different pH to evaluate the optimal pH at which complete regeneration occurs. Figure 4.15 represents, the results of desorption study of fluoride loaded mesoporous Fe-Al mixed oxide nanoparticle at different pH in aqueous medium. At pH greater than 8, large concentration of fluoride was leached out from the adsorbent surface and 93% of fluoride was eluted out at pH=12.

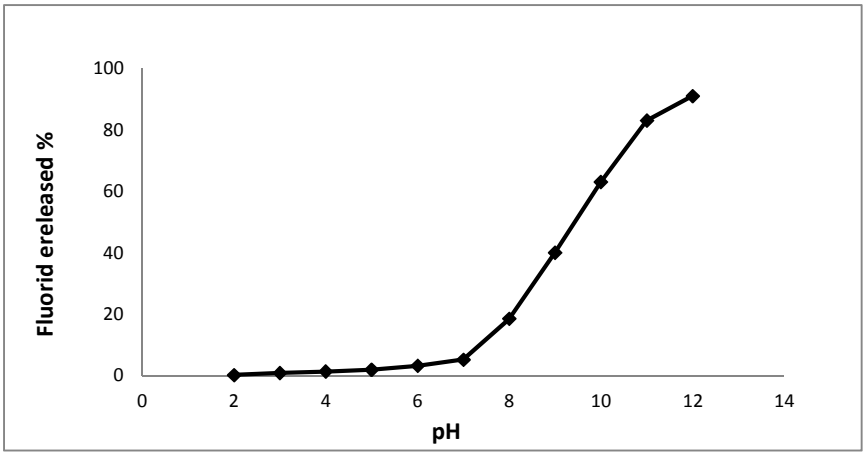

Figure 4.15 Desorption study

4.4 Column study

Fixed bed column process is the most widely accepted technique in field of water treatment due to simplicity of the process and high efficiency of purification. The performance of fixed bed study is generally influenced by bed height of adsorbent, initial concentration of adsorbate and flow rate. Results of the sorption process by the Fe-Al mixed oxide with variation of flow rate, initial concentration and bed mass/height on the sorption performance of hybrid material are presented in the form of breakthrough curves (BTC).

4.4.1 Flow rate effect on breakthrough

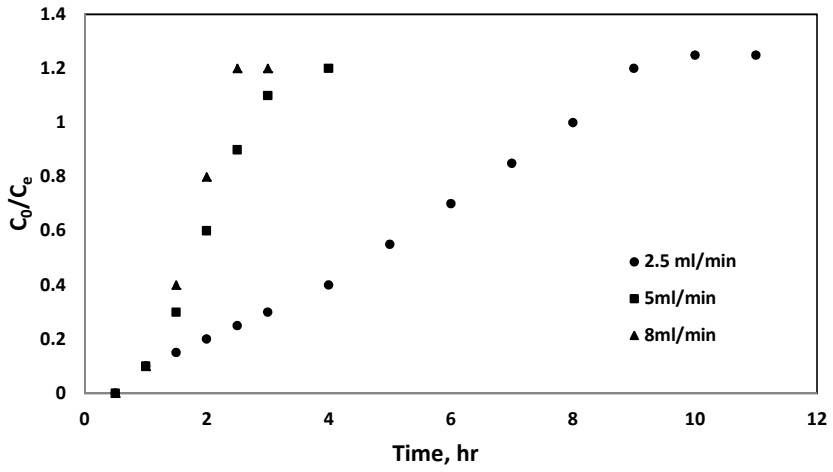

Figure 4.16 Breakthrough curves for F adsorption on Fe-Al mixed oxide nanoparticle at different flow rate

Figure 4.16 showed that the removal capacity of fluoride with an increase in the flow rate (2.5, 5.0 and 8.0 ml/min) was 556.5.3, 444 and 326.5 mg/kg, respectively. Considering the maximum allowable concentration of fluoride as 1.5mg/L, the breakthrough time for above said flow rates were 10, 4, and 2 hours, respectively.

With increase in the flow rate, the breakthrough curves becomes more steeper. This phenomenon is due to reduction in contact time between the adsorbing F^- and the adsorption media leading to fast approach towards the 10 mg/L initial concentration.

4.4.2 Initial fluoride concentration effect on breakthrough

The time of breakthrough decreased with increasing concentration of fluoride and were found to be 2, 4 and 8.5 hours for concentration of (15, 10 and 5 mg/l), respectively (Figure 4.17). The volume of water used corresponding to the initial fluoride concentration were 600, 1200 and 2500 ml.

The rate of adsorption is affected by the initial adsorbate concentration of a solute during the course of adsorption due to unavailability of the active sites. The bed volume (BV) and uptake capacity decreases with increasing initial concentration

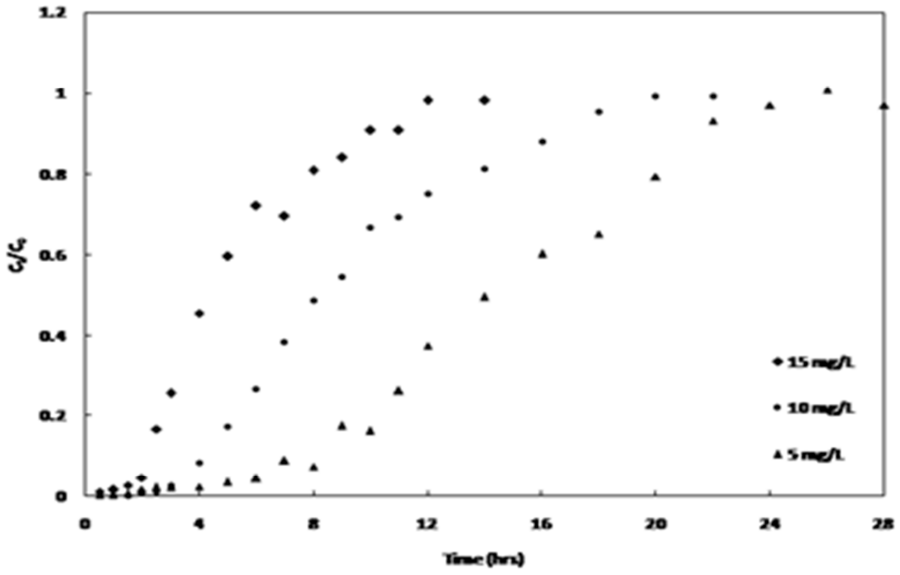

Figure 4.17 Breakthrough curves for adsorption of F on Fe-Al mixed oxide nanoparticle with concentration variation

4.4.3 Adsorbent mass (bed height) variation study on breakthrough

The experiment was carried out by taking arsenic solution with fluoride concentration; 10 mg/l and flow rate; 5 ml/min and flowed through fixed bed columns with different masses of of adsorbent (20, 30 and 40g). Time taken to reach a given effluent concentration increase with increasing adsorbent mass (Figure 4.18). This phenomenon is due to increased abundance of active sites for fluoride adsorption. The volumes of water tested till breakthrough point (1.5 ml/L), were found to be 1170, 1740 and 2220 ml, for 20, 30 and 40 g bed masses, respectively.

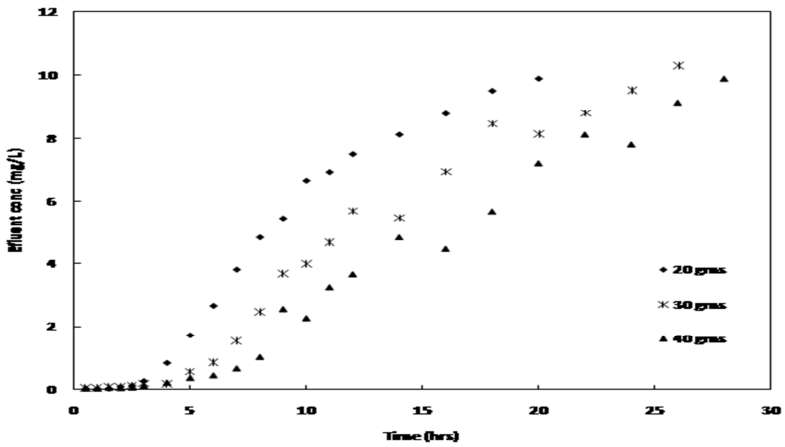

Figure 4.18 Breakthrough curves for adsorption of F on Fe-Al mixed oxide nanaoparticle with adsorbent mass variation

4.5 Chapter summary

Nano-structured rod-shaped Iron-Aluminium mixed oxide nano-particles were prepared by co-precipitation method at ambient temperature. Surface morphology of the material was investigated by SEM and TEM. The removal efficiency of fluoride on Fe-Al mixed oxide nanoparticle was investigated by batch as well as column adsorption process. The adsorption rate obeyed pseudo 2^{nd} order kinetic model and followed Langmuir adsorption isotherm model. The fluoride loaded adsorbent was successfully regenerated upto 93% at pH=12.

From the column study it was found that, Fe-Al mixed oxide nanoparticle was able to minimize fluoride concentration up to permissible limit.

Chapter 5

Synthesis of Chitosan encapsulated magnetic nanoparticle and its application for removal of fluoride from water

In the *present work, crosslinked ironoxide-chitosan nanoparticles (Fe_3O_4) was synthesized by microemulsion process for decontamination of fluoride from synthetic water. SEM, XRD, FTIR and magnetic property study was done for characterization of Ch-Fe_3O_4 nanoparticles. SEM, XRD and IR studies shows that the crosslinking of Fe_3O_4 with Chitosan resulted in formation of bigger size of particle compared to naked Fe_3O_4, indicating encapsulation of Fe_3O_4 with Chitosan. The fluoride removal capacity of Ch-Fe_3O_4 nanoparticle increases with increasing time and attains equilibrium within 120 min with 83.0% of fluoride removal. The rate of adsorption followed pseudo 2^{nd} order kinetic model and the adsorption process fitted well to Langmuir adsorption isotherm. The maximum adsorption capacity was calculated to be 33.62 mg/g from the experimental data. The thermodynamic study showed that the removal process was endothermic in nature. From column study showed that the adsorbent was capable of lowering the fluoride concentration to acceptable level.*

5.1 Introduction

Fluorine is one of the essential elements for human and animals. The benefits of low fluoride dosing (*Susheela et al. 2001; Agarwal et al. 1999*) and the risk of high fluoride dosing (*Hichour et al. 2000*) have been studied previously in literature.

In the field of water treatment use of nanoparticles is becoming difficult due to complicated separation process but in case of magnetic nanoparticles the separation is very easy by application of magnetic field. Hence magnetic nanoparticles are considered as effective adsorbents compared to other nanoparticles (*Murray et al. 1999*) in terms of environmental impact chemical stability and cost and maintenance. (*Taylor et al. 1984; shao e al, 2004*).

The objective of the present study was to study the simultaneous removal potential of fluoride by Magnetic chitosan nanoparticle. In order to achieve this, the magnetic nano particle was synthesized, characterized and their fluoride removal efficiency was studied.

5.2 Results and Discussions

5.2.1 Characterisation

Chemical analysis of the samples showed that the pure Fe_3O_4 nanoparticle sample contains 72.3% iron, Ch-Fe_3O_4 nanoparticle sample contains 67.5% iron and Glutaraldehyde added Ch-Fe_3O_4 nanoparticle contains 63.7% of Iron. The pH_{ZPC} of Gl-Ch- Fe_3O_4 nanoparticle was found to be 7.8.

5.2.2 XRD Analysis

From the XRD plot of naked Fe_3O_4 nanoparticle and Glutaraldehyde crosslinked Ch-Fe_3O_4 nanoparticle shown in Figure 5.1, six characteristic reflection peaks for Fe_3O_4(magnetite) were found that can be indexed to hkl = (220), (311), (400), (422), (511) and (440) for a cubic unit cell for both the samples, which can be indexed to JCPDS file (PDF No. 74-0748).

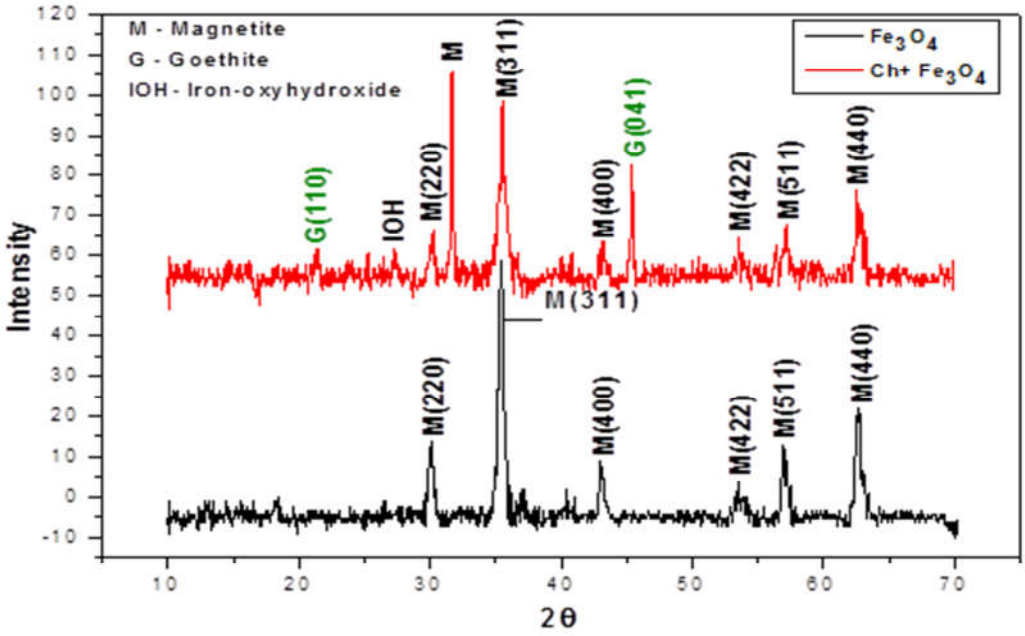

Figure 5.1 XRD pattern of naked Fe_3O_4 nanoparticle and Ch-Fe_3O_4 nanoparticle

For Gl-Ch- Fe_3O_4, two more reflection peaks for α-FeO(OH) (goethite) were obtained at hkl = (110) and(041) for a orthorhombic unit cell, which can be indexed to database in JCPDS file (PDF No. 17-0536). Another peak for amorphous Iron-oxide-hydroxide was obtained that could not be indexed to any hkl value and is consistent with the database in JCPDS file (PDF No. 05-0499). The analysis revealed that the synthesized naked Fe_3O_4 nanoparticle was pure magnetite and the coating process by chitosan resulted some phase changes resulting in a mixture of magnetite, goethite and Iron-oxide-hydroxide. The appearance of broad diffraction pattern indicates small particle size of Ch-Fe_3O_4 nanoparticle.

5.2.3 FTIR Analysis

FTIR spectra of the naked Fe_3O_4 nanoparticle, Ch-Fe_3O_4 nanoparticles and Glutaraldehyde crosslinked Ch-Fe_3O_4 nanoparticle were examined to realize the binding mechanism as shown in Figure 5.2. A wide band (3200~3500 cm^{-1}) is indexed N-H and O-H stretching vibrations of chitosan. The peaks at 570 (curve a) and 576 cm^{-1} (curve b) corresponds to both the stretching vibration mode and tensional vibration mode of Fe-O bond.

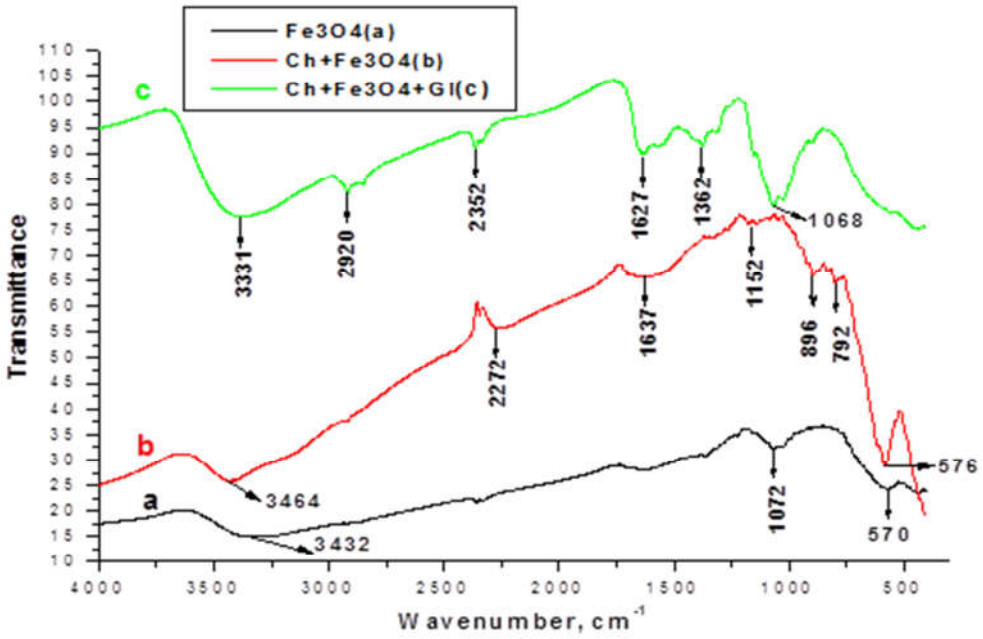

Figure 5.2 FTIR analysis (a) naked Fe_3O_4 nanoparticle, (b) Ch-Fe_3O_4 nanoparticle and (c) Glutaraldehyde cross linked Ch-Fe_3O_4 nanoparticle**.**

Characteristic band appeared at 1637cm^{-1} and 1627cm^{-1} for b and c respectively, can be indexed to N-H bending vibration of chitosan. In the spectrum of curve c, band at 1362cm^{-1} corresponds to -C-O stretching of alcoholic group of crosslinked glutaraldehyde. Band around 1068 cm^{-1} may be assigned to skeletal vibration of C-O stretch. The above results infered that chitosan was successfully coated to the magnetic Fe_3O_4 crosslinked with glutaraldehyde.

5.2.4 SEM Analysis

Surface morphology of both naked Fe_3O_4 nanoparticle and crosslinked Ch-Fe_3O_4 nanoparticle samples shown in Figure 5.3 were investigated using SEM and EDAX.

Figure 5.3(a) represents typical SEM micrograph of naked Fe_3O_4 nanoparticle. The SEM micrograph of crosslinked Ch-Fe_3O_4 [Figure 5.3(b)] presented relatively compact surface and some macropores. However, with the introduction of Fe_3O_4 nanoparticles into chitosan by microemulsion process, there were remarkable change was noticed on the surface morphology of crosslinked Ch-Fe_3O_4 nanoparticle [Figure 5.3(b)].

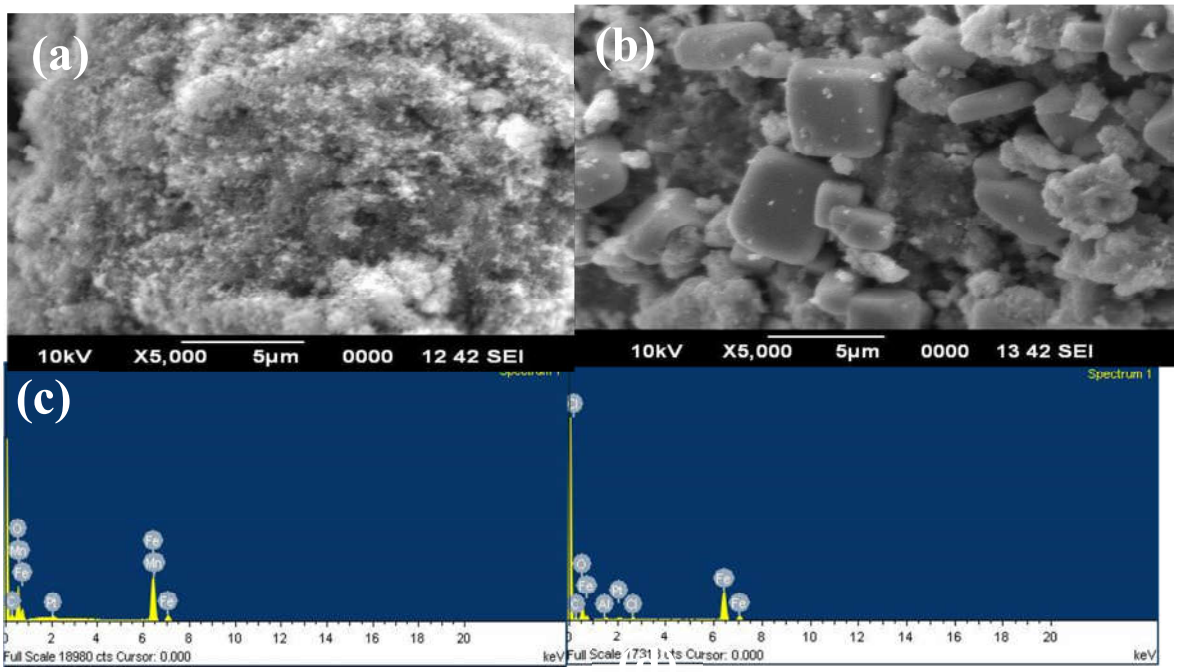

Figure 5.3 SEM and EDAX of naked Fe_3O_4 nanoparticle [(a) and (c)], and Ch-Fe_3O_4 nanoparticle [(b) and (d)]

The SEM micrograph of both the sample indicated that, the particle size of Ch-Fe_3O_4 nanoparticle was much bigger than that of naked Fe_3O_4 nanoparticle, indicating that naked Fe_3O_4 nanoparticle has been encapsulated by chitosan, which was in agreement with the XRD results.

5.2.5 Magnetic Property

Figure 5.4 demonstrates the magnetic hysteresis loop of Fe_3O_4 and Ch-Fe_3O_4 by VSM. For Fe_3O_4 nanoparticle an unsaturated hysteresis loop was obtained with application of magnetic field (1.5 T) indicating strong magnetic behavior (*Yogi and Varshney, 2013*). For Ch-Fe_3O_4, a saturated loop was observed with saturation magnetization (Ms= 25.23 emu/g) by application of same magnetic field. Thus Chitosan present in Ch-Fe_3O_4 induced complete orientation of magnetic domain in stable Fe_3O_4.

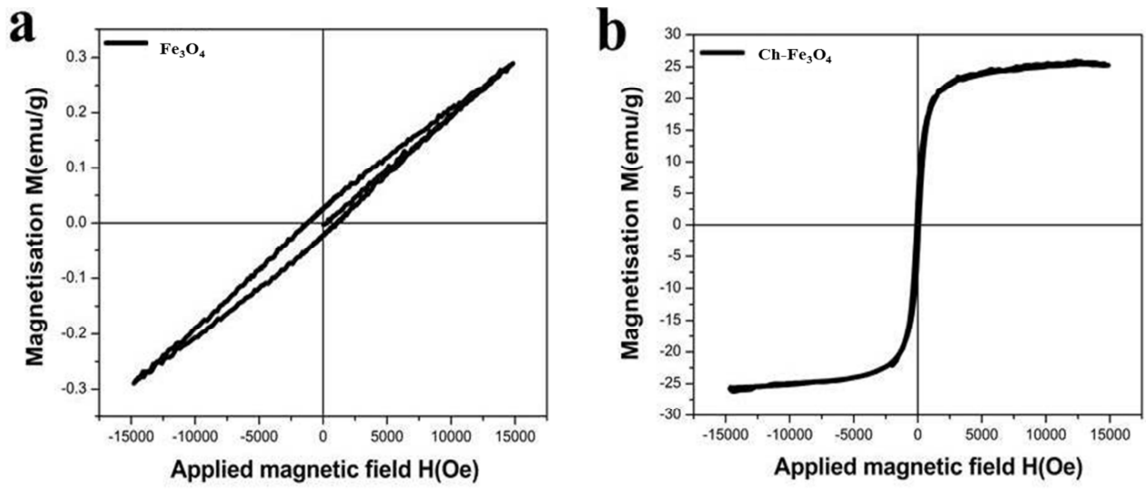

Figure 5.4 Magnetization curves of (a) iron oxide and (b) magnetic chitosan

5.3 Sorption Studies

5.3.1 Adsorbent dose variation

Figure 5.5 demonstrated the dose variation study of Ch-Fe_3O_4 for decontamination of fluoride for 10 mg/L of fluoride solution. The percentage removal of fluoride increased from 55-83% for a dose of 1~12g/L.

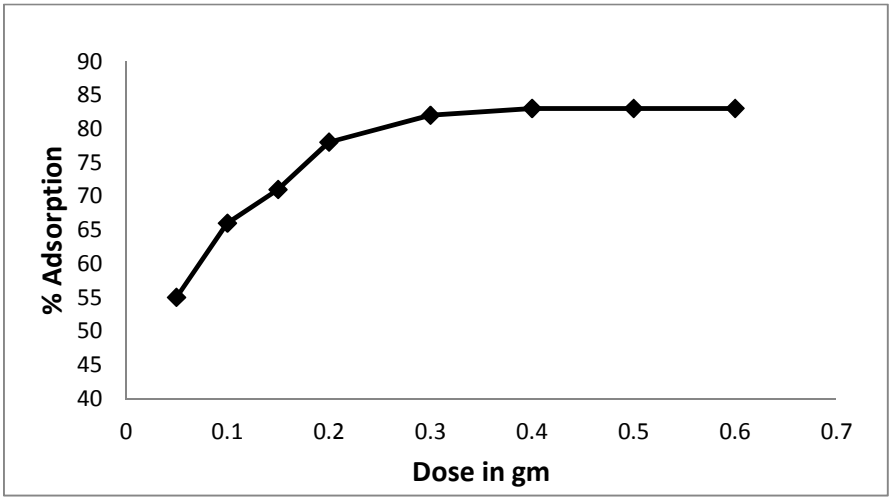

Figure 5.5 Adsorbent dose variation

After a dose of 8g/L, the removal percentage becomes almost constant as all the active sides were occupied at higher dose. Hence the optimal dose for removal process was considered as 8g/L.

5.3.2 Effect of pH

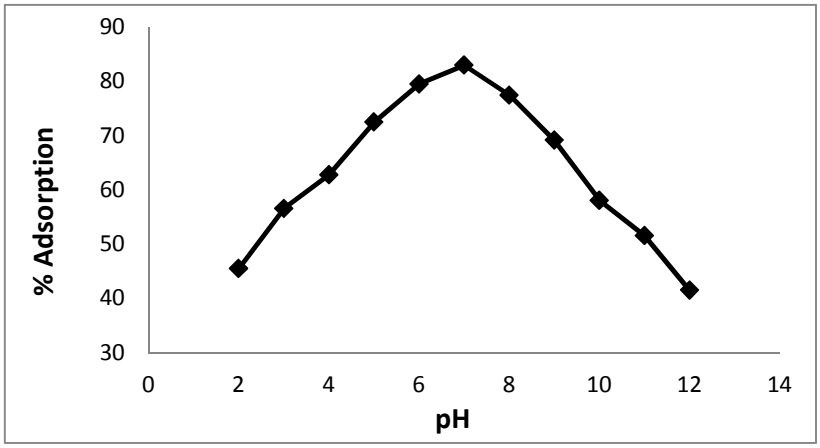

Figure 5.6 Effect of pH

Figure 5.6 showed the pH (2~12) variation study of Ch-Fe_3O_4 nanoparticle for fluoride removal for 10mg/L of fluoride concentration. There was an increase in the fluoride removal percentage with increase in pH ranging from 2~8 after which the removal percentage decreased. Hence the optimal pH for fluoride removal was around 7~8.

5.3.3 Kinetic Study

The rate of fluoride adsorption removal by Ch-Fe_3O_4 nanoparticle was investigated with the help of pseudo 1st order and pseudo 2nd order rate equation (Figure 5.7).

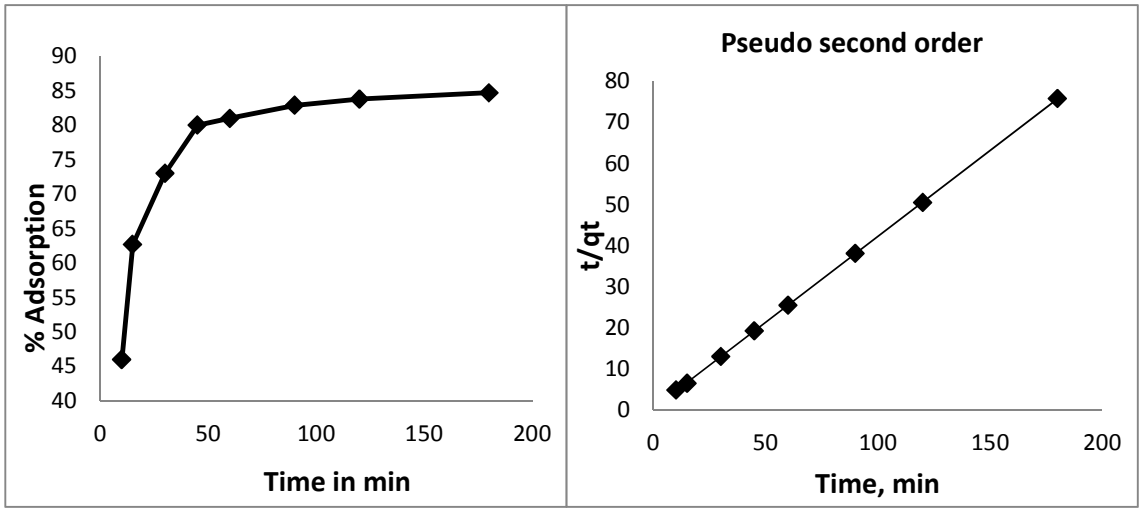

Figure 5.7 Time variation and kinetic study

Figure 5.7 showed time variation (10~180 mins) study of the adsorbent for fluoride removal. The percentage removal increased with increasing time up to 83.8% approaching equilibrium within 120 mins due to occupation of adsorbent adsorption sites in the adsorbent surface at higher concentration of fluoride. Hence rate of fluoride removal almost remains constant. The parameters obtained from both the kinetic model are given in Table 5.1, which shows that rate of adsorption was fitted better to pseudo 2nd order kinetic model (R^2=1).

Table 5.1: Parameters of kinetic rate equation

Pseudo 1st order				**Pseudo 2nd order**			
$q_{e,\ exp}$	**K_f**	**$q_{e,\ cal}$**	**R^2**	**$q_{e,\ exp}$**	**Ks**	**$q_{e,\ cal}$**	**R^2**
2.376	0.0483	2.791	0.908	2.376	0.3661	2.394	1

5.3.4 Adsorption isotherm

In the present investigation process of adsorption was analyzed through Langmuir (Figure 5.9) and Freundlich isotherm models. Figure 5.8 showed that the percentage removal of fluoride decreases with increase in the initial concentration (10~100 mg/L) due to unavailability of the coordination sites for adsorption at higher concentration of fluoride. The parameters calculated from Langmuir equation showed that the R_L= 0.0644 indicating favorable adsorption and q_{max}= 33.62mg/gm.

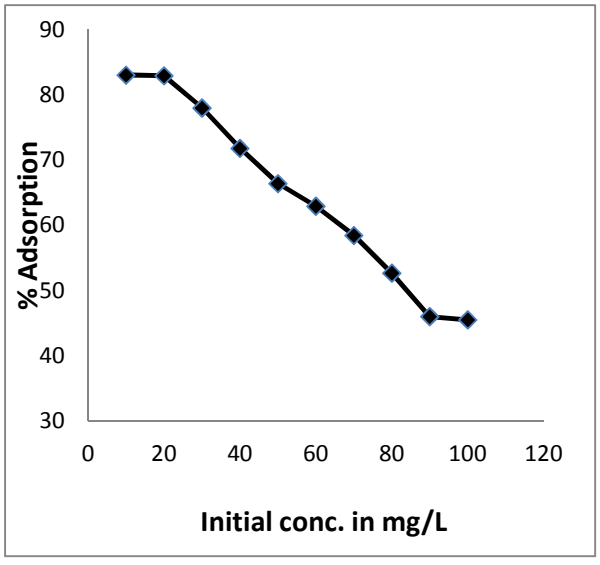

Figure 5.8 Effect of initial concentration

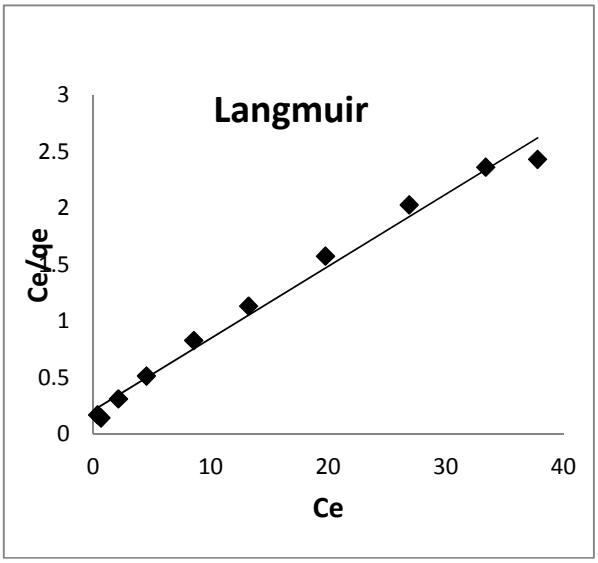

Figure 5.9 Adsorption isotherm

5.3.5 Temperature variation

Temperature variation study of the above said adsorbent for removal of fluoride with concentration (10mg/L) was shown in Figure 5.10. The removal percentage increased from 76 ~91%, for temperature (20°C~60°C) indicating the process to be endothermic.

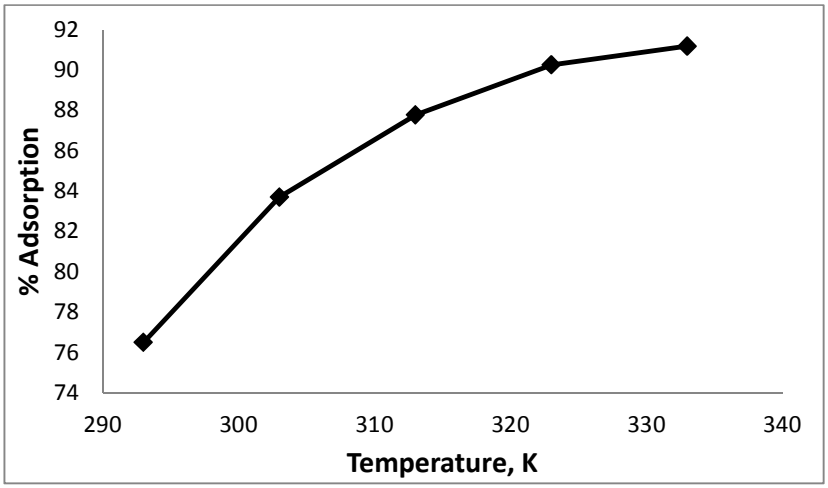

Figure 5.10 Temperature variation

5.4 Column Studies

Fixed bed column process is the most widely accepted technique in field of water treatment due to simplicity of the process and high efficiency of purification. The performance of fixed

bed study is generally influenced by bed height of adsorbent, initial concentration of adsorbate and flow rate. Results of the sorption process by the Ch-Fe_3O_4 nanoparticle with variation of flow rate, initial concentration and bed mass/height on the sorption performance of hybrid material are presented in the form of breakthrough curves (BTC).

5.4.1 Effect of flow rate on breakthrough

Figure 5.11 showed that the removal capacity of fluoride with an increase in the flow rate (2.5, 5.0 and 8.0 ml/min) was 547.5, 455 and 342.4 mg/kg, respectively. Considering the maximum allowable concentration of fluoride as 1.5mg/L, the breakthrough time for above said flow rates were 10, 4, and 2 hours, respectively.

With increase in the flow rate, the breakthrough curves become steeper. This phenomenon is due to reduction in contact time between the adsorbing F^- and the adsorption media leading to fast approach towards the 10 mg/L initial concentration.

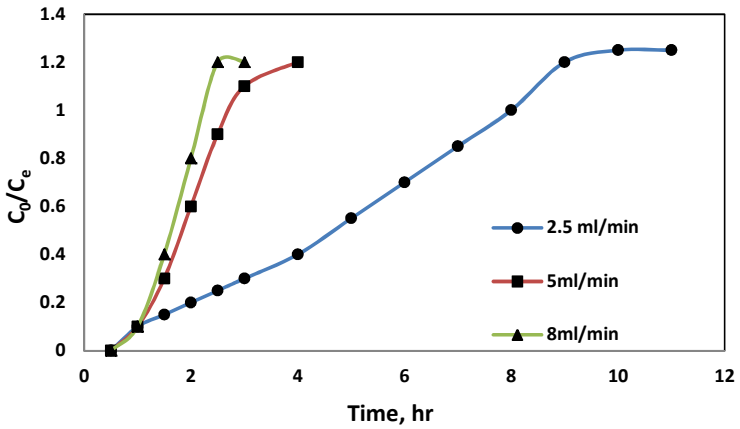

Figure 5.11 Breakthrough curves of F^- adsorption on Ch-Fe_3O_4 nanoparticle with flow rate variation

5.4.2 Initial fluoride concentration variation effect on breakthrough

The time of breakthrough decreased with increasing concentration of fluoride and were found to be 5, 12 and 16 hours for concentration of (15, 10 and 5 mg/l), respectively (Figure 5.12). The volume of water used corresponding to the initial fluoride concentration 800, 1600 and 3200 ml.

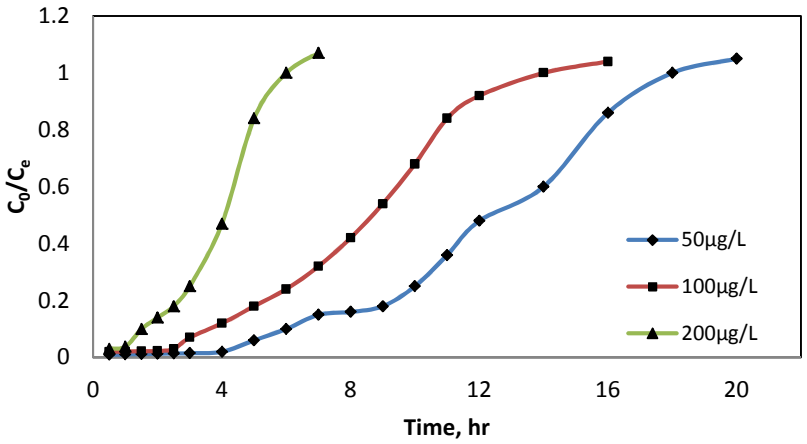

Figure 5.12 Breakthrough curves of F^- adsorption on Ch-Fe_3O_4 nanoparticle with concentration variation

The rate of adsorption was affected by the initial adsorbate concentration of a solute during the course of adsorption due to unavailability of the active sites. The BV (bed volume and uptake capacity) decreases with increasing initial concentration

5.4.3 Aadsorbent mass variation study on breakthrough

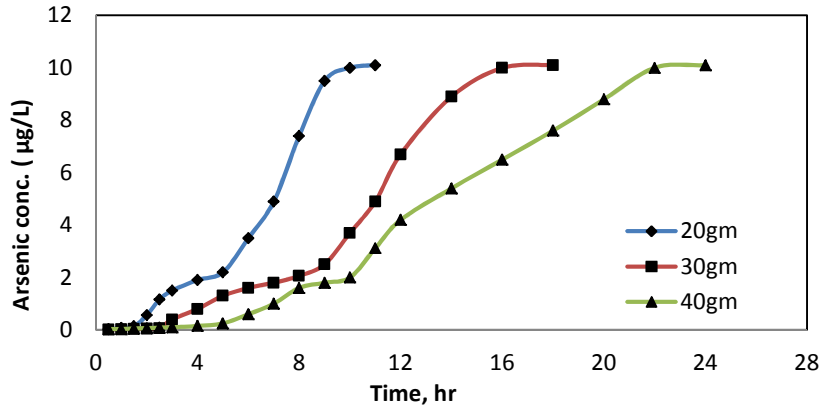

Figure 5.13 Breakthrough curves of F^- adsorption on Ch-Fe_3O_4 nanoparticle with adsorbent mass variation

The experiment was carried out by taking arsenic solution with fluoride concentration; 10 mg/l and flow rate; 5 ml/min and flowed through fixed bed columns with different masses of adsorbent (20, 30 and 40g). Time taken to reach a given effluent concentration increase with increasing adsorbent mass (Figure 5.13). This phenomenon is due to increased abundance of active sites for fluoride adsorption. The volumes of water tested till breakthrough point (1.5

ml/L), were found to be 1450, 2260 and 2740 ml, for 20, 30 and 40 g bed masses, respectively.

5.4.4 Application of Bed depth service time (BDST) model

The theoretical depth of adsorbent required to stop the concentration of adsorbate from exceeding the maximum allowable concentration limit is represented by bed depth C_b. Figure. 5.14 gives a plot of bed depth and service time to be a straight line.

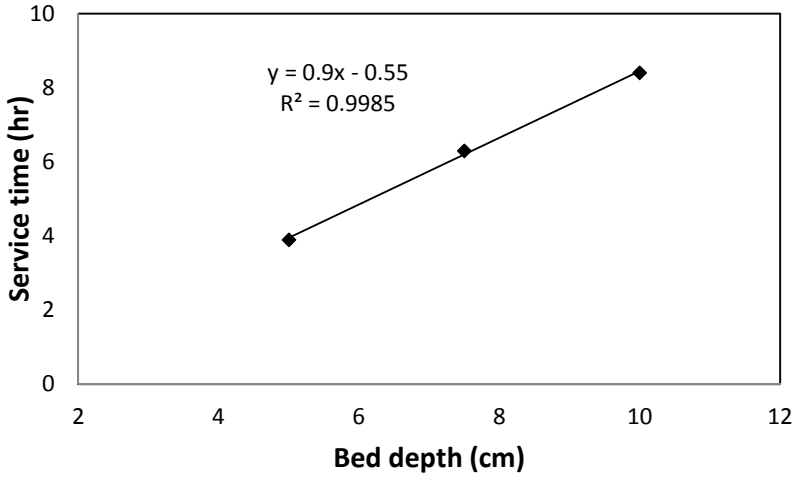

Figure 5.14 Linear BDST plot of bed depth and service time

The slope of BDST plot (Figure. 5.14) gives the time necessary for the adsorbate solution to cross a unit length through the adsorbent bed with certain experimental condition at a particular adsorbate concentration. In this study it was found to be 0.9hours for 1.5mg/L of fluoride.

The BDST parameter values (K, N_0 and x_0) are 0.583 l/mg hr, 563.02 mg/g and 0.781 cm, respectively. The K value determines the rate of mass transfer of the adsorbate from liquid phase to solid phase (adsorbent bed). Larger value of K indicates efficient removal of fluoride from contaminated water.

5.5 Chapter Summary

Ch-Fe_3O_4 nanoparticle was successfully synthesized by microemulsion technique and its application for fluoride decontamination from synthetic water. XRD, SEM and FTIR analysis were done for characterization of Fe_3O_4 and Ch-Fe_3O_4 nanoparticle. Maximum adsorption

occur in pH range (7~8). SEM, XRD and IR studies shows that the crosslinking of Fe_3O_4 with Chitosan resulted in formation of bigger size of particle compared to naked Fe_3O_4, indicating encapsulation of Fe_3O_4 with Chitosan. The rate of adsorption was fitted well to pseudo 2^{nd} order kinetics and the process obeyed Langmuir isotherm model. The maximum removal capacity is calculated to be 33.62 mg/g from the experimental data. The removal process is found to be endothermic and spontaneous in nature. Thus, the synthesized Ch-Fe_3O_4 can be considered as efficient adsorbent for fluoride removal. From the column study it is found that the synthesized adsorbent is capable of reducing the fluoride concentration up to permissible limit (1.5mg/L).

Chapter 6

Removal of fluoride by lanthanum incorporated porous Zirconium phosphate material

In the present work, porous Zirconium phosphate compound by incorporating Lanthanum onto it was synthesized using co-precipitation followed by hydrothermal method. The synthesized material was characterized using SEM, XRD, FTIR, TG-DTA, BET surface area analytical techniques. The removal efficiency fluoride by the mesoporous La-ZrP was examined by batch as well as column mode of adsorption. SEM and XRD analysis confirm the material to be mesoporous. Percentage removal of fluoride increased upto 96% with increasing contact time and attains equilibrium within 120min at optical condition of adsorbent dose; 4g/l, initial concentration; 10mg/L, pH; 7. The rate of removal process followed pseudo 2^{nd} order kinetic model and the isotherm data fitted better to Langmuir adsorption model. The maximum adsorption capacity was calculated to be 83.9 mg/g. Temperature variation study indicated endothermic nature of the process. Mesoporous La-ZrP material was successfully regenerated and reused upto five cycles of adsorption. Results of the column study showed that the mesoporous material lowered the fluoride concentration upto acceptable limit.

6.1 Introduction

According to WHO guidelines, the maximum permissible limit of fluoride in drinking water is 1.5mg/L, exceeding which can cause skeletal and dental fluorosis with various adverse effects. (*Samatya et al. 2007*). Adsorption process is comparatively economic, simple and suitable method for fluoride decontamination between all reported methods for water treatment (*Mohapatra et al. 2009; Ayoob et al. 2007*).

Generally porous materials are differentiated into three categories based on their pore size. The pore diameter of micro porous material is < 2nm and that of macro porous material is > 50nm, while the pore diameter of mesoporous material ranges from 2 ~ 50nm. A very few literatures reported the mesoporous ZrP with high surface area for removal of fluoride (*Tarafdar et al. 2006; Jung et al. 2007*). As fluoride has strong affinity towards Zr and the structural characteristics of Lanthanum also increases fluoride removal, thus mesoporous ZrP considered as good absorbent for fluoride remediation.

So, the present work is focused on synthesis and characterization of mesoporous La-ZrP by FTIR, XRD, SEM to study its efficiency of fluoride removal.

6.2 Results and Discussions

6.2.1 Characterisation

The pH_{ZPC} of the mesoporous La-ZrP was found to be 6.8 and the particle size was found to be 186nm. The material showed a lower pH_{ZPC} due to presence of higher number of singly coordinated groups on the surface.

6.2.2 XRD Analysis

Figure 6.1 shows the XRD data for three different La-ZrP (as synthesized, ethanol washed and calcined) in which sharp reflections were obtained in low angle range (<5°). Three sharp distinguishable peaks are indexed to hkl = (1 0 0), (1 1 0), and (2 0 0) planes for hexagonal unit cell.

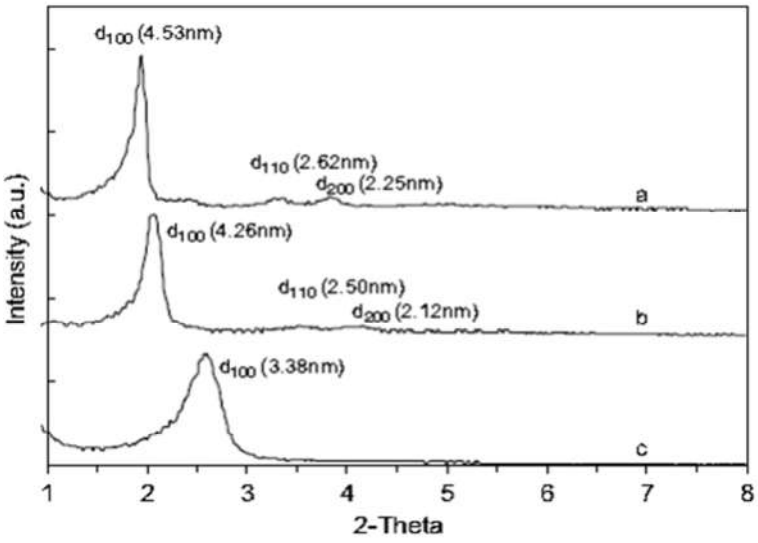

Figure 6.1 XRD plot (a) As synthesized, (b) Ethanol washed, (c) Calcined at 500°C

In as prepared La-ZrP, the peak of $d_{(1\,0\,0)}$: a=4.53nm is two times that of $d_{(2\,0\,0)}$; a=2.25nm showed presence of pores having hexagonal structure. For ethanol washed and calcined La-ZrP the XRD data showed intense peak at $d_{(1\,0\,0)}$ but comparatively weak peaks of $d_{(11\,0)}$ and $d_{(2\,0\,0)}$ due to removal of the surfactant after calcination at 500°C.

6.2.3 Thermal Analysis

The TGA plot for La-ZrP (as prepared) shown in Figure 6.2 demonstrates that an uninterrupted loss of weight occur up to 500°C and no decomposition occurs above that up to 500°C.

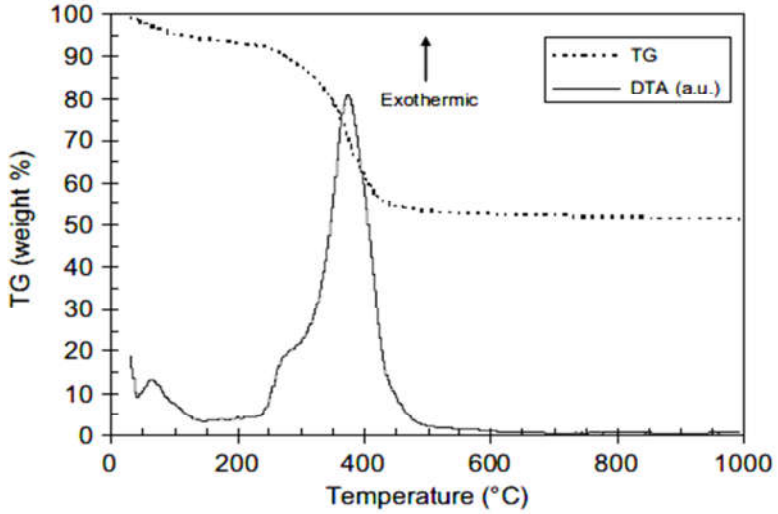

Figure 6.2 TG and DTA plot of as synthesized ZLP sample

The DTA plot demonstrates initial weight loss of 7.3% below 200°C, that may be because of elimination of interparticle and intraparticle water molecules. The a weight loss of 39% was observed from 200~500°C due to decomposition of organic surfactant. Again, total weight loss of 46% occurred 500–550°C indicating complete removal of surfactant.

6.2.4 FTIR Analysis

FTIR shown in Figure 6.3 demonstrates the complete removal of the surfactant from La-ZrP by calcination at 500°C. By comparing FTIR data, two sharp peaks at about 2846 cm^{-1} and 2917cm^{-1} (corresponding to C-H bond stretching of CH_3 group present in surfactant) are obtained for as prepared La-ZrP are absent for La-ZrP calcined at 500°C. This confirm that the surfactant was completely removed from the surface after calcination at 500°C. complete removal of surfactant. Presence of broad peak at 3392cm^{-1} represents asymmetric O-H bond stretching vibration of water molecule. Peaks at 2359cm^{-1} in both cases of as synthesized and calcined sample corresponds to P-O-H stretching vibration. Peaks observed at 1632cm^{-1} and 1639cm^{-1} in both the cases represents bending vibration of water (δ(O-H)). In the spectra of as synthesized sample peak at 1400cm^{-1} corresponding to deformation band of NH_4^+ disappears in that of the Calcined sample, which confirms removal surfactant NH_4^+. The peak obtained at 746 cm^{-1} correspond to P-O-P stretching vibration.

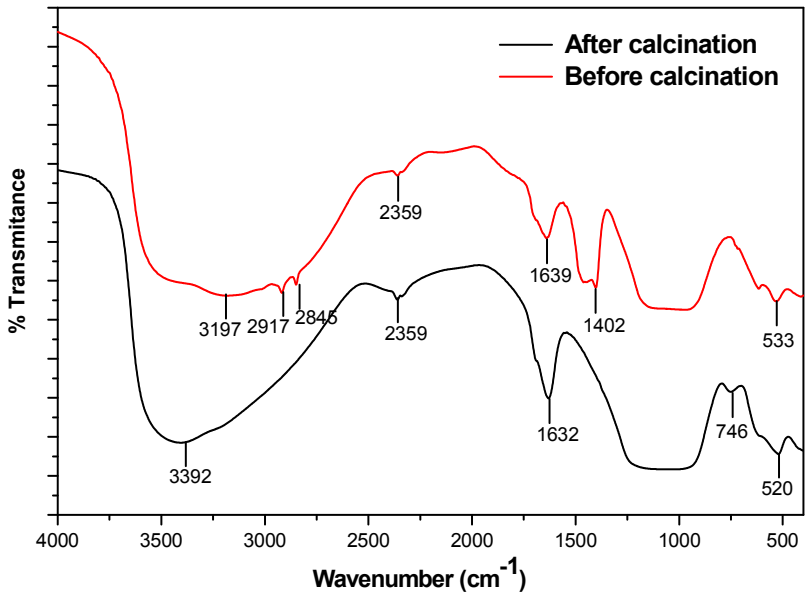

Figure 6.3 FTIR analysis of La-ZrP before and after calcination

6.2.5 SEM study

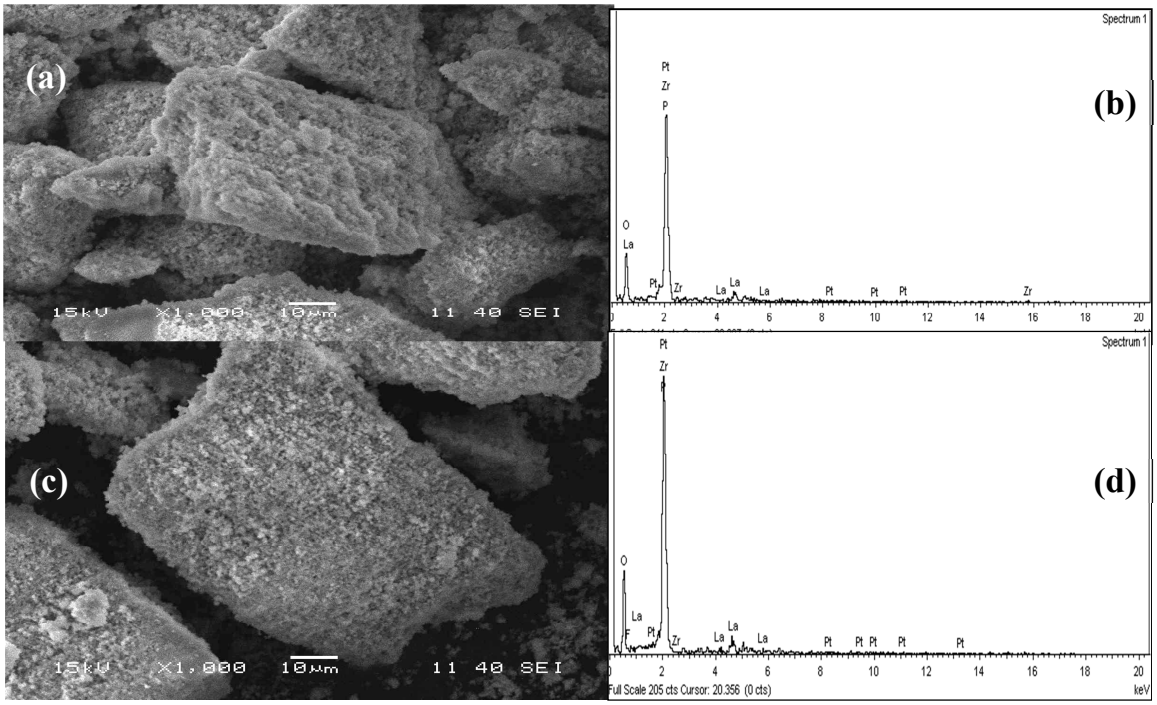

Figure 6.4 SEM image and EDAX plot of porous La-ZrP [(a), (b)] before adsorption, [(c), (d)] after adsorption.

SEM micrograph shown in Figure 6.4, for both Mesoporous ZrP [Figure 6.4(a)] and fluoride adsorbed La-ZrP [Figure 6.4(c)] shows accumulation of fluoride particles on La-ZrP surface after adsorption. The EDAX spectra showed signals for O, P, La, Zr and F in Figure 6.4(d) for the material after adsorption. Simultaneously, the molar ratio of La/Zr was found to be 2.15 from EDAX data.

6.2.6 BET surface analysis

Figure 6.5 describes the surface area and pore size distribution mesoporous ZrP [Figure 6.5(a)] and La-ZrP [Figure 6.5(b)] by nitrogen adsorption–desorption isotherm. The surface area of La-ZrP and ZrP were calculated to be 880.4 and 1266.3 m^2/g respectively.

The present analysis demonstrated that, doping of Lanthanum on ZrP decreased the pore diameter and surface area with increasing the pore volume and pore wall thickness. Hence both the mesoporous compound has narrow pore size distributions.

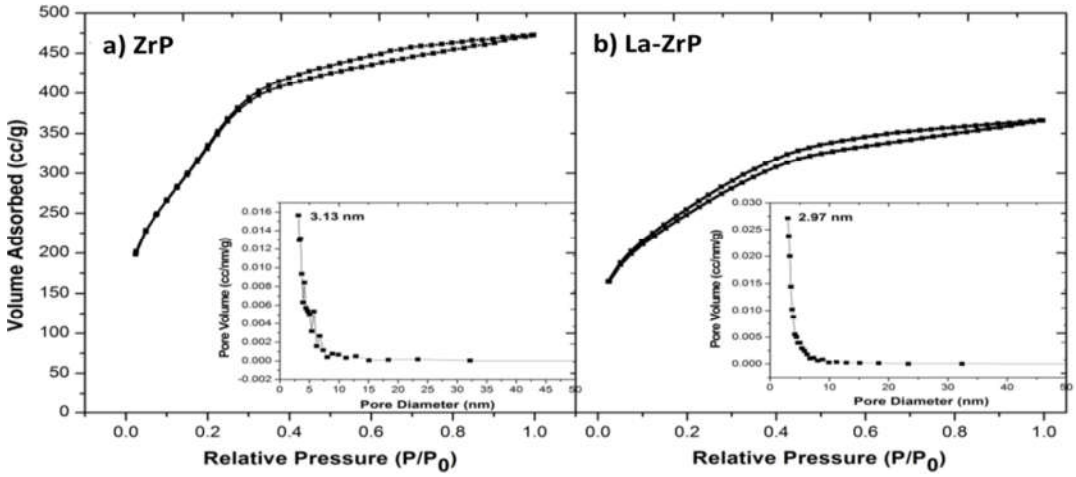

Figure 6.5 N_2 adsorption/desorption isotherms of (a) ZrP and (b) La-ZrP and the relevant pore size distribution curves (inset)

6.3 Sorption studies

6.3.1 Effect of adsorbent dose

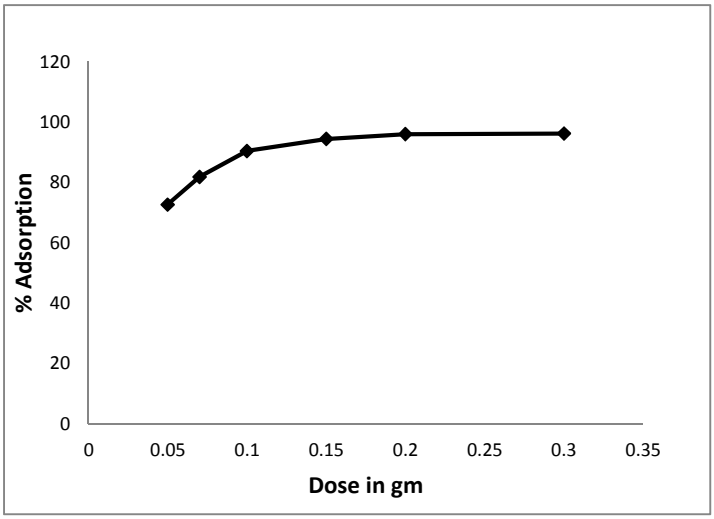

Figure 6.6 adsorbent dose variation

The fluoride removal efficiency of La-ZrP was carried out with variation of dose at contact time two hours and initial concentration 10mg/L. Figure 6.6 showed that the efficiency of fluoride adsorption was found to be 72.7~96.0% for 1~6g/L of adsorbent. The adsorption increased up to 0.2 gm of dose and becomes constant after that due to unavailability of active sides for adsorption. Thus, the optimal dose for fluoride adsorption was found to be 4g/L.

6.3.2 Effect of pH

Fluoride adsorption capacity of mesoporous La-ZrP was investigated with variation of pH= 2~12. From Figure 6.7, there was an increase in fluoride adsorption from pH (2~7) and decreases after that. Hence the optimal pH for fluoride removal was considered as pH=7. As the pH_{ZPC} of mesoporous La-ZrP was calculated to be 6.8, the favorable pH for adsorption is 6.5~7.

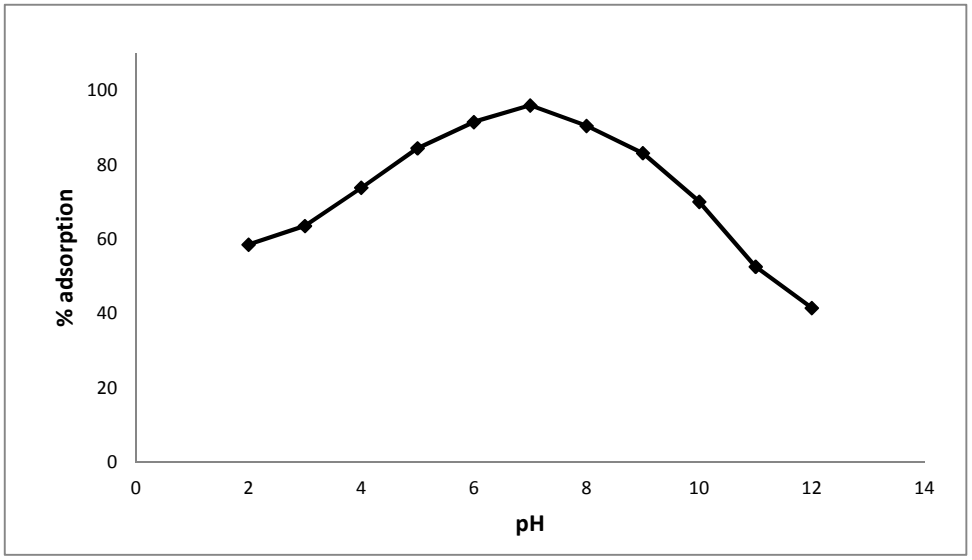

Figure 6.7 Effect of pH

6.3.3 Mechanism of adsorption

By considering the pH variation study, the following mechanism can be proposed for adsorption of fluoride :

(i) At pH less than pH_{ZPC}, the possible mechanism can be force of attraction (electrostatic) (6.1) or a ligand/anion exchange (6.2).

$$MOH(s) + H_3O^+ + F^- \rightarrow MOH_2 + \cdots F^- + H_2O \quad (6.1)$$

$$MOH(s) + H_3O^+ + F^- \rightarrow M^+ \cdots F^- + 2H_2O \quad (6.2)$$

where M stands for mesoporous La-ZrP. Hence fluoride is assumed to adsorbed by a surface phenomenon only.

(ii) At pH > $pH_{ZPC,}$ the adsorbent surface is negatively charged by decreasing the removal of fluoride due to repulsion effect. In this context adsorption may occur due to weak Vander Waal force (6.3) between Na^+ and F^- as Na^+ is attracted to the adsorbent surface.

$$MOH(s) + Na^{+}(aq) + F^{-}(aq) + OH^{-} \rightarrow MO\cdots Na^{+}\cdots F^{-} + H_2O \quad (6.3)$$

6.3.4 Kinetics of Adsorption

The kinetics study of fluoride removal efficiency of mesoporous ZrP was examined by means of pseudo 1st order and pseudo 2nd order rate equation.

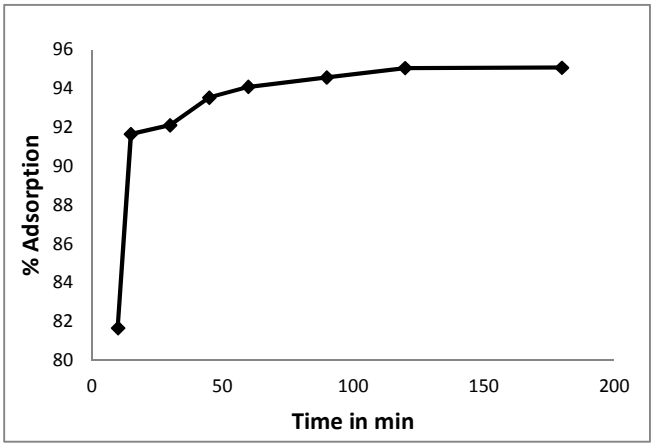

Figure 6.8 Time variation

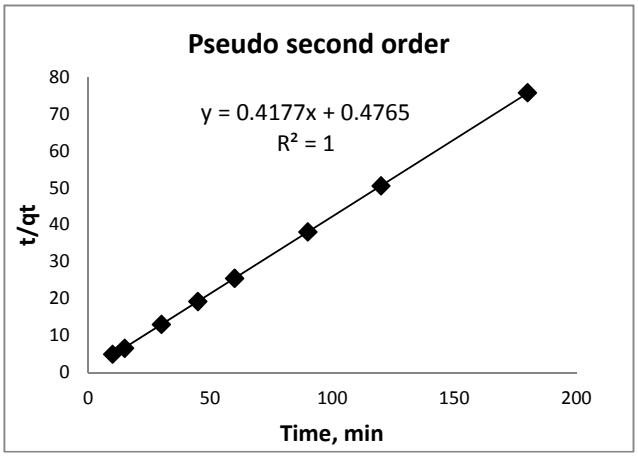

Figure 6.9 Kinetics study

The kinetic study of fluoride removal was done with variation of time (10~180 mins) represented in Figure 6.8. The fluoride removal capacity increase with increase in time and approached equilibrium within 120 mins with maximum adsorption of 96.4%. As initially, the availability of the adsorbent sides and adsorbate concentration was very high the adsorption increased. After equilibrium point, the fluoride adsorption rate becomes constant due to less number of adsorbent site and low fluoride concentration.

Figure 6.9 represents linear plot of pseudo 1st order and pseudo 2nd order kinetic rate equation. The parameters obtained from slope and intercept from the above plots are given in Table 6.1, which shows that, the values of q_e (exp) and q_e (cal) are similar and the correlation coefficient =1. Hence the adsorption kinetics for fluoride removal followed the pseudo 2nd order kinetic model.

Table 6.1: Parameters of kinetic rate equation

Pseudo 1st order				**Pseudo 2nd order**			
q_e(cal)	**q_e (exp)**	**K_f**	**R^2**	**q_e(cal)**	**q_e (exp)**	**K_S**	**R^2**
2.791	2.376	0.0483	0.908	2.394	2.376	0.3661	1

6.3.5 Adsorption isotherm

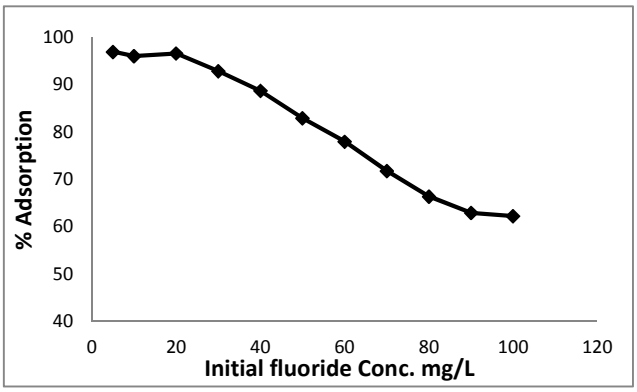

Figure 6.10 Effect of initial concentration

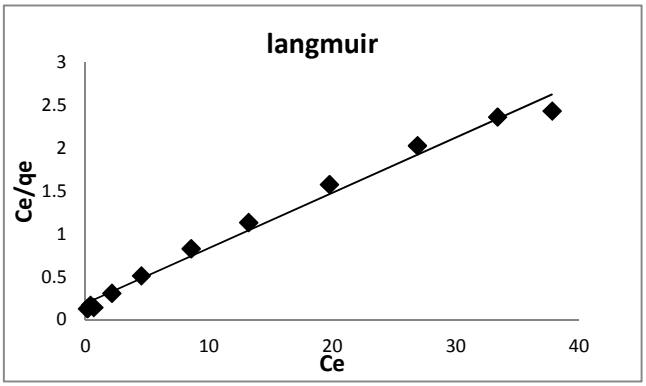

Figure 6.11 Adsorption isotherm

In this study, the equilibrium relationship of the adsorbent with the adsorbate was examined by Langmuir and Freundlich isotherm equations. Figure 6.10 shows that the

fluoride removal percentage decreases with increase in initial concentration of fluoride because of the fact that the binding capacity of mesoporous La-ZrP becomes saturated with increasing concentration.

The parameters obtained from linear plots of Freundlich and Langmuir model justifies the feasibility of process (Table 6.2). The value of R_L value < 1 shows favorable removal, while R_L value greater than one shows unfavorable removal (*Dey et al. 2010*). In the present study, R_L value was calculated to be 0.0644, justifying favorable adsorption process. From the estimated parameters given in Table: 6.2, it is found that model Langmuir fitted better than Freundlich model and the monolayer surface coverage, q_m was found to be 5.285mg g^{-1}. Thus, it could be inferred that La-ZrP surface has good affinity for fluoride.

Table 6.2: Parameters of isotherm models

Freundlich model			**Langmuir model**		
R^2	**1/n**	**K_f**	**R^2**	**K_L(L/mg)**	**q_m(mg/g)**
0.927	0.41	3.908	0.99	2.953	5.258

6.4 Effect of temperature

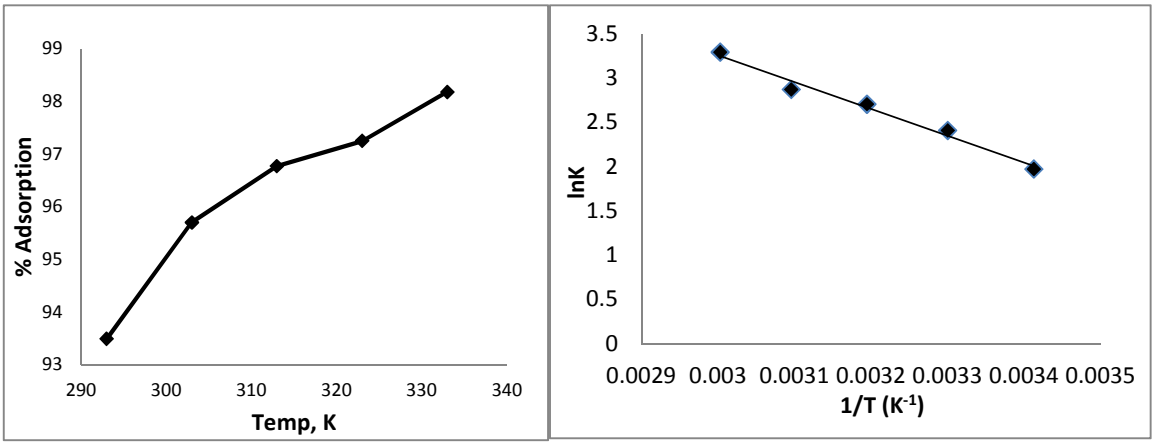

Figure 6.12 Effect of temperature and Vant-hoff's curve

Figure 6.12 showed temperature variation study on fluoride removal efficiency of mesoporous La-ZrP. The removal % increased from 93.4 ~ 98.1 with increasing temperature (20~60°C) indicating endothermic nature of adsorption.

6.4.1 Regeneration-Reuse Studies

The adsorbent material gets exhausted and its removal capacity decrease at the end of the process. So, it needs to be regenerated for further use. In this study regeneration was carried out by leaching out of fluoride at different pH to evaluate the optimal pH at which complete regeneration occurs.

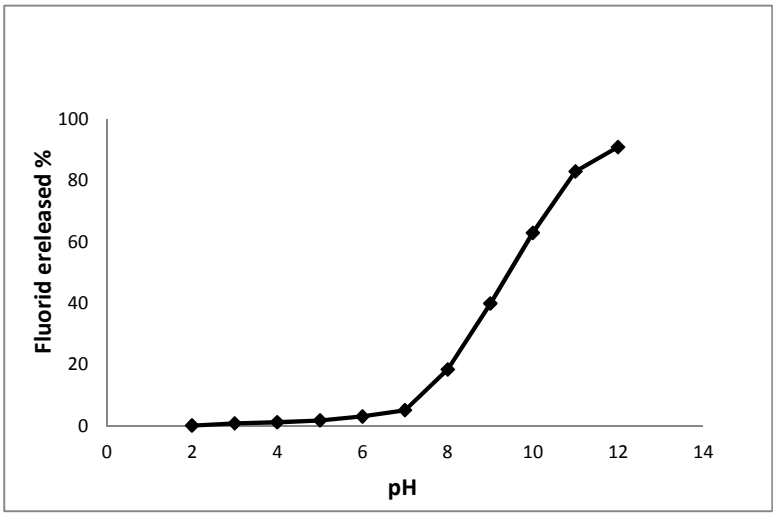

Figure 6.13 Desorption study

Figure 6.13 represents, the results of desorption study of fluoride loaded mesoporous La-ZrP at different pH in aqueous medium. At pH greater than 8, large concentration of fluoride was leached out from the adsorbent surface and 91% of fluoride was eluted out at pH=12. Thus, the regenerated material could be used for five number of cycles in a batch process (Figure 6.14).

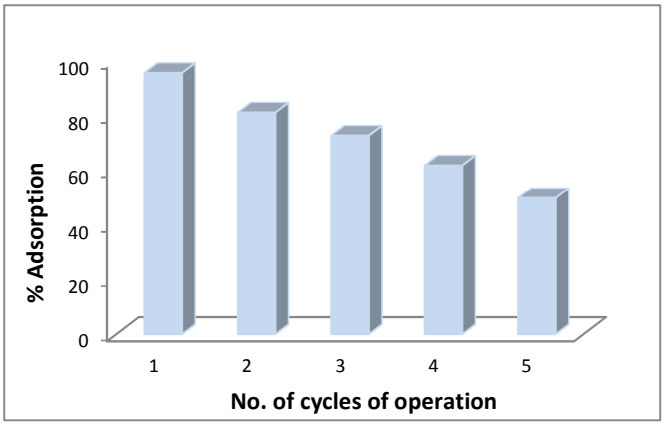

Figure 6.14 The reusability study

The fluoride removal percentage of mesoporous La-ZrP decreased from 95.5 to 49.8% for first to fifth cycle of batch adsorption study.

6.4.2 Effect of interfering ions

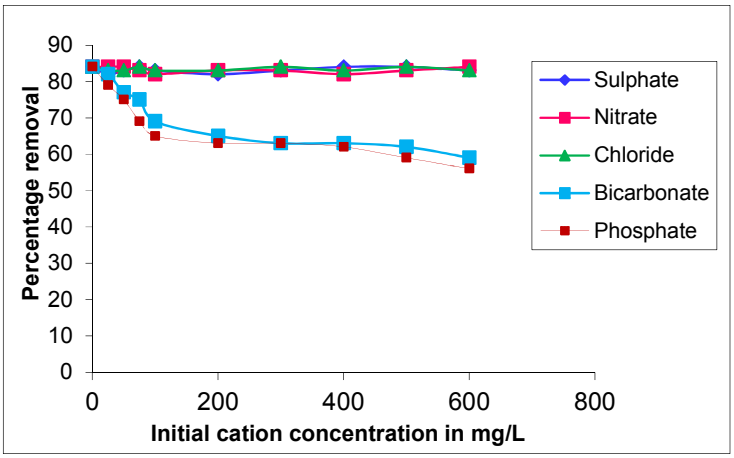

Figure 6.15 Effect of competitive ions on fluoride removal

Effect of competitive ions upon adsorption of fluoride was analysed using sodium salts of chloride, phosphate, bicarbonate, nitrate and sulphate ions as co-ions by keeping the fluoride concentration (10 mg/L) with variation of initial concentration of competitive ions (25~600mg/L). The graphical result shown in the Figure 6.15 indicates that the fluoride removal process had been significantly affected in presence of PO_4^{3-} and HCO^{3-} ions. However, presence of NO^{3-}, Cl^-, SO_4^{2-} had less comparable effect on adsorption of fluoride. This might be due to difference in pH of the solutions of the co-ions.

The pH of the solutions were 6.7, 6.2, 7.1, 8.6 and 10.2 for NO^{3-}, Cl^-, SO_4^{2-}, PO_4^{3-} and HCO^{3-} respectively. From the studies on effect of pH it was concluded that uptake of fluoride was most favourable within the pH range of 6 to 7 and decreases with increase in the pH towards alkaline range. As the pH of the solutions of NO^{3-}, Cl^-, SO_4^{2-} ions are in the range of 6-7 fluoride adsorption was not much affected in their presence than that in case of PO_4^{3-} and HCO^{3-} as their pH are in the alkaline range.

6.5 Column Study

The performance of fixed bed study is generally influenced by bed height of adsorbent, initial concentration of adsorbate and flow rate. Results of the sorption process by the

mesoporous La-ZrP with variation of flow rate, initial concentration and bed mass/height on the sorption performance of hybrid material are presented in the form of breakthrough curves (BTC).

6.5.1 Flow rate effect on breakthrough

From Figure 6.16, it was found that the adsorption capacity of fluoride with an increase in the flow rate of 2.5, 5.0 and 8.0 ml / min was 556.3, 438 and 342.0 mg/kg, respectively. Considering the maximum allowable concentration of fluoride as 1.5 mg/L, the breakthrough time for above said flow rates were 10, 4, and 2 hours, respectively. With increase in the flow rate, the breakthrough curves become steeper.

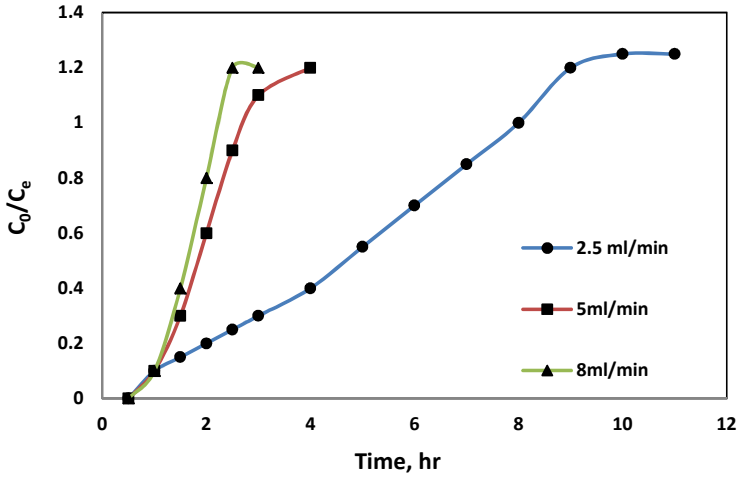

Figure 6.16 Breakthrough curve for fluoride removal on La-ZrP with flow-rate variation

6.5.2 Effect of initial fluoride concentration on breakthrough

The time of breakthrough decreased with increasing concentration of fluoride and were found to be 4, 13 and 17 hours for concentration of 15, 10 and 5 mg/l, respectively (Figure 6.17). The volume of water used corresponding to the initial fluoride concentration were 800, 1600 and 3200 ml.

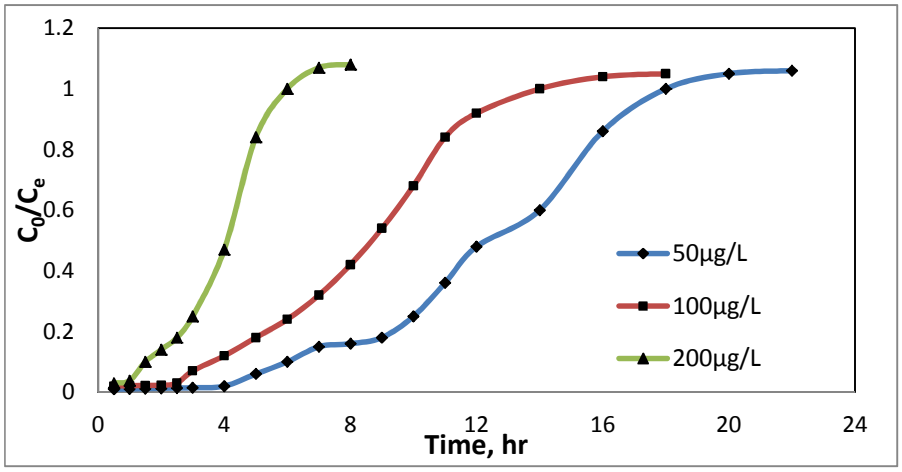

Figure 6.17 Breakthrough curves for fluoride removal on La-ZrP with concentration variation

6.5.3 Adsorbent mass/bed variation on height on breakthrough

The experiment was carried out by taking fluoride solution with initial concentration of 10 mg/l and flow rate 5 ml/min and crossed through columns with different adsorbent masses of 20, 30 and 40g. Time taken to reach a given effluent concentration increase with increasing adsorbent mass (Figure 6.18). This phenomenon is due to increased abundance of active sites for fluoride adsorption.

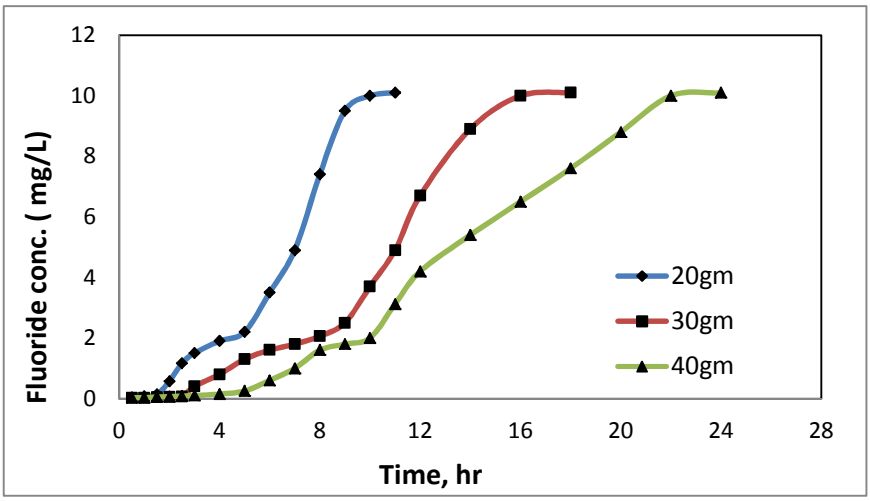

Figure 6.18 Breakthrough curves for fluoride removal on La-ZrP with bedmass variation

6.6 Chapter Summary

In this research, mesoporous La-ZrP was synthesized for fluoride remediation from synthetic water. The main outcomes of the study are

- Maximum adsorption of fluoride (83.9mg/g) occurs at pH=7.
- The rate of adsorption obeyed pseudo 2nd order kinetic model.
- The removal process best fitted to Langmuir isotherm model with a monolayer adsorption.
- Temperature variation study confirms the process to be endothermic and spontaneous.
- From desorption experiment, it was found that the material could be regenerated and reprocessed for several cycles.
- Thus decontamination of fluoride by mesoporous La-ZrP was cost effective to reach the maximum allowable limit of fluoride in water.

The La-ZrP mesoporous compound was successfully used in removal of fluoride using fixed bed columns.

Chapter 7

Mg/Fe layered double hydroxide nanoplates and their adsorption behaviour of As(V) from water

In the present study, Layered double hydroxides (LDHs) are studied for adsorption of arsenic due to their exceptional ion exchange capacity. Mg/Fe LDH nanoplates with different molar ratios of (3:1, 4:1, 5:1) are synthesized by a solvothermal method. The results obtained through comparative study, show that variation in molar ratio (Mg/Fe) has a strong effect on adsorption of As(V) by as-synthesized LDHs. The samples with (Mg/Fe) molar ratio of 4:1 shows highest adsorption rate and adsorption capacity that is ascribed to the higher surface area.

7.1 Introduction

Layered double hydroxides (LHDs) have gotten incredible consideration because of their high anion exchange capacity and crystal structure comprises of +vely charged brucite-like sheets and the intercalation of anions in the hydrated interlayer areas, which balance the positive charges (*Hong et al. 2014; Zhong et al. 2013; Yaun et al. 2013; Wu et al. 2013*). Recently assessment of removal capacity of organic and inorganic anionic pollutants by LDH have been attemped by means of adsorption and ion exchange process due to, high anion exchange ability of LDH caused by weak interlayer bonding (*Ku et al. 2003; Genj et al. 2013; Zheng et al. 2012*). There are various literature reporting of arsenic removal by LDHs and calcined LDHs (*Turk et al. 2009; Carja et al. 2008;Kang et al. 2013*)

Considering arsenic as one of the highly toxic and carcinogenic material and arsenic toxicity as priority issue (*WHO*), decontamination of drinking water from it has been an insurmountable problem in field of water treatment (*Upadhyaya et al. 2010; Gonzalez-Contreras et al. 2010; Pallier et al. 2010*).

A number of researches have been reported on sorption of arsenic onto LDH minerals (*Zhu et al. 2012; Zhang et al. 2013*). As arsenic is frequently found on the surface of iron oxides in natural habitat, it has high chances of getting adsorbed adsorption on iron oxide surface. So LDHs containing iron can be better adsorbents for arsenic decontamination.

Therefore, objective of this research work is to develope Mg/Fe-CO_3 LDHs with different molar ratios of Mg/Fe by solvothermal method and to examine the removal capacity of arsenic. The material was characterized by FTIR, SEM with (EDS) Technique, (TEM) and (XRD).

7.2 Results and Discussions

7.2.1 Characterisation

The elemental analysis results for all materials are given in Table 7.1. The calculated Mg/Fe molar ratios of the as synthesized samples are approximately similar to the quantity added during preparation. This indicates that co-precipitation has been done successfully.

Table 7.1: Chemical composition

Sample	Mg^{2+} (mass %)	Fe^{3+} (mass %)	Mg/Fe (molar ratio)
Mg3Fe	19.05	16.15	2.943
Mg4Fe	22.72	13.16	4.002
Mg5Fe	24.37	12.42	4.974

7.2.2 XRD Analysis

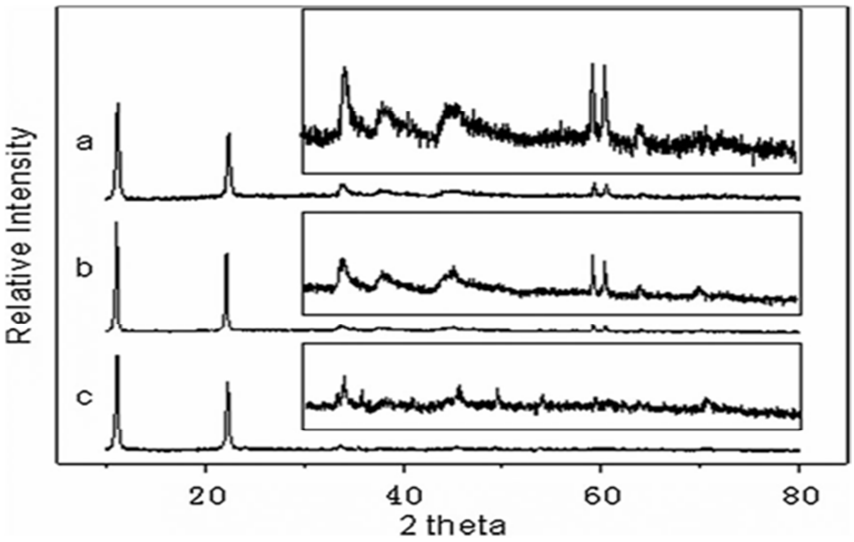

Figure 7.1 XRD plot of samples [Mg/ Fe: (a) 5:1; (b) 4:1; (c) 3:1.]

The XRD analysis of the as synthesized LDHs with different molar ratios of (Mg/Fe) (Figure 7.1) demonstrates two sharp peaks at 111(7.92 Å) and 221(3.97 Å), that can be recorded to (003) and (006) of hydrotalcite-like structure. The two strong peaks obtained for all three as synthesized samples are similar indicating presence of analogue interlayer structure in the as-prepared LDHs . The weak peaks (inset of Figure 7.1) can be attributed to the facets attached to the intra-layer structure. The difference in the peak intensity may be due to difference in Mg/Fe molar ratio. Crystal cell parameters of the as synthesized LDH were calculated as a = 3.10 Å and c = 23.76 Å through analysis of XRD results. The XRD pattern didn't show any secondary phases for $Mg(OH)_2$ and $Fe(OH)_3$ for as synthesized samples. Thus the XRD results show that all three as synthesized samples are Confirmed to be LDHS containing hydrotalcite like structures.

7.2.3 Morphological Analysis

SEM images (Figure 7.2a and 7.2b) shows presence of circular nanoplates in as synthesis Mg3Fe. (Figure 7.2c and d) shows front and side view of the sample, which calculates the diameter and thickness of the nanoplates about to be 300 nm and 30 nm respectively. Figure 7.2d, demonstrates, presence of layered structures and the inter layer distance was found to be about 2.4 nm, which is approximately similar with (23.76 Å) /(001) face obtained from XRD results.

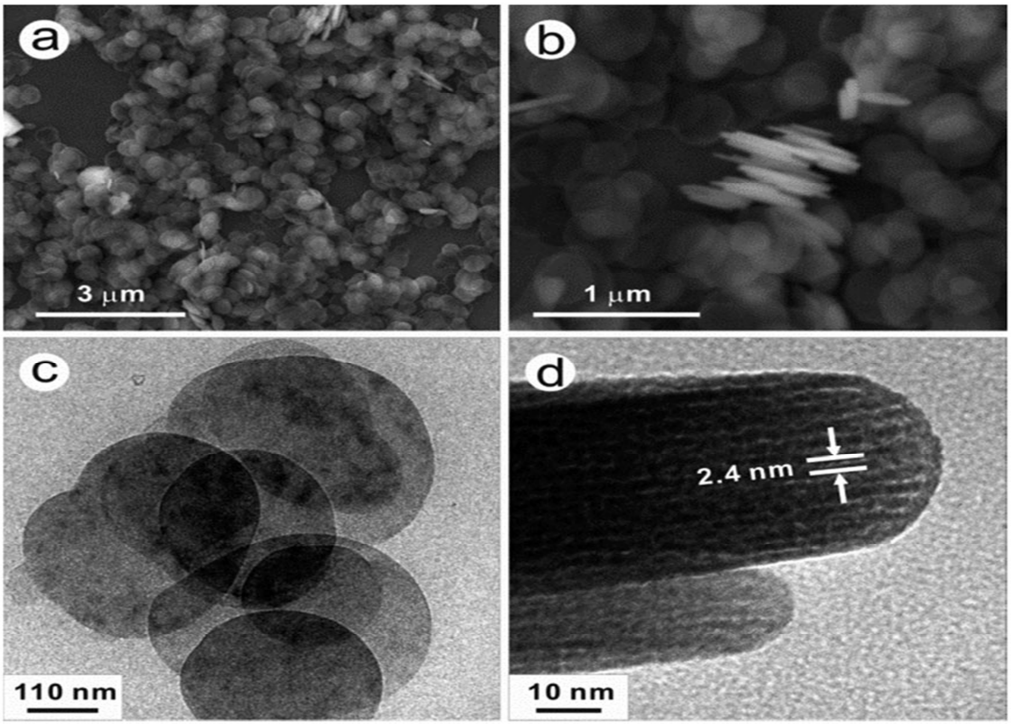

Figure 7.2 Morphological study of the as synthesized (Mg3Fe): (a), (b) SEM images; (c), (d) TEM images

7.2.4 BET analysis

From Figure 7.3, BET surface area of calcined Mg3Fe, Mg4Fe and Mg5Fe was found to be be 108, 144, and 130 m^2g^{-1} respectively by N_2 adsorption/desorption isotherms. Hence calcined Mg4Fe LDH exhibits highest surface area among all three LDHs. Generally higher surface area provides more active sites for adsorption. Thus higher adsorption capacity of As(V) on calcined Mg4Fe surface can be justified by its higher surface area compared to other samples.

The correlation of As(V) adsorption capacity of the calcined LDHs with BET surface area is given in Table 7.2.

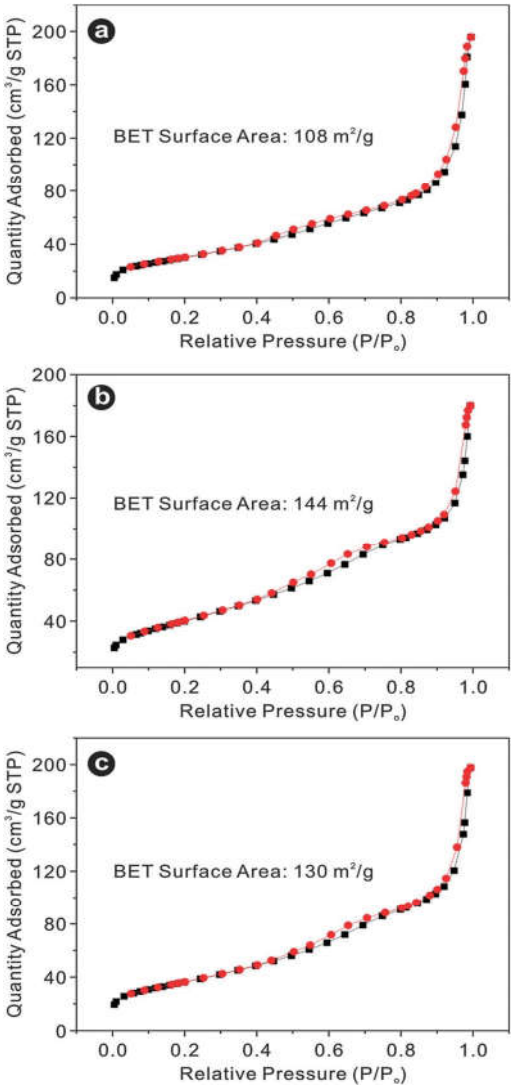

Figure 7.3 BET analysis (a) Mg3Fe (b)Mg_4Fe and (c)Mg_5Fe at 350°C for 5 hr

Table 7.2: Correlation of BET surfaces area and maximum adsorption capacity

Calcined LDHs	Mg/Fe 3 : 1	Mg/Fe 4 : 1	Mg/Fe 5 : 1
q_{max} (mg g^{-1})	145.77	271.00	166.39
$q_{max}/q_{max(Mg/Fe=3:1)(\%)}$	100	186	114
$SBET$(m^2 g^{-1})	108	144	130
$S_{BET}/S_{BET(Mg/Fe=3:1)}$ (%)		133	100

7.3 Sorption Study

7.3.1 Adsorption Kinetics

Kinetics of adsorption describes the rate of absorption representing the efficiency of adsorbents and potential use of the adsorbents. The kinetics study carried out to investigate the dynamics of As(V) removal on the three LDHs is given in Figure 7.4. From the kinetic data it is found that, Mg4Fe followed fastest rate of adsorption and attained equilibrium within 5 minutes suggesting to be a better adsorbent.

The correlation coefficient of linear plot for pseudo 2nd order kinetic model (inset of Figure 7.4) for all three LDHs approaches 1(Table 7.3), which indicates that the adsorption kinetics is best described by pseudo 2nd order rate equation. The k_2 value calculated from second order rate equation (Table 7.3) showed that Mg4Fe exhibited faster rate of adsorption.

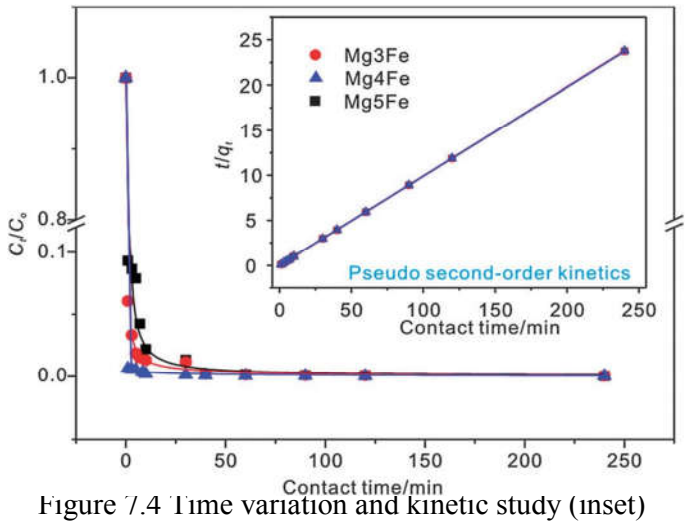

Figure 7.4 Time variation and kinetic study (inset)

Table 7.3: Pseudo 2nd order kinetic parameters for the adsorption of As(V) on the calcined LDHs

Mg/Fe molar ratio		**3:1**	**4:1**	**5:1**
Pseudo 2nd order model	k_2	0.41	4.91	0.75
	$q_{e,\ exp}\ (mg\ g^{-1})$	10.08	10.09	10.08
	$q_{e,\ cal}\ (mg\ g^{-1})$	10.13	10.09	10.12
	R^2	1	1	1

7.3.2 Adsorption Isotherm

The adsorption isotherm study of As(V) on the three calcined LDH surfaces was done by considering two empirical equations of Freundlich and Langmuir isotherm models by analyzing the experimental results (Figure 7.5). The calculated Langmuir and Freundlich parameters from the experimental data were presented in Table 7.4. The correlation coefficient value of Langmuir model approaches to 1 better than Langmuir model, showing that the adsorption data fitted to Langmuir isotherm model well.

Langmuir isotherm model suggests a surface phenomenon and no chemical reaction takes place between the adsorbate and the adsorbent.

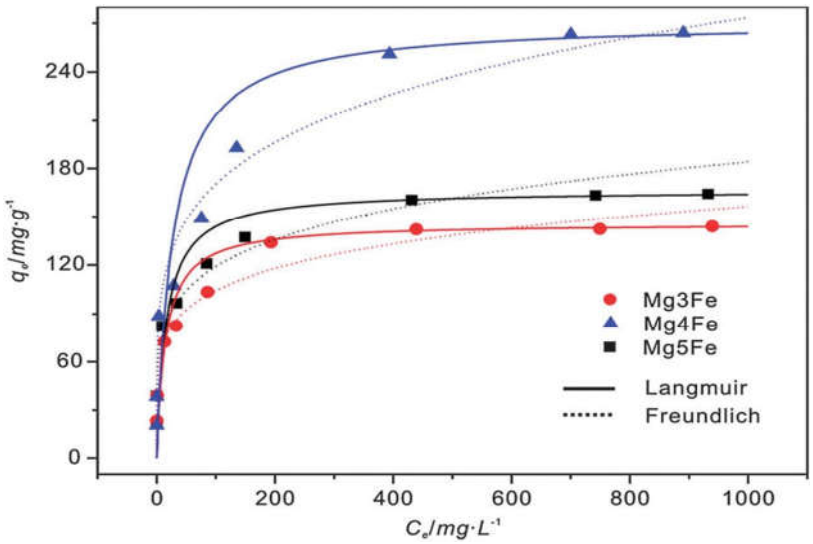

Figure 7.5 Langmuir and Freundlich adsorption isotherm for calcined LDHs

Table 7.4: Langmuir and Freundlich parameters for As(V) adsorption

Mg/Fe molar ratio		**3: 1**	**4 : 1**	**5: 1**
Langmuir	q_m (mg g^{-1})	145.8	271.0	166.4
	K_L	0.068	0.037	0.064
	R^2	0.998	0.995	0.998
Freundlich	n	5.70	4.86	5.27
	K_F	46.51	65.94	49.69
	R^2	0.985	0.976	0.989

The calcined Mg4Fe showed maximum removal capacity q_m = 271.0 mg g^{-1} calculated from Langmuir isotherm model (Table 7.4) compared to that of Mg3Fe and Mg5Fe.

SEM micrograph of the calcined Mg4Fe LDHs after adsorption, clearly demonstrates new phases other than hydrotalcite-like structures (Figure 7.6b). The XRD patterns of the Calcined LDHs are given in Figure 7.6d, in which pattern for Mg4Fe showed new phase that can be indexed to $FeAsO_4$ (JCPDS No. 11-0048).

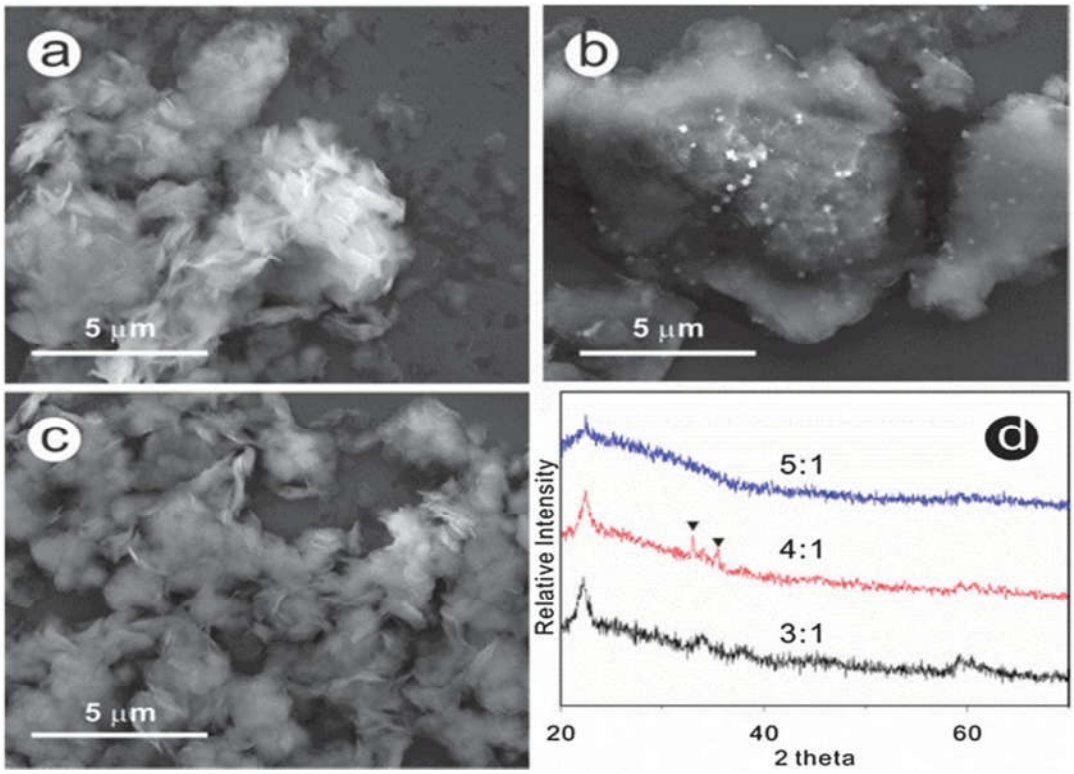

Figure 7.6 SEM micrograph of LDHs after adsorption (a) 3:1; (b) 4:1; (c) 5:1; and (d) XRD pattern of LDHs after adsorption

By analyzing the above results, it is found that the Mg4Fe exhibits metastable hydrotalcite-like structure, which forms a precipitation with arsenic ($FeAsO_4$) during the process of adsorption, increasing the adsorption capacity.

7.4 Column Study

The performance of fixed bed study is generally influenced by bed height of adsorbent, initial concentration of adsorbate and flow rate. Results of the sorption process by the LDH

with variation of the above said factors on the sorption performance of hybrid material are presented in the form of breakthrough curves (BTC).

7.4.1 Flow rate effect on breakthrough

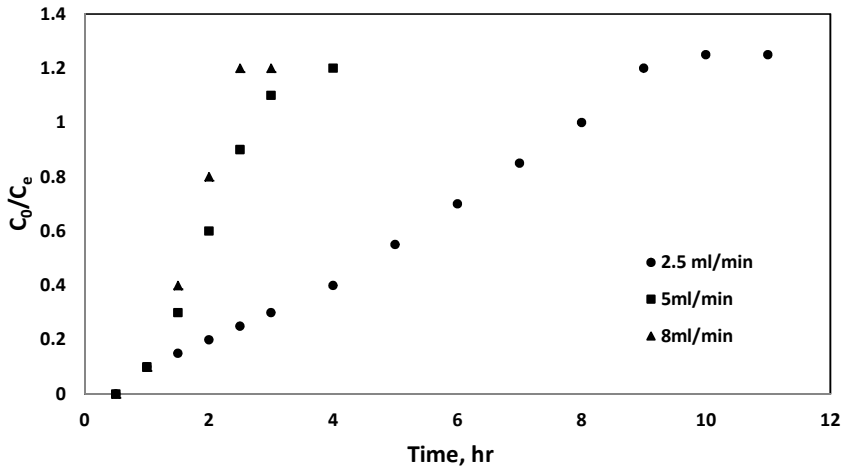

Figure 7.7 Breakthrough curves of As(V) adsorption on Mg/Fe-CO_3 LDH at different flow rate

From Figure 7.7, it was found that the removal capacity of As (V) with an increase in the flow rate of (2.5, 5.0 and 8.0) ml/min was 547.3, 455 and 342.4 mg/kg, respectively. Considering the maximum allowable concentration of As(V) as 0.01mg/L, the breakthrough time for above said flow rates were 10, 4, and 2 hours, respectively.

With increase in the flow rate, the breakthrough curves become more steeper. This phenomenon is due to reduced contact time between the adsorbing As (V) and the adsorption media leading to fast approach towards the 10 mg/L initial concentration.

7.4.2 Initial As(V) concentration variation study on breakthrough

The time of breakthrough decreased with increasing concentration of As(V) and were found to be 5, 12 and 16 hours for concentration of (15, 10 and 5) mg/l, respectively (Figure 7.8). The volume of water used corresponding to the initial As(V) concentration were 800, 1600 and 3200 ml.

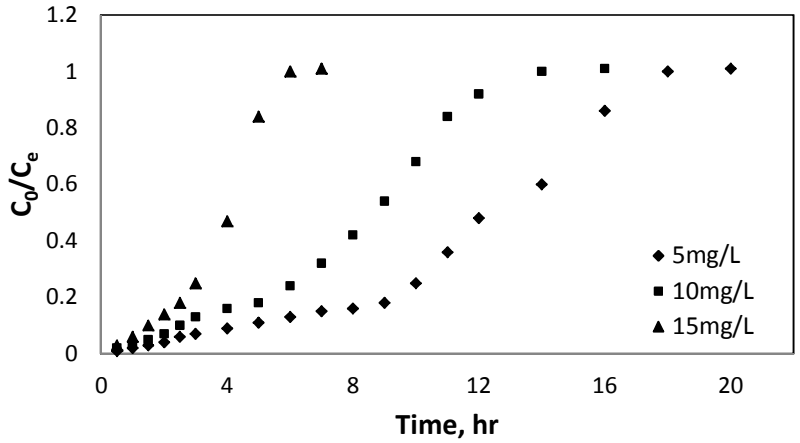

Figure 7.8 Breakthrough curves of As(V) adsorption with varying adsorbent concentration

The rate of adsorption is affected by the concentration of adsorbate during the course of adsorption due to fully occupied active sites. The BV (bed volume and uptake capacity) decreases with increasing initial concentration.

7.4.3 Adsorbent mass (bed height) variation study on breakthrough

The experiment was carried out by taking initial arsenic concentration (10 mg/l) and rate of flow (5 ml/min) and flowed through columns with different masses of adsorbent of 20, 30 and 40g. Time taken to reach a given effluent concentration increase with increasing adsorbent mass (Figure 7.9). This phenomenon is due to increased abundance of active sites for As(V) adsorption. The volumes of water tested till breakthrough, were found to be 1450, 2260 and 2740 ml, for 20, 30 and 40 g bed masses, respectively.

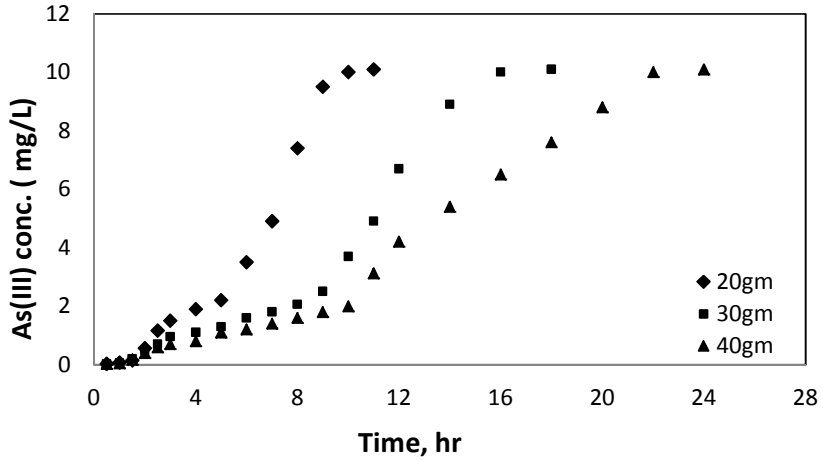

Figure 7.9 Breakthrough curves for As(V) with varying adsorbent mass

7.4.4 (BDST) Bed depth service time model

The height of adsorbent required to stop the adsorbate concentration from exceeding maximum allowable concentration limit is represented by critical bed depth C_b. Figure. 7.10 gives a plot of bed depth and service time to be a straight line.

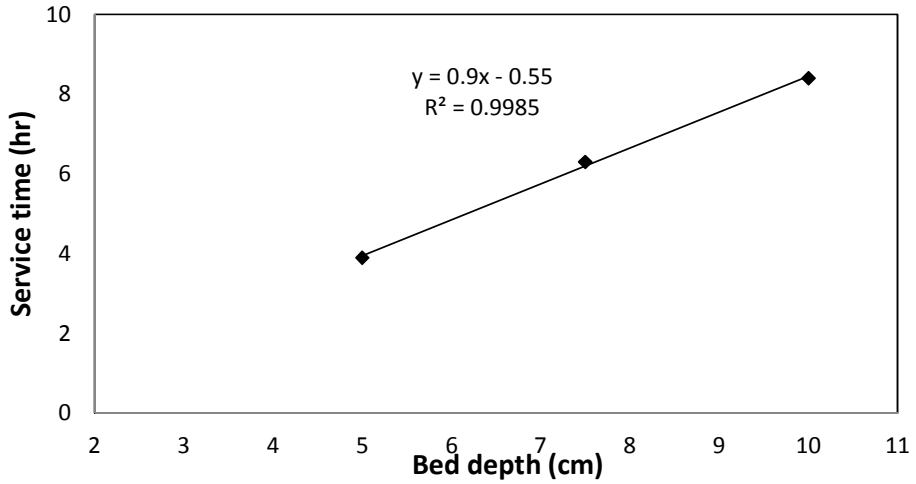

Figure 7.10 Linear BDST plot of bed depth and service time

The slope of BDST plot determines the time necessary for the adsorbate solution to cross a path of unit length through the adsorbent bed with certain experimental condition at a particular concentration of adsorbate. In this study it was found to be 0.9hours for 0.01mg/L of As(V).

The BDST parameter values (K, N_0 and x_0) are 0.863 l/mg hr, 853.05 mg/g and 0.984 cm, respectively. The K value determines the rate of mass transfer of the adsorbate from liquid phase to solid phase (adsorbent bed). Larger value of K indicates efficient removal of As(V) from contaminated water.

7.5 Chapter Summary

The LDHs were prepared by solvothermal process with different molar ratio of Mg/Fe (3:1, 4:1 and 5:1) and tested for adsorption of As(V) after calcination at 350°C for 5 hrs. The calcined LDH with Mg/Fe molar ratio (4:1) showed outstanding adsorption of As(V) with high removal capacity of 271mgg^{-1} and high adsorption rate acquiring equilibrium within 5 minutes. Thus Mg/Fe molar ratio was an important factor affecting adsorption process.

The Mg/Fe-CO_3 LDH was used for removal of As(V) in fixed bed columns. The breakthrough nature was affected by flow rate, bed height and initial As(V) concentration.

Chapter 8

Conclusions and Suggestions for Future Research

8.1 Conclusion

In past few decades, contamination of ground water with hazardous anions like fluoride and arsenic has drawn much attention for its highly adverse effects on human health. Active research for remediation of toxic anions from contaminated water by novel adsorbents has been carried out. The novelty of the present work was to synthesize simple and efficient adsorbent materials to solve problem of water treatment making it cost-effective and environment friendly.

In this research work, different adsorbent materials such as; Fe-Al mixed oxide nano particle, magnetic chitosan (Ch-Fe_3O_4) nano particle, Lanthanum doped Zirconium phosphate mesoporous material (La-ZrP) and Mg/Fe carbonate LDH were synthesized successfully by different wet chemical, coprecipitation, and hydrothermal method. Different physico-chemical properties and adsorption capacity of the synthesized adsorbent were investigated by means of various instrumental techniques like SEM, XRD, TGA/DSC, BET, FTIR, AAS and ion selective electron. The synthesized novel materials were used as adsorbent for the adsorption of the toxic anions like fluoride and arsenic by both batch and column adsorption process from aqueous solution.

The following major contributions are inferred from this research work.

1. Nano-structured rod-shaped Iron-Aluminium mixed oxide nano-particles were synthesized at ambient temperature under controlled conditions. Shape and size of the particles were observed by transmission electron microscopy (TEM). The detail batch sorption studies for fluoride were carried out to know the removal efficiency. The

kinetics and thermodynamics of fluoride adsorption on mixed oxide nano-particles have been studied by the sets of experiments at various conditions (initial fluoride concentration, adsorbent dose, pH, adsorption time and temperature). Pseudo 2^{nd} order kinetic model best described the reaction rate. The isothermal data for fluoride removal fitted to the Langmuir model best than any other model, fluoride uptake increased with an increase of Cl^- concentration and presence of SO_4^{2-} had also a beneficial effect on the sorption. Reusability of the mixed oxide nano-particle was tested up to seven consecutive cycles. Quantitative desorption of fluoride from the adsorbent was found to be more than 93% at pH 7.

The Iron-Aluminium (Fe-Al) mixed oxide nanoparticle was used in water defluoridation using fixed bed columns. The nature of breakthrough was influenced by the flow rate, column bed height and initial fluoride concentration. With increased initial fluoride concentration sharp breakthrough curves were obtained. On the other hand, the breakthrough curves became gentler as the bed height increased.

2. XRD, SEM and FTIR images were used to characterize nano scale Fe_3O_4 and crosslinked Ch-Fe_3O_4. Adsorption kinetics and isotherm of fluoride removal from aqueous synthetic solution was studied by batch model as a function of adsorbent dose, pH of solution, contact time, initial fluoride and temperature. The iron oxide nanoparticles showed an excellent ability to remove fluoride (F^-) from water over a wide range of pH. SEM, XRD and IR studies shows that the crosslinking of Fe_3O_4 with Chitosan resulted in formation of bigger size of particle compared to naked Fe_3O_4, indicating encapsulation of Fe_3O_4 with Chitosan. The removal amount of fluoride increases with increased in time and reached a saturation level in120 min and 93.0% of fluoride removal was achieved. Adsorption kinetic study revealed that the adsorption process followed pseudo 2^{nd} order kinetics. The removal process followed the Langmuir adsorption isotherm. The Maximum loading capacity was found to be 33.62 mg/g with 100 mg/l concentration of fluoride. The iron oxide nanoparticles can be used as an efficient adsorbent for fluoride decontamination of water. The removal process was endothermic in nature with temperature variation (20~60°C). The Ch-Fe_3O_4 nanoparticle was successfully used for fluoride decontamination using fixed bed columns and the breakthrough was affected by bed mass, initial concentration of fluoride and flow rate.

3. Mesoporous La-ZrP was synthesized by co-precipitation followed by hydrothermal method for decontamination of fluoride from synthetic water. The surface morphology and other physico-chemical properties studies confirmed the material to be mesoporous. The maximum adsorption capacity of .fluoride removal was found to be 83.9 mg/g at pH 7 approaching equilibrium within 120 minutes. The rate of adsorption followed pseudo 2^{nd} order kinetic equation and the removal process was better fitted to Langmuir isotherm model with monolayer adsorption. Temperature variation study showed the process of adsorption was endothermic in nature. The loaded material was regenerated successfully and reused for several cycles. The results of the column study inferred that the material was able to bring down the fluoride concentration upto permissible limit and adsorption was affected by flow rate, column bed height and initial fluoride concentration.
4. Mg/Fe-CO_3 was synthesized by solvothermal method with different molar ratio of Mg/Fe (3:1, 4:1 and 5:1). Then the as synthesized LDH was calcined at 350°C and used for adsorption of As(V) from water. The calcined LDH exhibited higher adsorption capacity compared to as synthesized LDH. Further investigation showed the LDH with molar ratio of Mg/Fe (4:1) has the highest surface area and adsorption capacity (271 mg g^{-1}) approaching equilibrium within 5 minutes. The process of adsorption followed Langmuir isotherm model mand rate of adsorption obeyed pseudo 2^{nd} order kinetic model. As the initial concentration of As(V) increases the breakthrough curve becomes sharp whereas, gentler breakthrough curves were with increased bedmass.

All the above results show that the synthesized novel adsorbent materials are excellent adsorbents for decontamination of both arsenic and fluoride from water. Hence the materials can be used as low-cost adsorbents for potential application for water treatment.

8.2 Scope for Future Research

The followings scope of studies may be considered in future research .

1. Enhancement of adsorption capacity of the adsorbents prepared by further surface modification.
2. Large-scale utilization of the above prepared materials for remediation of actual contaminated water.

3. Design of a column model using the adsorbent material in different segments/layers for field application.

4. Investigation of the adsorption capacities of the adsorbent with real industrial effluents by mean of a column model as discussed in the fixed bed column method.

References

Abdul, K.S.M., Jayasinghe, S.S., Chandana, E.P.S., Jayasumana, C., Silva, P.M.C.S.D., 2015, "Arsenic and human health effects: A Review". *Environmental Toxicology and Pharmacology*, 40, 828-846.

Agarwal, K.C., Gupta, S.K., and Gupta, A.B., 1999, "Development of new low cost defluoridation technology (KRASS)". *Water Sci. Technology*, 40, 167-173.

Akin, I., Arslan, G., Tor, A., Ersoz, M., and Cengeloglu, Y., 2012, "Arsenic (V) removal from underground water by magnetic nanoparticles synthesized from waste red mud". *J. Hazard Mater.* 235–236, 62–68.

Alberti, G., Casciola, M., Marmottini, F.,and Vivani, R., 1996,"Preparation of mesoporous zirconium phosphate-pyrophosphate with a large amount of thermally stable acid groups on the pore surface". *J. Porous Mater.,* 6, 299–305.

Algarra, M., Vazquez, M. I., Alonso, B., Casado, C. M., Casado, J., and Benavente, J., 2014, "Characterization of an Engineered Cellulose Based Membrane by ThiolDendrimer for Heavy Metals Removal". *Chem. Eng. J.,* 253, 472–477.

Allen, S.J., Mckay, G., Porter, J.F., 2004, "Adsorption isotherm models for basic dye adsorption by peat in single and binary component systems". *J. Colloid Interface Sci.,* 280, 322-333.

Ambashta, R.D., and Sillanpaa, M., 2010, "Water purification using magnetic assistance: a review". *J Hazard Mater,* 180, 38–49.

Amini, M., Abbaspour, K.C., Berg, M., Winkel, L., Hug, S.J., Hoehn, E., Yang, H., and Johnson, C.A., 2008, "Statistical modeling of global geogenic arsenic contamination in groundwater". *Environ. Sci. Technol.,* 42, 3669–3675.

Amor, Z., Bariou, B., Mameri, N., Taky, M., Nicolas, S., and Elmidaoui, A., 2001, "Fluoride removal from brakish water by electrodialysis, Desalination". 133, 215-223.

Anderson, L.C.D., and Bruland, K.D., 1991, "Biochemistry of arsenic in natural waters: the importance of methylated species", *Environ. Sci. Technol*. 25, 420–429.

Anwar, F., 2003, "Assessment and analysis of industrial liquid waste and sludge disposal at unlined landfill sites in arid climate". *Waste Manage*, 23 (9), 817–824.

Araya, H., Tomita, A., Hayashi, M., 2005, "The novel formulation design of O/W microemulsion for improving the gastrointestinal absorption of poorly water soluble compounds". *Int. J. Pharm.* 305, 61–74.

Arce, V. B., Gargarello, R. M., Ortega, F., Romañano, V., Mizrahi, M., Ramallo-Lopez, J. M., Cobos, C. J., Airoldi, C., Bernardelli, C., and Donati, E. R., et al., 2015, "EXAFS and DFT Study of the Cadmium and Lead Adsorption on Modified Silica Nanoparticles". *Spectrochim.Acta - Part AMol. Biomol. Spectrosc*. 151, 153–163.

Arenas, J. P., and Crocker, M. J., 1994, "Physical and biophysical chemistry division commission on colloid and surface chemistry including catalysis". *Pure & Appl. Chem,* 66, 1739-1758.

Asgari, B., and Bowen, J., 2017, "Gallium (III)–metalloporphyrin grafted magnetite nanoparticles for fluoride removal from aqueous solutions". *Natural Products Chemistry & Research.* 11, 5(5).

Ayoob, S., Gupta, A.K., Bhakat, P.B., and Bhat, V.T., 2008, "Investigations on the kinetics and mechanisms of sorptive removal of fluoride from water using alumina cement granules". *Chem. Eng. J.*, 140, 6-14.

Babu, C. M., Palanisamy, B., Sundaravel, B., Palanichamy, M., and Murugesan, v., 2013, "A Novel Magnetic Fe3O4/SiO2 Core-Shell Nanorods for the Removal of Arsenic". *J. Nanosci. Nanotechnol.,* 13, 2517-2527.

Badoga, S., Sharma, R., Dalai, A. K., and Adjaye, J., 2015, "Synthesis and Characterization of Mesoporous Aluminas with Different Pore Sizes: Application in NiMo Supported Catalyst for Hydrotreating of Heavy Gas Oil". *Appl. Catal. A Gen.* 489, 86–97.

Bajpai, S., and Chaudhuri, M., 1999, "Removal of arsenic from ground water by manganese dioxide-coated sand". *J. Environ. Eng.* 125, 782–784.

Bakon, K.H., S.J. Palmer, and Frost, R.L., 2010, "Thermal analysis of synthetic reevesite and cobalt substituted reevesite (Ni,Co)6Fe2(OH)16(CO3)·4H2O". *J.Therm.Anal.Calorim.* 100(1):p.125-131.

Banga, S., Johnson, M.D., Korfiatisa G.P., and Meng, X., 2005, "Chemical reactions between arsenic and zero-valent iron in water", *Water Res*. 39, 763–770.

Bektas, N., Aydin, S., and Oncel, M. S., 2011, "The Adsorption of Arsenic Ions Using Beidellite, Zeolite, and Sepiolite Clays: A Study of Kinetic, Equilibrium and Thermodynamics". *Sep. Sci. Technol.,* 46, 1005–1016.

Bell, M.C., and Ludwig, T.G., 1970, "The supply of fluoride to man: ingestion from water, in: Fluorides and Human Health WHO Monograph", Series 59, World Health Organization, Geneva.

Bellezza, F., Cipiciani, A., Costantino, U.,and Marmottini, F., 2006, "Adsorption of myoglobin onto porous zirconium phosphate and zirconium benzenephosphonate obtained with template synthesis". *Langmuir* 22, 5064–5069.

Berg, M., Tran, H.C., Nguyen, T.C., Pham, H.V., Schertenleib, R., and Giger, W., 2001, "Arsenic contamination of ground water and drinking water in Vietnam: a human health threat", *Environ. Sci. Technol.* 35, 2621–2626.

Bhandare, A. A., and Argekar, A. P., 2002, "Separation and Recovery of Platinum and Rhodium by Supported Liquid Membranes Using bis(2-Ethylhexyl)phosphoric Acid (HDEHP) as a Mobile Carrier". *J. Memb. Sci.* 201, 233–237.

Bhatnagara, A., Kumara, E., and Sillanpaab, M., 2011, "Fluoride removal from water by adsorption-A review". *Chemical Engineering Journal,* 171, 811– 840.

Bhattacharjee, S., Chakravarty, S., Maity, S., Dureja, V., and Gupta, K.K., 2005, "Metal contents in the ground water of Sahebgunj district, Jharkhand, India, with special reference to arsenic", *Chemosphere* 58,1203–1217.

Bhattarai, N., Edmondson, D., Veiseh, O., Matsen, A. F., and Zhang, M., 2005, "Electrospun chitosan-based nanofibers and their cellular compatibility". *Biomaterials,* 26, 6176–6184

Bhaumik, M., Leswifi, T.Y., Maity, A., Srinivasu, V.V., and Onyango, M.S., 2011, "Removal of fluoride from aqueous solution by polypyrrole /Fe3O4 magnetic nanocomposite". *J. Hazard. Mater.* 186, 150-159.

Bian, S.W., Ma, Z., Zhang, L.S., Niu, F., and Song, W.G., 2009, "Silica nanotubes with mesoporous walls and various internal morphologies using hard/soft dual templates". *Chem. Commun.,* 1261–1263.

Biswas, K., Debnath, S., and Ghosh, U.C., 2010, "Physicochemical Aspects on Fluoride Adsorption for Removal from Water by Synthetic Hydrous Iron(III) –Chromium(III) Mixed Oxide". *Separ. Sci.Technol.,* Vol. 45, pp. 472–485.

Blue, L. Y., Jana, P., and Atwood, D. A., 2010, "Aqueous Mercury Precipitation with the Synthetic Dithiolate", *BDTH2.Fuel,* 89 (6), 1326–1330.

Blue, L. Y., Van Aelstyn, M. A., Matlock, M., and Atwood, D. A., 2008, "Low-Level Mercury Removal from Groundwater Using a Synthetic Chelating Ligand". *Water Res.* 42 (8–9), 2025–2028.

Boutonnet, M., Kizling, J., and Stenius, P., 1982, "The preparation of monodisperse colloidal metal particles from microemulsions". *Colloids Surf.* 5, 209–225.

Bouzaid, J. and R.L. Frost, 2007, Thermal decomposition of stichtite. *J. Therm.Anal.Calorim.,* 89(1):p.133-135.

Bujňáková, Z., Baláž, P., Zorkovská, A., Sayagués, M.J., Kováč, J., and Timko, M., 2013, "Arsenic sorption by nanocrystalline magnetite: an example of environmentally promising interface with geosphere". *J Hazard Mater* 262, 1204–1212.

Cai, H., Chen, G., Peng, C., Xu, L., Zhu, X., Zhang, Z., Dong, Y., Shang, G., Ke, F., and Gao, H., et al., 2015, "Enhanced Removal of Fluoride by Tea Waste Supported Hydrous Aluminium Oxide Nanoparticles: Anionic Polyacrylamide Mediated Aluminium Assembly and Adsorption Mechanism". *RSC Adv.* 5, 29266–29275.

Cai, W., Tan, L., Yu, J., Jaroniec, M., Liu, X., Cheng, B., and Verpoort, F., 2014, "Synthesis of Amino-Functionalized Mesoporous Alumina with Enhanced Affinity towards Cr (VI) and CO2". *Chem. Eng. J.,* 239, 207–215.

Cao, G., and Wang, Y., 2011, "Nanostructures and Nanomaterials". *Second Edi. World Scientific.*

Carja, G., Ratoi, S., Ciobanu, G., and Balasanian, I., 2008, "Uptake of As(V) from aqueous solution by anionic clays type FeLDHs". *Desalination,* 223, 243–248.

Castel, C., Schweizer, M., Simonnot, M.O., Sardin, M., 2000, "Selective removal of fluoride ions by a two-way ion-exchange cyclic process". *Chem. Eng. Sci.* 55, 987–993.

Chadrasekaran, Krishna.K., Karunasagar, D., Arunachalam, J., 2001, "A combined treatment approach using Fenton's reagent and zero-valent iron for the removal of arsenic from drinking water". *J. Hazard. Mater.* 84, 229–240.

Chakravarty, S., Dureja, V., Bhattacharyya, G., Maity, S., and Bhattacharjee, S., 2002, "Removal of arsenic from ground water using low cost ferruginous manganese ore". *Water Res.* 36, 625–632.

Charinpanitkul, T., Chanagul, A., and Dutta, J., 2005, "Effects of cosurfactant on ZnS nanoparticle synthesis in microemulsion". *Sci. Technol. Adv. Mater.* 6, 266–271.

Chaturvedi, A. K., Yadav, K.P., Pathak, K. C., and V. N., 1990, "Defluoridation of water by adsorption on fly ash". *Water, Air, Soil Pollut.,* 49, 51-61.

Chen, C., Gunawan, P., and Xu, R., 2011, "Self-assembled Fe3O4-layered double hydroxide colloidal nanohybrids with excellent performance for treatment of organic dyes in water". *J. Mater. Chem.* 21, 1218–1225.

Chen, F., Luo, G.S., and Wang, Y.J., 2005, "Studies on adsorption properties of chemically modified chitosan resins to diuretics". *Acta Polymerica Sinica,* 1, 53–59.

Chen, L., Wang, T.J., Wu, H.X., Jin, Y., Zhang, Y., and Dou, X.M., Jan 2011, "Optimization of a Fe–Al–Ce nano-adsorbent granulation process that used spray coating in a fluidized bed for fluoride removal from drinking water". *Powder Technol.,* Vol. 206, Issue 3, pp.291–296.

Chen, M. L., Gu, C. B., Yang, T., Sun, Y., and Wang, J. H., 2013, "A green sorbent of esterified egg-shell membrane for highly selective uptake of arsenate and speciation of inorganic arsenic". *Talanta,* 116, 688–694.

Chen, N., Zhang, Z., Feng, C., Li, M., Zhu, D., and Sugiura, N., Jan 2011, "Studies on fluoride adsorption of iron impregnated granular ceramics from aqueous solution". *Mater. Chem. Phys.* Vol. 125, Issues 1-2, pp. 293–298.

Chen, N., Zhang, Z., Feng, C., Zhu, D., Yang, Y., and Sugiura, N., Feb 2011, "Preparation and characterization of porous granular ceramic containing dispersed aluminum and iron oxides as adsorbents for fluoride removal from aqueous solution". *J. Hazard. Maters.,* Vol. 186, Issue 1, pp. 863–868.

Chetia, M.,Goswamee, R. L., Banerjee, S., Chatterjee, S., Singh, L., Srivastava, R. B., and Sarma, H. P., 2012,"Arsenic removal from water using calcined Mg–Al layered double hydroxide". *Clean Technol. Environ.* 14, 21-27

Chin, A.B., and Yaacob, I.I., 2007, "Synthesis and characterization of magnetic iron oxide nanoparticles via w/o micro emulsion and Massart's procedure". *Journal of materials processing technology*. 191, 235–237.

Choubisa, S.L., and Sompura, K., 1996, "Dental fluorosis in tribal villages of Dungerpur district (Rajasthan)", *Poll. Res.* 15 (1), 45–47.

Chowdhury, S. R., and Yanful, E. K., 2010, "Arsenic and chromium removal by mixed magnetite–maghemite nanoparticles and the effect of phosphate on removal". *J. Environ. Manage.,* 91, 2238–2247.

Christen, K., 2000, cleaning technologies can remove arsenic, butatcost". *Environ. Sci. Technol*. 34, 75–79.

Ciesla, U., Froba, M., Stucky, G., and Schuth, F., 1999, "Highly ordered porous zirconias from surfactant-controlled syntheses: zirconium oxide-sulfate and zirconium oxo phosphate". *Chem. Mater.* 11, 227–234.

Clifford, D.A., 2006, "Ion-exchange and inorganic adsorption. Water Quality and Treatment: A Handbook of Community Water Supplies (5th Ed.)". *American Water Works Association,* McGraw-Hill, New York.

Cobelo-Garcia, A., Turner, A., Millward, G. E., and Couceiro, F., 2007, "Behaviour of palladium (II), platinum(IV), and rhodium(III) in Artificial and Natural Waters: Influence of Reactor Surface and Geochemistry on Metal Recovery". *Anal.Chim.Acta.* 585(2), 202–210.

Cui, Y., Ge, Q., Liu, X. Y., and Chung, T. S., 2014, "Novel Forward Osmosis Process to Effectively Remove Heavy Metal Ions". *J. Memb. Sci.*467, 188–194.

Dahi, E., Mtalo, F., Njau, B., and Bregnhj, H., 1996, "Defluoridation Using. Nalgonda Technique in Tanzania". 22nd WEDC Conference, New Delhi, India.

Das, S.K., Bhunia, M.K., Sinha, A.K., and Bhaumik, A., 2011, "Synthesis, characterization, and biofuelapplication of mesoporous zirconium oxophosphates". *ACS Catal.* 1, 493–501.

Das, D.P., Das, J., and Parida, K.J., 2002, "Physicochemical characterization and adsorption behavior of calcined". *Colloid Interface Sci.* 261, 213–220.

Daus, B., Wennrich, R., and Weiss, H., 2004, "Sorption materials for arsenic removal from water: a comparative study". *Water Res.,* 38, 2948–2954.

Deng, W. L., and Flytzani-Stephanopoulos, M., 2006, "On the Issue of the Deactivation of Au–Ceria and Pt–Ceria Water–Gas Shift Catalysts in Practical Fuel-Cell Applications". *Angew. Chem. Int. Ed.,* 45, 2285-2289.

Dey, R.K., Jha, U., Singh, A.C., Samal, S., and Ray, A.R., 2006, "Extraction of metal ions using chemically modified silica gel covalently bonded with 4,4'-diaminodiphenylether and 4,4'-diaminodiphenylsulfone-salicylaldehyde Schiff bases.". *Anal. Sci.,* 8, 1105-1110.

Diaz-Nava, C., Solache-Rios, M., and Olguin, M.T., 2003, "Sorption of fluoride ions from aqueous solutions and well drinking water by thermally treated hydrotalcite", *Sep. Sci. Tech.,* 38,131–147.

Ding, Y. Xi, Z., He, H., Frost, R.L., 2005, "Influence of binders on infrared laser ablation of powdered tungsten carbide pressed pellets in comparison with sintered tungsten carbide hardmetals studied by inductively coupled plasma atomic emission spectrometry". *Spectrochim. Acta A.,* 61, 515–524.

Dnekbas, E.B., Kilic, E., Birlikseven, C., and Ozturk, E., 2002, "Magnetic chitosan microspheres: preparation and characterization Reactive and Functional Polymers", 50, 225–232.

Dobrowolski, R., and Otto, M., 2013, "Preparation and evaluation of Ni-loaded activated carbon for enrichment of arsenic for analytical and environmental purposes". *Microporous Mesoporous Mater.,* 179, 1–9.

Dou, X., Zhang, Y., Wang, H., Wang, T., and Wang, Y., 2011, "Performance of granular zirconium iron oxide in the removal of fluoride from drinking water". *Water Res.* 45, 3571-3578.

Dousova, B., Lhotka, M., Grygar, T., Machovic, V., and Herzogova, L., 2011, "In situ co-adsorption of arsenic and iron/manganese ions on raw clays". *Appl. Clay Sci.,* 54, 166–171.

Drouiche, N., Lounici, H., Drouiche, M., Mameri, N., and Ghaffour, N., 2009, "Removal of fluoride from photovoltaic wastewater by electrocoagulation and products characteristics", *Desalination Water Treat.,* 7, 236-241.

Edwards, M., 1994, "Chemistry of arsenic removal during coagulation and Fe–Mn oxidation". *J. Am. Water Works Assoc*. 86, 64–78.

Elwakeel, K. Z., El-Sayed, G. O., and Darweesh, R. S., 2013, "Fast and Selective Removal of silver (I) from Aqueous Media by Modified Chitosan Resins". *Int. J. Miner. Process*. 120, 26–34.

Emamjomeh, M.M., and Sivakumar, M., 2006, "An empirical model for defluoridation by batch monopolar electrocoagulation/flotation (ECF) process". *J. Hazard. Mater.*131, 118-125.

Erickson, K.L., Bostrom,T.E. and Frost, R.L., 2004,"A study of structural memory effects in synthetic hydrotalcites using environmental SEM". *Mater. Lett.* 59(2-3):p.226-229.

Fan, R., Chen, X.H., and Gui, Z., et al., 2001, "A new simple hydrothermal preparation of nanocrystalline magnetite Fe3O4". *Materials Research Bulletin.* 36(3–4), 497–502.

Farrell, W.J., Peggy, O.D., and Colklin, M., 2001, "Electrochemical and spectroscopic study of arsenate removal from water using zero-valent ion media". *Environ. Sci. Technol.* 35, 2026–2032.

Fendorf, S., Eick, M., Grossl, P., and Sparks, D.L., 1997, "Arsenate and chromate reduction mechanisms on goethite. 1. Surface structure". *Environ. Sci. Technol.* 31, 315–320.

Feng, D., Aldrich, C., and Tan, H., 2000, "Treatment of Acid Mine Water by use of Heavy Metal Precipitation and Ion Exchange". *Miner. Eng.* 13 (6), 623–642.

Frost, R.L., Bakon, K.H., and S.J. Palmer, 2010, Raman spectroscopic study of synthetic reevesite and cobalt substituted reevesite (Ni,Co)6Fe2(OH)16(CO3)· 4H2O. *J.RamanSpectrosc.,* 41(1): p.78-83.

Fu, Q., Saltsburg, H., and Flytzani-Stephanopoulos, M., 2003, "Active Nonmetallic Au and Pt Species on Ceria-Based Water-Gas Shift Catalysts". *Science,* 301, 935-938.

Gallegos-Garcia, M., Ramirez-Muniz, K., and Song, S. X., 2012, "Advanced nanomaterials for waste water remediation". *Miner. Process. Extr. Metall. Rev.,* 33, 301–315.

García-Sánchez, J.J., Solache-Ríos, M., Martínez-Miranda, V., and Solís-Morelos, C., Oct. 2013, "Removal of fluoride ions from drinking water and fluoride solutions by aluminum modified iron oxides in a column system", *J. Colloid Interface Sci.* Vol. 407, pp. 410–415.

Gehrke, Ilka., Andreas, Geiser., and Annette, Somborn–Schulz., 2015, "Innovations in nanotechnology for water treatment". *Nanotechnology Science App.* 8, 1–17.

Genç-Fuhrman, H., Tjell, J. C., and McConchie, D., 2004. "Adsorption of arsenic from water using activated neutralized red mud". *Environmental Science & Technology,* 38(8), pp. 2428–2434.

Geng, C. Y., Xu, T. H., Li, Y. P., Chang, Z., Sun, X. M., and Lei, X. D., 2013," Effect of synthesis method on selective adsorption of thiosulfate by calcined MgAl-layered double hydroxides". *Chem. Eng. J.,* 232, 510–518.

Gitari, W.M., Ngulube, T., Masindi, V., and Gumbo, J.R., 2015, "Defluoridation of groundwater using Fe3+ modified bentonite clay: optimization of adsorption conditions". *Desalination Water Treat*. Vol. 53, pp. 1578–1590.

Goikolea, E., Insausti, M., Lezama, L., Garitaonandia, J.S., 2008, "Magnetic and structural characterization of silver-iron oxide nanoparticles obtained by the microemulsion technique", 354, 5216–5218.

Gong, W. X., Qu, J. H., Liu, R. P., and Lan, H. C., 2012, "Adsorption of Fluoride onto Different Types of Aluminas". *Chem. Eng. J.* 189–190, 126–133.

Gonzalez-Contreras, P., Weijma, J., vander -Weijden, R., and Buisman, C. J. N., 2010, "Biogenic Scorodite Crystallization by Acidianus sulfidivorans for Arsenic Removal". *Environ. Sci. Technol.,* 44, 675–680.

Gonzalez-Velasco, J. R., Gutierrez-Ortiz, M. A., Marc, J. L., Botas, J. A., Gonzalez-Marcos, M. P., and Blanchard, G., 1999, "Contribution of cerium/zirconium mixed oxides to the activity of a new generation of TWC". *Appl. Catal. B: Environmental,* 22, 167-178.

Gupta, A., Yunus, M., and Sankararamakrishnan, N., 2012, "Zerovalent iron encapsulated chitosan nanospheres- a novel adsorbent for the removal of total inorganic Arsenic from aqueous systems," *Chemosphere,* vol. 86, no. 2, pp. 150–155.

Gupta, S.K., and Chen, K.Y., 1978, "Arsenic removal by adsorption". *J. Water Pollut. Control Fed.* 50, 493–506.

Gupta, V.K., Ali, I., and Saini, V.K., 2007, "Defluoridation of waste waters using waste carbon slurry". *Water Res.* 41, 3307-3316.

Han, C., Pu, H., Li, H., Deng, L., Huang, S., He, S., and Luo, Y., 2013, "The Optimization of As (V) Removal over Mesoporous Alumina by Using Response Surface Methodology and Adsorption Mechanism". *J. Hazard. Mater.* 254–255 (1), 301–309.

Han, J., Dou, Y., Wei, M., Evans, D.G., and Duan, X., 2010, "Erasable nanoporous antireflection coatings based on the reconstruction effect of layered double hydroxides". *Angew Chem. Int. Ed.* 49, 2171–2174.

Harvey, C.F., Swartz, C.H., Badruzzaman, A.B.M., Keon-Blute, N., Yu, W., Ali, M.A., Jay, J., Beckie, R., Niedan, V., Brabander, D., Oates, P.M., Ashfaque, K.N., Islam, S., Hemond, H.F., and Ahmed, M.F., 2002, "Arsenic mobility and groundwater extraction in Bangladesh", *Science* 298 ,1602–1606.

Hering, J.G., Chen, P.Y., Wilkie, J.A., and Elimelech, M., 1996, "Arsenic removal by ferric chloride". *J. Am. Water Works Assoc.* 88,155–167.

Hichour, M., Persin, F., Sandeaux, J., and Gavach, C., 2000, "Fluoride removal from waters by Donnan dialysis". *Sep. Purif. Technol.* 18, 1–11.

Hoar, T.P., and Schulman, J.H., 1943, "Transparent water-in-oil dispersions: the oleopathic hydro-micelle". *Nature* 152, 102.

Hong, J., Zhu, Z. L., Lu, H. T., and Qiu, Y. L., 2014, "Effect of metal composition in lanthanum-doped ferric-based layered double hydroxides and their calcined products on adsorption of arsenate". *RSC Adv.,* 4, 5156–5164.

Hu, C.Y., Lo, S.L., Kuan, W. H., and Lee, Y. D., 2005, "Removal of Fluoride from Semiconductor Wastewater by Electrocoagulation- Flotation". *Water Res.* 39 (5), 895–901.

Hu, K., and Dickson, J. M., 2006, "Nano filtration Membrane Performance on Fluoride Removal from Water". *J. Memb. Sci.* 279 (1–2), 529–538.

Huang, L., Wang, J., Gao, Y.,Qiao, Y., Zheng, Q.,Guo, Z., Zhao, Y., O'Hare, D., and Wang, Q. J., 2014, "Synthesis of LiAl2-layered double hydroxides for CO2 capture over a wide temperature range Meter". *Chem. A,* 2, 18454-18462.

Huang, P. P., Cao, C. Y., Wei, F., Sun, Y. B., and Song, W. G., 2015, "MgAl layered double hydroxides with chloride and carbonate ions as interlayer anions for removal of arsenic and fluoride ions in water". *RSC Adv.5,* 10412-10417.

Huisman, J. L., Schouten, G., and Schultz, C., 2006, "Biologically Produced Sulphide for Purification of Process Streams, Effluent Treatment and Recovery of Metals in the Metal and Mining Industry". *Hydrometallurgy,* 83 (1–4), 106–113.

Hyeon, T., Lee, S.S., and Park, J., et al., 2001, "Synthesis of highly crystalline and monodispersemaghemite Nano crystallites without asize–selection process". *J Am Chem Soc.* 123(51), 12798–12801.

Iben, Nasser, I., Ibn El Haj Amor, F., Donato, L., Algieri, C., Garofalo, A., Drioli, E., and Ahmed, C., 2016, "Removal and Recovery of Ag(CN)2- from Synthetic Electroplating Baths by Polymer Inclusion Membrane Containing Aliquat 336 as a Carrier". *Chem. Eng. J.* 295, 207–217.

Islam, M., and Patel, R.K., 2007, "Evaluation of removal efficiency of fluoride from aqueous solution using quick lime". *Journal of Hazardous Material*, 143, 303-310.

Jagtap, S., Yenkie, M. K. N., Labhsetwar, N., and Rayalu, S., 2011, "Defluoridation of Drinking Water Using Chitosan Based Mesoporous Alumina". *Micropor. Mesopor. Mat.* 142 (2–3), 454–463.

Jain, A., Ravene, K.P., and Loeppert, R.H., 1999, "Arsenite and arsenate adsorption on ferrichydrite: surface charge reduction and net OH− release stoichiometry". *Environ. Sci. Technol.* 33, 1179–1184.

Jia, Z., Yujun, W., Yangcheng, L., Jingyu, M., and Guangsheng, L., 2006, "In situ preparation of magnetic chitosan/Fe3O4 composite nanoparticles in tiny pools of water-in-oil microemulsion". *Reactive and functional polymers*. 66, 1552–1558.

Jiang, D., Long, S.Y., Huang, J., Xiao, H.Y., and Zhou, J.Y., 2005, "Immobilization of Pycnoporus sanguineus laccase on magnetic chitosan microspheres". *Biochemical Engineering Journal,* 25, 15–23.

Jimenez-Jimenez, J., Maireles-Torres, P., Olivera-Pastor, P., Rodriguez-Castellon, E.,Jimenez-Lopez, A., Jones, D.J.,and Roziere, J.,1998, "Surfactant-assisted synthesis of a

mesoporous form of zirconium phosphate with acidic properties". *Adv. Mater*.10, 812–815.

Jiménez-Núñez, M.L., Olguín, M.L.,Solache-Ríos, M., 2007, "Fluoride Removal from Aqueous Solutions by Magnesium, Nickel, and Cobalt Calcined Hydrotalcite-like Compounds". *Sep. Sci. Technol*. 42 (16), 3623–3639.

Jin, Y., Liu, F., Tong, M., and Hou, Y., 2012, "Removal of arsenate by cetyltrimethylammonium bromide modified magnetic nanoparticles". *J Hazard Mater* 227–228, 461–468.

Joshi, A., and Chaudhuri, M., 1996, "Removal of arsenic from ground water by iron-oxide coated sand". *J. Environ. Eng.* 122, 769–776.

Kabay, N., Arar, O., Samatya, S., Yuksel, U., and Yuksel, M., 2008, "Separation of Fluoride from Aqueous Solution by Electrodialysis: Effect of process Parameters and Other Ionic Species". *J. Hazard. Mater*. 153(1–2), 107–113.

Kammerer, J., Carle, R., and Kammerer, D. R., 2011, "Adsorption and Ion Exchange: Basic Principles and Their Application in Food Processing". *J. Agric. Food Chem.* 59 (1), 22–42.

Kang, D. J., Yu, X. L., Tong, S. R., Ge, M. F., Zuo, J. C., Cao, C. Y., and Song, W. G., 2013, "Performance and mechanism of Mg/Fe layered double hydroxides for fluoride and arsenate removal from aqueous solution". *Chem. Eng. J.,* 228, 731–740.

Kannan, K., and Sundaram, M.M., 2001, "Kinetics and mechanism of removal of methylene blue by adsorption on various carbons - a comparative study". *Dyes Pigment*., 51, 25-40.

Kartinen, E., and Martin, J.C.J., 1995, "An overview of arsenic removal processes". *Desalination*, 103, 79–88.

Kausar, A., Bhatti, H. N., and MacKinnon, G., 2013. "Equilibrium, kinetic and thermodynamic studies on the removal of U (VI) by low cost agricultural waste". *Colloids and Surfaces B: Biointerfaces*, 111, pp. 124–133.

Khan, A, B., S. J., Maqbool, T., and Hankins, N. P., 2017, "Heavy Metals Removal by Osmotic Membrane Bioreactor (OMBR) and Their Effect on Sludge Properties". *Desalination,* 403, 117–127.

Khan, A.A., and Singh, R.P., 1987, "Adsorption thermodynamics of carbofuran on Sn(IV) arsenosilicate in H+, Na+ and Ca2+ forms". *Colloids Surf.,* 24, 33-42.

Khatibikamal, V., Torabian, A., Janpoor, F., and Hoshyaripour, G., 2010, "Fluoride removal from industrial wastewater using electrocoagulation and its adsorption kinetics". *J. Hazard. Mater.,* 179, 276–280.

Kim, D.K., Zhang, Y., Voit, W., and Muhammed, M., 2001, "Synthesis and characterization of surfactant coated superparamagnetic monodispersed iron oxide nanoparticles". *Journal of Magnetism and Magnetic Materials*. 225, 30-36.

Kim, Y., Kim, C., Rengaraj, S., and Yi, J., 2004, "Arsenic Removal Using Mesoporous Alumina Prepared via a Templating Method". *Environ. Sci. Technol. 38 (3),* 924–931.

Kleitz, F., Thomson, S.J., Liu, Z.,Terasaki, O., andSchuth, F., 2002, "Porous mesostructured zirconium oxophosphate with cubic (Ia3d) symmetry". *Chem. Mater.* 14, 4134–4144.

Korngold, E., Belfer, S., and Urtizberea, C., 1996, "Removal of Heavy Metals from Tap Water by a Cation Exchanger". *Desalination,* 104 (3), 197–201.

Kreilgaard M.M., 2002, "Influence of microemulsions on cutaneous drug delivery". *Bulletin Technique Gattefosse,* 95, 79-100.

Ku, Y., and Chiou, H.M., 2002, "The adsorption of fluoride ion from aqueous solution by activated alumina". *Water Air Soil Pollution*, 133, 349–360.

Ku, Y., and Chiou, H.M., 2006, "The adsorption of fluoride ion from aqueous solution by activated alumina ground water by electrodialysis: continuous operation". *Desalination,* 189, 215-220.

Kumar, E., Bhatnagar, A., Kumar, U., Sillanpa, M., 2011, "Defluoridation from aqueous solutions by nano-alumina: characterization and sorption studies", *J. Hazard. Mater*. 186, 1042-1049.

Kumar, E., Bhatnagar, A., Minkyu, J., Jung, W., Lee, S., Kim, S., Lee, G., Song, H., Choi, J., Yang, J., and Jeon, B., Feb 2009, "De fluoridation from aqueous solutions by granular ferric hydroxide (GFH)".*Water Res.,* Vol. 43, Issue 2, pp. 490–499.

Kwok, K. C. M., Koong, L. F., Chen, G., and McKay, G., 2014, "Mechanism of arsenic removal using chitosan and nanochitosan". *Journal of Colloid and Interface Science,* vol. 416, pp. 1–10.

Laurent, S., Forge, D., Port, M., Roch, A., Robic, C., Elst, L.V., and Muller, R.N., 2008, "Magnetic Iron Oxide Nanoparticles: Synthesis, Stabilization, Vectorization, Physicochemical Characterizations, and Biological Applications". *Chem. Rev.* 108, 2064–2110.

Lee, G., Chen, C., Yang, S. T., and Ahn, W. S., 2010, "Enhanced Adsorptive Removal of Fluoride Using Mesoporous Alumina". *Microporous Mesoporous Mater.* 127 (1–2), 152–156.

Leist, M., Casey, R.J., and Caridi, D., 2000, "The management of arsenic wastes: problems and prospects", *J. Hazard. Mater.* 76, 125–138.

Letichevsky, S., Tellez, C. Z., Avillez, R. R., Silva, M. I. P., Fraga, M. A., and Appel, L. G., 2005, "Obtaining CeO2–ZrO2 mixed oxides by co-precipitation: role of preparation conditions". *Appl. Catal. B: Environmental,* 58, 203-210.

Lhassani, A., Rumeau, M., Benjelloun, D.,and Pontié, M., 2001, "selective demineralization of water by nanofiltration application to the deflouridation to the brackish water ". *Wat. Res.,* 35, 3260–3264.

Li, F. H., Li, Y. N., Zhang, C. C., and Fan, Z. G., 2010, "Recovery of Valuable Elements from Spent YBa2Cu 3O7-x/Ag Composite Superconductor Bulks". *Trans. Nonferrous Met. Soc.* China (English Ed. 20(SUPPL.1), s192–s197.

Li, G. Z., and Guo, R., 1995, "Theory and Application of microemulsion". *Petroleum Industry Press*, 47-180.

Li, G., Jiang, Y., Huang, K., Ding, P., and Chen, J., 2008, "Preparation and properties of magnetic Fe3O4-chitosan nanoparticles". *Journal of Alloys and Compounds*, 466, 451–456.

Lin, Y. F., and Chen, J. L., 2013, "Synthesis of mesoporous maghemite (γ-Fe2O3) nanostructures with enhanced arsenic removal efficiency". *RSC Adv.,* 3, 15344–15349.

Lin, Y.H., etal., 2005, "Thermogravimetric analysis of hydrotalcites based on the takovite formula NixZn6-xAl2(OH)16(CO3).4H2O". *J. Therm. Anal.Calorim*.81:p.83-89.

Liu, A., Ming, J., and Ankumah, R.O., 2005, "Nitrate contamination in private wells in rural Alabama". *Sci. Tot. Environ.* 346 (1–3), 112–120.

Liu, L., Cui, Z., and Ma, Q., et al., 2016, "One–step synthesis of magnetic iron– aluminum oxide/graphene oxide nanoparticles as a selective adsorbent for fluoride removal from aqueous solution". *RSC Advances.* 6(13), 10783–10791.

Liu, R. P., Sun, L. H., Qu, J. H., and Li, G. B., 2009, "Arsenic removal through adsorption, sand filtration and ultrafiltration: In situ precipitated ferric and manganese binary oxides as adsorbents". *Desalination,* 249, 1233–1237.

Liu, R., Gong, W., Lan, H., Yang, T., Liu, H., and Qu, J., May 2012, "Simultaneous removal of arsenate and fluoride by iron and aluminum binary oxide: Competitive adsorption effects". *Sep. Purif. Technol.,* Vol. 92, pp. 100–105.

Lofrano, G., and Ed., 2012 "Emerging Compounds Removal from Wastewater". Springer Briefs in Molecular Science; Springer Netherlands: Dordrecht.

Lopez-Muñoz, M. J., Arencibia, A., Cerro, L., Pascual, R., and Melgar, A., 2016, "Adsorption of Hg (II) from Aqueous Solutions Using TiO2 and Titanate Nanotube Adsorbents". *Appl. Surf. Sci.* 367, 91–100.

Lunge, S., Singh, S., and Sinha, A., 2014, "Magnetic iron oxide (Fe3O4) nanoparticles from tea waste for arsenic removal". *J MagnMagn Mater* 356, 21–31.

Luo, F., and Inoue, K., 2004, "The removal of fluoride ion by using metal (III)-loaded amberlite resins". *Solvent Extr. Ion Exch.* 22, 305-322.

Lv, L., et al., 2006, "One-pot synthesis of carbon supported calcined-Mg/Al layered double hydroxides for antibiotic removal by slow pyrolysis of biomass waste". *J. Hazard. Mater.* 133 (1–3), 119–128.

Ma, J. Q., Shen, Y., Shen, C. S., Wen, Y. Z., and Liu, W. P., 2014, "Aldoping chitosan-Fe(III) hydrogel for the removal of fluoride from aqueous solutions". *Chemical Engineering Journal,* vol. 248, pp. 98–106.

Ma, J., and Wu, B., 2013, "Effect of surfactants on preparation of nanoscale α-Al2O3 powders by oil-in-water microemulsion". *Advanced powder technology*, 24, 354-358.

Ma, L., Islam, S. M., Liu, H., Zhao, J., Sun, G., Li, H., and Kanatzidis, M. G., 2017, "Selective and Efficient Removal of Toxic Oxoanions of As(III), As(V), and Cr(VI) by Layered Double Hydroxide Intercalated with MoS42−". *Chem. Mater*.29, 3274-3284.

Madrakian, T., Afkhami, A., Zadpour, B., and Ahmadi, M., 2015, "New Synthetic MercaptoethylaminoHomopolymer-Modified Maghemite Nanoparticles for Effective Removal of Some Heavy Metal Ions from Aqueous Solution". *J. Ind. Eng. Chem*. 21, 1160–1166.

Mahmood, I, Lopes, C.B., Lopes, I., Ahmad, I., Duarte, A.C., and Pereira, E., 2013, "Nanoscale materials and their use in water contaminants removal-a review". *Environment Sci. Pollution Res.* 20, 1239–1260.

Malik, M.A., Wani, M.Y., and Hashim, M.A., 2012, "Microemulsion method: A novel route to synthesize organic and inorganic nanomaterials". *Arabian journal of Chemistry*, 5, 397-417.

Mameri, N., Yeddou, A.R., Lounici, H., Grib, H., Belhocine, D., and Bariou, B., 1998, "Defluoridation of septentrional Sahara water of North Africa by electrocoagulation process using bipolar aluminium electrodes", *Water Res.* 32 (5),1604–1610.

Manning, and Goldberg, S., 1997, "Adsorption and stability of arsenic (III) at the clay mineral–water interface". *Environ. Sci. Technol.* 31, 2005–2011.

Mansour, M., Ossman, M., and Farag, H., 2011. "Removal of Cd (II) ion from waste water by adsorption onto polyaniline coated on sawdust". *Desalination*, 272(1), pp. 301–305.

Markeb, A.A., Alonso, A., and Sánchez, A., et al., 2017, "Adsorption process of fluoride from drinking water with magnetic core–shell Ce–Ti@ Fe3O4 and Ce–Ti oxide nanoparticles". Sci Total Environ. 598, 949–958.

Matlock, M. M., Howerton, B. S., and Atwood, D. A., 2001, "Irreversible Precipitation of Mercury and Lead", *J. Hazard. Mater*. 84 (1), 73–82.

Matlock, M. M., Howerton, B. S., and Atwood, D. A., 2002, "Chemical Precipitation of Heavy Metals from Acid Mine Drainage". *Water Res.* 36 (19), 4757–4764.

McNeill, L.S., and Edwards, M., 1997, "Predicting arsenate removal during metal hydroxide precipitation", *J. AWWA* 89, 75–86.

Meenakshi, S., and Viswanathan, N., 2007, "Identification of Selective Ion-Exchange Resin for Fluoride Sorption". *J. Colloid Interface Sci.* 308 (2), 438–450.

Meenakshi, S., Garg, V.K., Kavita., Renuka., and Malik, A., 2004, "Ground water quality in some villages of Haryana, India: focus on fluoride and fluorosis", *J. Hazard. Mater*. B 106, 85–97.

Mehdipour, S., Vatanpour, V., and Kariminia, H. R., 2015, "Influence of Ion Interaction on Lead Removal by a Polyamide Nanofiltration Membrane". *Desalination* 362, 84–92.

Melo, C.R., Riella, H.G., Kuhnen, N.C., Angioletto, E., Melo, A. R., Bernardin, A.M., da Rocha, M.R., and da Silva, L., 2012, "Synthesis of 4A zeolites from kaolin for obtaining 5A zeolites through ionic exchange for adsorption of arsenic". *Mater. Sci. Eng.,* 177, 345–349.

Miller, S. M., and Zimmerman, J. B., 2010, "Novel, bio-based, photoactive arsenic sorbent: TiO 2-impregnated chitosan bead". *Water Research*, vol. 44, no. 19, pp. 5722–5729.

Miyata, S., 1983, "Anion Exchange Properties of Hydrotalcite-like Compounds Clays and Clay Minerals".31(4):p.305-311.

Mohan Rao, N. V. R., and Bhaskaran, C.S., 1988, "studies on deflouridation of water". *Journal of fluorine Chemistry,* 41, 17-24.

Mohan, D., and Pittman, C. U., 2007, "Arsenic removal from water/wastewater using adsorbents—A critical review". *J. Hazard. Mater.,* 142, 1–53.

Mohapatra, M., Anand, S., Mishra, B. K., Giles, D. E., and Singh, P., 2009, "Review of Fluoride Removal from Drinking Water". *J. Environ. Manage.* 91 (1), 67–77.

Mohapatra, M., Hariprasad, D., Mohapatra, L., Anand, S., and Mishra, B.K., March 2012, "Mg-doped nano ferrihydrite—A new adsorbent for fluoride removal from aqueous solutions". *Appl. Surface Sci.,* Vol. 258, Issue 10, pp. 4228–4236.

Monárez-Cordero, B., Amézaga-Madrid, P., Antúnez-Flores, W., LeyvaPorras, C., Pizá-Ruiz, P., and Miki- Yoshida, M., 2014, "Highly efficient removal of arsenic metal ions with high superficial area hollow magnetite nanoparticles synthetized by AACVD method". *J Alloys Compd.* 586, S520–S525.

Morris, S.M., Horton, J.A., and Jaroniec, M., 2010, "Soft-templating synthesis and properties of mesoporous alumina–titania". *Microporous and Mesoporous Materials*, 128, 180–186.

Mukh–Qasem, R.A., and Gedanken, A., 2005, "Sonochemical synthesis of stable hydrosol of Fe3O4 nanoparticles". *Journal of colloid and interface science*. 284(2), 489–494.

Mulligan, C.N., Yong, R.N., and Gibbs, B.F., 2001, "Remediation technologies for metal contaminated soils and groundwater: an evaluation", *Eng. Geol.* 60 (1–4), 193–200.

Mulwanda, J., and Dorfling, C., 2015, "Recovery of Dissolved Platinum Group Metals from Copper Sulphate Leach Solutions by Precipitation". *Miner. Eng.* 80, 50–56.

Murray, E. P., Tsai, T., and Barnett, S. A., 1999, "A direct-methane fuel cell with a ceria-based anode". *A. Nature.* 400, 649-651.

Nickson, R.T., McArthur, J.M., Shrestha, B., Kyaw-Myint, T.O., and Lowry, D., 2005, "Arsenic and other drinking water quality issues, Muzaffargarh District, Pakistan", *Appl. Geochem* 20, 55–68.

Nikoloski, A. N., Ang, K. L., and Li, D., 2015, "Recovery of Platinum, Palladium and Rhodium from Acidic Chloride Leach Solution Using Ion Exchange Resins". *Hydrometallurgy.* 152, 20–32.

Nishiyama, Y., Tanaka, S., Hillhouse, H.W., Nishiyama, N., Egashira, Y.,and Ueyama, K., 2006, "Synthesis of ordered mesoporous zirconium phosphate films by spin coating and vapor treatments". *Langmuir,* 22, 9469–9472.

Nordstrom, D.K., and Alpers, C.N., 1999, "Negative pH, efflorescent mineralogy, and consequences for environmental restoration at the Iron Mountain Superfund Site, California", *Proc. Natl. Acad. Sci. U.S.A.* 96, 3455–3462.

Nur, T., Loganathan, P., Nguyen, T.C., Vigneswaran, S., Singh, G., and Kandasamy, J., 2014, "Batch and column adsorption and desorption of fluoride using hydrous ferric oxide: Solution chemistry and modelling". *Cical Eng. J.,* Vol. 247, pp. 93-102.

Oehmen, A., Viegas, R., Velizarov, S., Reis, M. A. M., and Crespo, J. G., 2006, "Removal of Heavy Metals from Drinking Water Supplies through the Ion exchange Membrane Bioreactor". *Desalination.* 199(1–3), 405–407.

Oguz, E., 2007, "Equilibrium isotherm and kinetics studies for the sorption of fluoride on light weight concrete materials". *Colloid Surf. A: Physicochem. Eng. Asp.,* 295, 258-263.

Oller, I., Malato, S., and Sanchez-Perez, J. A., 2011, "Combination of Advanced Oxidation Processes and Biological Treatments for Wastewater Decontamination-A Review". *Sci. Total Environ.* 409(20), 4141–4166.

Omueti, J. A. I., and Jones, R. L., 1977, "Fluoride adsorption by Illinois soil". *Journal of Soil Science*, 28, 564-572.

Oremland, R. S., and Stolz, J.F., 2003, "Ecology of arsenic", *Science* 300, 939–944.

Pallier,V., Feuillade-Cathalifaud, G., Serpaud, B., and Bollinger, J. C., 2010, "Effect of organic matter on arsenic removal during coagulation/flocculation treatment". *J. Colloid Interface Sci.,* 342, 26–32.

Palmer, S.J.,Soisonard, A., Frost, R.L.J.,2009, "Determination of the mechanism(s) for the inclusion of arsenate, vanadate, or molybdate anions into hydrotalcites with variable cationic ratio", *Colloid Interface Sci.* 329 (2), 404–409.

Patel, H.A., Byun, J., and Yavuz, C.T., 2012, "Arsenic removal by magnetic nanocrystalline barium hexaferrite". *J. Nanopart Res* 14, 881.,

Patra, J.K., and Baek, K.H., 2017, "Green biosynthesis of magnetic iron oxide (Fe3O4) nanoparticles using the aqueous extracts of food processing wastes under photo catalysed condition and investigation of their antimicrobial and antioxidant activity". *J. Photochem. Photobiol.,* B, 173,291–300.

Phillips, D. H., Sen Gupta, B., Mukhopadhyay, S., and Sen Gupta, A.K., 2018, "Arsenic and fluoride removal from contaminated drinking water with Haix-Fe-Zr and Haix-Zr resin beads". *Journal of Environmental Management,* 215,132-142.

Pihlar, B., and Cencic, Z.l., 1993, "Investigation of a zirconium electrode as a sensor for fluoride ions". *Anal. Chim. Acta,* 273, 267–274.

Prashanth, P.A., Raveendra, R.S., HariKrishna, R., Ananda, S., Bhagya, N.P., Nagabhushana, B.M., Lingaraju, K., and Naika, H.R., 2015, "Synthesis, characterizations, antibacterial

and photoluminescence studies of solution combustion-derived α-Al 2O3 nanoparticles". *J. Asian Ceram. Soc.,* 3, 345–351.

Prathna, T.C., Sharma, S.K., and Kennedy, M., 2017, "Development of iron oxide nanoparticle adsorbents for arsenic and fluoride removal". *Desal. Wat. Treatment,* 67, 187–195.

Qdais, H. A., and Moussa, H., 2004, "Removal of Heavy Metals from Wastewater by Membrane Processes: A Comparative Study". *Desalination,* 164 (2), 105–110.

Qiao, J., Cui, Z., Sun, Y., Hu, Q., Guan, X., 2014, "Simultaneous removal of arsenate and fluoride from water by Al-Fe hydroxides". *Front. Environ. Sci. Eng.,* 8, 169–179.

Rajbhandari, R., Shrestha, L. K., and Pradhananga, R. R., 2012, "Nanoporous Activated Carbon Derived from Lapsi (Choerospondias Axillaris) Seed Stone for the Removal of Arsenic from Water". *J. Nanosci. Nanotechnol.,* 12, 7002–7009.

Rives, V., and Editor, 2001, "Layered Double Hydroxides: Present and Future", *New York: Nova Science PubInc*: p. 439.

Rodriguez, J.A., and Fernandez-Garcia, M., 2007, "Synthesis, Properties, and Applications of Oxide Nanomaterials". *John Wiley and Sons, Hoboken*, NJ.

Ruixia, L., Jinlong, G., and Hongxiao, T., 2002, "Adsorption of Flouride, Phosphate, and Arsenate Ions on a New Type of Ion Exchange Fiber". *J. Colloid Interface Sci.*248, 268–274.

Sahu, A.K., Pitchumani, S., Sridhar, P., and Shukla, A.K., 2009, "Co-assembly of a nafion-mesoporouszirconium phosphate composite membrane for PEM fuel cells". *Fuel Cells*, 9, 139–147.

Samantaray, S.K., and Parida, K., 2001, "Effect of phosphate ion on the textural and catalytic activity of titania-silica mixed oxide". *Appl. Catal. A,* 220, 9–20.

Sari, A., and Tuzen, M., 2008, "Biosorption of Pb(II) and Cd(II) from aqueous solution using green alga (Ulva lactuca) biomass". *J. Hazard. Mater.,* 152 ,302-308.

Schoeman, J. J., and Steyn, A., 2000, "Defluoridation, denitrification and desalination of water using ion-exchange and reverse osmosis technology". *Water Research Commission, Pretoria.* ISBN: 1 86845 597 1.

Schoeman, J. J., and Steyn, A., 2000, "Defluoridation, denitrification and desalination of water using ion-exchange and reverse osmosis technology". *Water Research Commission, Pretoria.* ISBN: 1 86845 597 1.

Schulman, J. H., Stoeckenius, W., and Prince, M. J., 1959, "Mechanism of formation and structure of microcmulsions by electron microscopy". *Phys. Chem.* 63, 1677.

Sehn, P., 2008, "Fluoride Removal with Extra Low Energy Reverse Osmosis Membranes: Three Years of Large Scale Field Experience in Finland". *Desalination*, 223, 73–84.

Sen, M., and Pal, P., 2009, "Treatment of arsenic-contaminated groundwater by a low cost activated alumina adsorbent prepared by partial thermal dehydration". *Desalin. Water Treat.,* 11, 275–282.

Serbezov, A., Moore, J. D., and Wu, Y., 2011, "Adsorption Equilibrium of Water Vapor on Selexsorb-CDX Commercial Activated Alumina Adsorbent". *J. Chem. Eng. Data,* 56 (5), 1762–1769.

Shao, M.F., Ning, F.Y., Zhao, J.W., Wei, M., Evans, D.G., and Duan, X., 2012, "Preparation of Fe3O4@SiO2@layered double hydroxide core–shell microspheres for magnetic separation of proteins". *J. Am. Chem. Soc*. 134, 1071–1077.

Shao, Z. P., and Haile, S. M., 2004, "A high-performance cathode for the next generation of solid-oxide fuel cells". *Nature*, 431, 170-173.

Sharma, M., Kalita, P., and Garg, A., et al., 2018, "Magnetic nanoparticles as an effective adsorbent for removal of fluoride–a review". *MOJ Eco Environ Sci*. 3(3), 207–210.

Sharma, V.K., and Sohn, M., 2009, "Aquatic arsenic: toxicity, speciation, transformations, and remediation". *Environ Int.* 35, 743–759.

Shen, J., Li, Z., Wu, Y., Nan., Zhang, B., and Li, F., 2015, "Dendrimer-Based Preparation of Mesoporous Alumina Nanofibers by Electrospinning and Their Application in Dye Adsorption". *Chem. Eng. J.* 264, 48–55.

Shen, S., Tian, B., Yu, C., Xie, S., Zhang, Z., Tu, B., and Zhao, D., 2003, "Synthesis of highly ordered thermally stable cubic mesostructured zirconium oxophosphate templated by tri-eadgroup quaternary ammonium surfactants". *Chem. Mater.* 15, 4046–4051.

Shinde, R. N., Pandey, A. K., and Acharya R., et al. 2013, "Chitosantransition metal ions complexes for selective arsenic (V) preconcentration". *Water Research*, vol. 47, no. 10, pp. 3497–3506.

Shipley, H.J., Yean, S., Kan, A.T., and Tomson, M.B., 2010, "A sorption kinetics model for arsenic adsorption to magnetite nanoparticles". *Environ SciPollut Res* 17, 1053–1062.

Sing, K.S.W., Everett, D.H., Haul, R.A.W., Moscou, L., Pierotti, R.A., Rouquerol, J., and Siemieniewska, T., 1985, "Reporting Physisorption Data for gas/Solid Systems with

Special Reference to the Determination of Surface Area and Porosity". *Pure Appl. Chem*. 57(4), 603–619.

Singh, R., and Maheshwari, R.C., 2001, "Defluoridation of drinking water–a review", Ind. *J. Environ. Protec*. 21 (11), 983–991.

Sjöblom, J., Lindberg, R., and Friberg, S. E., 1996, "Microemulsions: Phase equilibria characterization, structures, applications and chemical reactions". *Adv. Colloid Interface Sci*., 95, 125.

Srimurali, M., Pragathi, A., Karthikeyan, J., 1998, "A study on removal of fluorides from drinking water by adsorption onto low-cost materials". *Environmental Pollution*, 99, 285-289.

Stajcic, A., Nastasovic, A., Stajic-Trosic, J., Markovic, J., Onjia, A., andRadovanovic, F., 2015, "Novel Membrane-Supported Hydrogel for Removal of Heavy Metals". *J. Environ. Chem. Eng.* 3, 453–461.

Sun, Y., Chen, C., Tan, X., Shao, D., Li, J., Zhao, G., Yang, S., Wang, Q., and Wang, X., 2012, "Enhanced Adsorption of Eu (III) on Mesoporous Al2O3/expanded Graphite Composites Investigated by Macroscopic and Microscopic Techniques". *Dalton Trans.* 41 (43), 13388–13394.

Sun, Z. M., Yu, Y. C., Pang, S. Y., and Du, D. Y., 2013, "Manganese-modified activated carbon fiber (Mn-ACF): Novel efficient adsorbent for Arsenic". *Appl. Surf. Sci.,* 284, 100–106.

Susheela, A.K., 1999, "Fluorosis management programme in India", *Curr. Sci*. 77 (10), 1250–1256.

Susheela, A.K., 2001, "Treatise on Fluorosis". *Fluorosis Research and Rural Development Foundation*, India.

Swain, S. K., Patnaik, T., Singh, B. K., Jha, U., Patel, R. K., and Dey, A.K., 2011, "Kinetics, equilibrium and thermodynamic aspects of removal of fluoride from drinking water using meso-structured zirconium phosphate". *Chemical engineering journal,* 171, 1218-1226.

Swain, S.K., Padhi, T., Patnaik, T., Patel, R.K., Jha, U., Dey, R.K., 2010, "kinetics and thermodynamics of fluoride removal using cerium-impregnated chitosan", *Desalination Water Treat.,* 13, 369–381.

Tadanaga, K., Furukawa, Y., Hayashi, A., and Tatsumisago, M., 2010, "Direct ethanol fuel cell using hydrotalcite clay as a hydroxide ion conductive electrolyte". *Adv. Mater*. 22, 4401–4404.

Tahaikt, M., El Habbani, R., AitHaddou, A., Achary, I., Amor, Z., Taky, M., Alami, A., Boughriba, A., Hafsi, M., and Elmidaoui, A., 2007, "Fluoride Removal from Groundwater by Nano filtration". *Desalination*. 212, 46–53.

Tang, Y., Wang, J., and Gao, N., 2010, "Characteristics and model studies for fluoride and arsenic adsorption on goethite". *J. Environ. Sci.,* 22, 1689–1694.

Tarafdar, A., Panda, A.B., Pradhan, N.C., andPramanik, P., 2006,"Synthesis of spherical mesostructured zirconium phosphate with acidic properties". *Microporous Mesoporous Mater.* 95, 360–365.

Taylor, K.C., 1993, "Nitric Oxide Catalysis in Automotive Exhaust Systems". *Catalysis Reviews: Science and Engineering,* 35, 457-481.

Taylor, K.C., Anderson, J. R., and Boudart, M., 1984, "Selectivity Control and Catalyst Design in the Fischer-Tropsch Synthesis: Sites, Pellets, and Reactors". *Catalysis-Science and Technology*. Berlin, Springer-Verlag.

Teja, A.S., and Koh, P.Y., 2009, "Synthesis, properties, and applications of magnetic iron oxide nanoparticles". *Progress in crystal growth and characterization of material*, 55, 22-45.

Teychene, B., Collet, G., Gallard, H., and Croue, J. P., 2013, "A comparative study of boron and arsenic (III) rejection from brackish water by reverse osmosis membranes". *Desalination*, 310, 109–114.

Tian, B.Z., Liu, X.Y., Tu, B., Yu, C.Z., Fan, J., Wang, L.M., Xie, S.H., Stucky, G.D.,and Zhao, D.Y., 2003, "Self-adjusted synthesis of ordered stable mesoporous minerals by acid-base pairs". *Nat. Mater.* 2, 159–163.

Tomar, V., Prasad, S., and Kumar, D., 2014, "Adsorptive Removal of Fluoride from Aqueous Media Using Citrus Limonum (Lemon) Leaf". *Microchem. J.* 112, 97–103.

Tor, A., 2007, "Removal of fluoride from water using anion-exchange membrane under Donnan dialysis condition". *J. Hazard. Mater.* 141,814-818.

Turk, T.,Alp, I., and Deveci, H., 2009, "Adsorption of As (V) from water using Mg/Fe based hydrotalcite (FeHT)". *J. Hazard. Mater*., 171, 665–670.

Turner, B. D., Binning, P., and Stipp, S. L. S., 2005, "Fluoride Removal by Calcite: Evidence for Fluorite Precipitation and Surface Adsorption". *Environ. Sci. Technol.* 39(24), 9561–9568.

Um, W., Mattigod, S., Serne, R.J., Fryxell, G.E., Kim, D.H.,and Troyer, L.D., 2007,"Synthesis of nanoporous zirconium oxophosphate and application for removal of U(VI)". *Water Res*. 41, 3217–3226.

Underwood, E.J., 1997, "Trace Elements in Human and Animal Nutrition". *Academic Press,* New York, 545.

Upadhyaya, G., Jackson, J., Clancy, T. M., Hyun, S. P., Brown, J., Hayes, K. F., and Raskin, L., 2010, "Challenges in determining causation in structure–function studies using molecular biological techniques". *Water Res*., 44, 4958–4969.

Upadhyayula, V.K.K., Deng, S., Mitchell, M.C., and Smith, G.B., 2009, "Application of carbon nanotube technology for removal of contaminants in drinking water: a review". *Sci. Total Environ.*, 408, 1–13.

Van-Dorn, D., Ravalli, M.T., Small, M.M., Hillery, B., and Andreescu. S., 2011, "Adsorption of arsenic by iron oxide nanoparticles: a versatile, inquiry-based laboratory for a high school or college science course". *J Chem. Educ*. 88, 1119–1122.

Veressinina, Y., Trapido, M., Ahelik, V., and Munter, R., 2001, "Fluoride in drinking water: the problems and its possible solutions". *Proc. Estonian Acad. Sci. Chem.,* 50, 81-88.

Virolainen, S., Tyster, M., Haapalainen, M., and Sainio, T., 2014, "Ion exchange Recovery of Silver from Concentrated Base Metal-Chloride solutions". *Hydrometallurgy*.152, 100–106.

Viswanathan, N., and Meenakshi, S., 2009, "Role of Metal Ion Incorporation in Ion Exchange Resin on the Selectivity of Fluoride". *J. Hazard. Mater.* 162 (2–3), 920–930.

Viswanathan, N., and Meenakshi, S., 2010, "Selective fluoride adsorption by a hydrotalcite/chitosan composite". *Appl. Clay Sci.,* 48, 607–611.

Vogel, A.I., 2000, "A Text Book of Quantitative Inorganic Analysis, English Language Book Society", *Longmans Green*, London.

W. Li., Cao, C. Y., Wu, L. Y., Ge, M. F., and Song, W.G., 2011, "Superb fluoride and arsenic removal performance of highly ordered mesoporous aluminas". *Journal of Hazardous Materials*, 198, 143–150.

Waghmare, S.S., and Arfin, T., 2015, "Fluoride removal from water by mixed metal oxide adsorbent materials: a state-of-the-art review". *International journal of engineering sciences & research technology.* 4(9), 51-536.

Wan, Y., Wu, H., Yu, A., and Wen, D., 2006, "Biodegradable polylactide/chitosan blend membranes; Biodegradable Polylactide/Chitosan Blend Membranes". *Biomacromolecules* 7, 1362–1372.

Wang, H., et al., 2007, "Defluoridation of Drinking Water by Mg/Al Hydrotalcite-Like Compounds and Their Calcined Products". *Appl. Clay Sci*. 35 (1–2), 59–66.

Wang, S., Ma, Y., Shi, Y., Gong, W., 2009, "Defluoridation performance and mechanism of nano-scale aluminum oxide hydroxide in aqueous solution". *Journal of Chemical Technology and Biotechnology*, 84 (7), 1043-1050.

Wei, X., and Viadero, R.C., 2007, "Synthesis of magnetic nanoparticles with ferric iron recovered from acid mine drainage". *Colloids and surface A: Physiochemical and Engineering Aspects,* 294, 280-286.

WHO, 2011, "Guidelines for Drinking Water Quality", *World Health Organization*, Vol. 1, 4th ed., p. 178.

Wongwailikhit, K., and Horwongsakul, S., 2011, "The preparation of iron (III) oxide nanoparticles using W/O microemulsion". 65, 2820–2822.

Worch, E., 2012, "Adsorption Technology in Water Treatment - Fundamentals, Processes, and Modeling". De Gruyter: Berlin/Boston.

Wu, H.X., Wang, T.J., Dou, X.M., Zhao, B., Chen, L., and Jin, Y., 2008, "Spray Coating of Adsorbent with Polymer Latex on Sand Particles for Fluoride Removal in Drinking Water". *Ind. Eng. Chem. Res*. Vol. 47, Issue 14, pp. 4697–4702.

Wu, X. L., Tan, X. L., Yang, S.T., Wen, T., Guo, H. L., Wang, X. K., and Xu, A.W., 2013, "Coexistence of adsorption and coagulation processes of both arsenate and NOM from contaminated groundwater by nanocrystallined Mg/Al layered double hydroxides". *Water Res.,* 47, 4159–4168.

Wu, X., Zhang, Y., Dou, X., Yang, M., 2007, "Fluoride removal performance of a novel Fe-Al-Cetrimetal oxide adsorbent, Chemosphere". 69,1758-1764.

Xi, Y., Ding, Z., He, H., Frost, R.L., 2005, "Infrared spectroscopy of organoclays synthesized with the surfactant octadecyltrimethyl ammonium bromide". *Spectrochim. Acta A.,* 61, 515–525.

Xu, P., Capito, M., and Cath, T. Y., 2013, "Selective removal of arsenic and monovalent ions from brackish water reverse osmosis concentrate". *J. Hazard. Mater.,* 260, 885–891.

Xu, R. X., Yu, X.Y., Gao, C., Liu, J. H., Compton, R.G., and Huang, X. J., 2013, "Enhancing selectivity in stripping voltammetry by different adsorption behaviors: the use of

nanostructured Mg–Al-layered double hydroxides to detect Cd (II)". *Analyst*, 138, 1812–1818.

Xu, Y., Dai, Y., Zhou, J., Xu, Z.P., Qian, G., and Lu, G.Q.M., 2010, "Removal efficiency of arsenate and phosphate from aqueous solution using layered double hydroxide materials: intercalation vs. precipitation". *J. Mater. Chem.* 20, 4684–4691.

Yahyaei, B., and Azizian, S., 2014, "Rapid Adsorption of Binary Dye Pollutants onto the Nanostructured Mesoporous Alumina". *J. Mol. Liq.* 199, 88–95.

Yamani, J. S., Miller, S. M., Spaulding, M. L., and Zimmerman, J. B., 2012, "Enhanced arsenic removal using mixed metal oxide impregnated chitosan beads". *Water Research,* vol. 46, no. 14, pp. 4427–4434.

Yang, L.,Shahrivari, Z., Liu, P. K.,Sahimi, M., and Tsotsi, T. T., 2005,"Removal of Trace Levels of Arsenic and Selenium from Aqueous Solutions by Calcined and Uncalcined Layered Double Hydroxides (LDH)s". *Ind. Eng. Chem. Res*. 44, 6804-6815.

Yang, W., Dou, X., and Li, Y., et al., 2016, "Performance and mass transfer of aqueous fluoride removal by a magnetic alumina aerogel". *RSC Advances.* 6(114), 112988–112999.

.

Yari, M., Rajabi, M., Moradi, O., Yari, A., Asif, M., Agarwal, S., and Gupta, V. K., 2015, "Kinetics of the Adsorption of Pb (II) Ions from Aqueous Solutions by Graphene Oxide and Thiol Functionalized Graphene Oxide". *J. Mol. Liq.* 209, 50–57.

Yoon, S. H., and Lee, J. H., 2007, "Optimal Control of a Continuous Distillation Column". *J. Ind. Eng. Chem.,* 13, 97–104.

Yoshida, T., Yamanchi, H., and Jun, G.F., 2004, "Chronic health effect in people exposed to arsenic via the drinking water: dose–response relationship in review", *Toxicol. Appl. Pharmacol.* 198, 243–252.

You, Y. W., Zhao, H. T., and Vange, G. F., 2000, "Removal of Arsenic from Aqueous Solutions by Anion Clays". *Environ. Technol*. 22, 6804.

Yuan, X. Y., Wang, Y. F., Wang, J., Zhou, C., Tang, Q., and Rao, X. B., 2013," Calcined graphene/MgAl-layered double hydroxides for enhanced Cr(VI) removal". *Chem. Eng. J.*, 221, 204–213.

Yuan, Z.Y., Ren, T.Z., Azioune, A., Pireaux, J.J., and Su, B.L., 2005, "Marvelous self-assembly of hierarchically nanostructured porous zirconium phosphate solid acids with high thermal stability". *Catal.* Today 105, 647–654.

Yulin, T., Xiaohong, G., Jianmin, W., Naiyun, G., Martin, R. M., and Charles, C. C., Nov 2009, "Fluoride adsorption onto granular ferric hydroxide: Effects of ionic strength, pH, surface loading, and major co-existing anions". *Journal of Hazardous Materials* Vol. 171, Issues 1-3, pp. 774–779.

Zewail, T. M., and Yousef, N. S., 2015, "Kinetic Study of Heavy Metal Ions Removal by Ion Exchange in Batch Conical Air Spouted Bed". *Alexandria Eng. J.* 54, 83–90.

Zhang, C., Li, Y., and Wang, T.J., et al., 2016, "Adsorption of drinking water fluoride on a micron–sized magnetic Fe3O4@ Fe–Ti composite adsorbent". *Applied Surface Science*. 363, 507–515.

Zhang, C., Li, Y., and Wang, T.J., et al., 2017, "Size–Dependent Fluoride Removal Performance of a Magnetic Fe3O4@Fe-Ti Adsorbent and Its Defluoridation in a Fluidized Bed". *Industrial & Engineering Chemistry Research*. 56(9), 2425-2432.

Zhang, H., Huang, F., Liu, D.-L., and Shi, P., 2015, "Highly Efficient Removal of Cr (VI) from Wastewater via Adsorption with Novel Magnetic Fe3O4@C@MgAl-Layered Double-Hydroxide". *Chinese Chem. Lett*. 26(9), 1137–1143.

Zhang, L., and Fang, M., 2010, "Nanomaterials in Pollution Trace Detection and Environmental Improvement". *Nano Today*, 5 (2), 128–142.

Zhang, M., Gao, B., Varnoosfaderani, S., Hebard, A., Yao, Y., and Inyang, M., 2013, "Preparation and characterization of a novel magnetic biochar for arsenic removal". *Bioresour. Technol.,* 130, 457–462.

Zhang, T., et al., 2012, "Synthesis of Li–Al layered double hydroxides (LDHs) for efficient fluoride removal". *Ind. Eng. Chem. Res*.

Zhao, X., Höll, W. H., and Yun, G., 2002, "Elimination of Cadmium Trace Contaminations from Drinking Water". *Water Res.* 36 (4), 851–858.

Zhao, X., Wang, J., and Wu, F., et al., 2010, "Removal of fluoride from aqueous media by Fe3O4@Al (OH)3 magnetic nanoparticles". *J Hazard Mater.* 173(1), 102–109.

Zhao, Y., He, S., Wei, M., Evans, D.G., and Duan, X., 2010, "Hierarchical films of layered double hydroxides by using a sol–gel process and their high adaptability in water treatment". *Chem. Commun*. 46, 3031–3033.

Zheng, Y. M., Li, N., and Zhang, W. D., 2012, "Preparation of nanostructured microspheres of Zn–Mg–Al layered double hydroxides with high adsorption property". *Colloids Surf., A*, 415, 195–201.

Zhi, J., Wang, Y.J., and Luo, G.S., 2005, "Adsorption of diuretic furosemide onto chitosan nanoparticles prepared with a water-in-oil nano-emulsion system", *Reactive and Functional polymers*, 65, 249–257.

Zhong, Y., Yang, Q., Luo, K., Wu, X. Q., Li, X. M., Liu, Y., Tang, W. W., Zeng, G. M., and Peng, B., 2013, "Fe(II)–Al(III) layered double hydroxides prepared by ultrasound-assisted co-precipitation method for the reduction of bromate". *J. Hazard. Mater*. 250, 345–353.

Zhou, Z.H., Wang, J., and Liu, X., et al., 2001, "Synthesis of Fe3O4 nanoparticles from emulsions". *Journal of Materials Chemistry*. 11(6), 1704–1709.

Zhu, B. J., Yu, X. Y., Jia, Y., Peng, F. M., Sun, B., Zhang, M. Y., Luo, T., Liu, J. H., and Huang, X. J., 2012, "Iron and 1,3,5-Benzenetricarboxylic Metal–Organic Coordination Polymers Prepared by Solvothermal Method and Their Application in Efficient As(V) Removal from Aqueous Solutions". *J. Phys. Chem. C*, 116, 8601–8607.

Zhu, J., Zhao, H., and Ni, J., 2007, "Fluoride distribution in electrocoagulation defluoridation process". *Sep. Purif. Technol.* 56,184-191.

Zhu, W. P., Gao, J., Sun, S. P., Zhang, S., and Chung, T. S., 2015, "Poly (amidoamine) Dendrimer (PAMAM) Grafted on Thin Film Composite (TFC) Nanofiltration (NF) Hollow Fiber Membranes for Heavy Metal Removal". *J. Memb. Sci*. 487, 117–126.

Thesis Dissemination

Dissemination

Internationally indexed journals

[1] S K Swain, **Tapaswin Padhi**,,Tanushree Patnaik,V K Singh,Usha Jha, **R K Patel** and R K Dey ,Kinetics and thermodynamics of fluoride removal using cerium-impregnated chitosan Desalination and Water Treatment, 13, (2010) 369-381. doi.org/10.5004/dwt.2010.995

[2] Sandip Mandal, **Tapswani Padhi**, & R K Patel, Studies on the removal of arsenic (III) from water by a novel hybrid material. Journal of Hazardous Materials, 192(2), (2011) 899–908. doi:10.1016/j.jhazmat.2011.05.099.

[3] Sandip Mandal, Swagatika Tripathy, **Tapswani Padhi**, Manoj Kumar Sahu, **Raj Kishore Patel**, Removal efficiency of fluoride by novel Mg-Cr-Cl layered double hydroxide (LDH) by batch process from water, Journal of Environmental Sciences, 25(5), (2013) 1-9. doi.org/10.1016/S1001-0742(12)60146-6.

[4] Mamta Mohapatra, **Tapaswini Padhi**, Sashi Anand, & Barada Kanta Mishra,. Ca–Mg-Doped Surface-Modified Nano-Sized Ferrihydrite Powder Synthesized by Surfactant Mediation–Precipitation Technique: A Novel Super Adsorbent for Cations. Adsorption Science & Technology, 30(5), (2012) 383–397. doi:10.1260/0263-6174.30.5.383

[5] Mamta Mohapatra, **Tapaswini Padhi**, Sashi Anand, & Barada Kanta Mishra, CTAB mediated Mg-doped nano Fe2O3: synthesis, characterization, and fluoride adsorption behavior. Desalination and Water Treatment, 50(1-3), (2012) 376–386. doi:10.1080/19443994.2012.720411.

[6] Mamta Mohapatra, **Tapaswini Padhi**, Tukuni Dash, Pritam Singh, Sashi Anand, & Barada Kanta Mishra,. Ambient temperature synthesis of nanorod 6-line ferrihydrite and its cation sorption behavior. Toxicological & Environmental Chemistry, 93(5), (2011) 844–859. doi:10.1080/02772248.2011.566878

Submitted Articles

[1] T. Padhi, R. K. Patel, Ambient temperature synthesis of rod shaped Iron-Aluminium mixed oxides and its fluoride sorption behavior.

[2] T Padhi. N.Pandey, R.K.Patel; Studies on the removal efficiency of Fluoride by porous Lanthanum incorporated Zirconium Phosphate.

[3] T. Padhi, R. K. Patel, Synthesis of Chitosan encapsulated magnetic nanoparticle and its application for removal of fluoride and Arsenic from water by column method.

Conferences

[1] Sandip Mandal ,**Tapaswini Padhi**, Anil Giri, **Rajkishore Patel**, Studies on the removal efficiency of fluoride by Mg-Cr-Cl layer double hydroxide ,1st International Conference on Desalination and Environment: A Water Summit (ICODE 2011), 29 October - 1 November, 2011, in Beach Rotana, Abu Dhabi.

[2] **T.Padhi, R.K.Patel**, S.Mandal, M. Ku. Sahu, Synthesis of Magnetic Iron-oxide Nanoparticles Through Micro Emulsion for Environmental Application, ICMAT13-A-2294, Material research society, seventh international conference on materials for advanced technologies 30.06.2013 to 5.07.2013, Suntec, Singapore.

[3] Sandip Mandal ,**Tapaswini Padhi**, M Islam, Anil Giri, **Rajkishore Patel**, Adsorption behavior of calcined Ca/Al CO_3hydrotalcite-like compound towards removal of As (V) from Groundwater The twenty-sixth international conference on solid waste technology and management ,Philadelphia, PA U.S.A. March 27-30, 2011.

Biodata

Name of the Candidate : **Ms. Tapaswini Padhi**

Mother's Name : **Mrs. Subasini Padhi**

Father's Name : **Mr. Krushna Chandra Padhi**

Date of Birth : **18. 06. 1985**

PresentAddress : **Department of Chemistry, National Institute of Technology, Rourkela -769008, INDIA**

Email : **tps.padhi@gmail.com**

Educational Qualification:

(i) **B.Sc.** in Chemistry, from Bhadrak Autonomous College, Bhadrak Odisha with percentage of 78%.

(ii) **M. Sc.** in Chemistry, from National Institute of Techinology, Rourkela, Odisha, India with CGPA of 8.36.

Research Experience:

She is a research Scholar in Dept. of Chemistry, NIT, Rourkela from Jun. 2010.

Professional Experience:

PROJECT ASSISTANT-II (Sept 2008 - Jan 2010)

Hydro and Electro Metallurgy department

Institute of Minerals and Materials Technology, Bhubaneswar

Permanent Address: AT-Mangalpur, PO-Nischintakoel, PS: Salipur, DIST-Cuttack, Odisha, India**.**